

8-2020

Changes in Neural Network Connectivity of Normal Young Adults in Response to Power Wheelchair Trainer using EEG Coherence

Ruby Phung
Grand Valley State University

Follow this and additional works at: <https://scholarworks.gvsu.edu/theses>



Part of the [Biomedical Engineering and Bioengineering Commons](#)

ScholarWorks Citation

Phung, Ruby, "Changes in Neural Network Connectivity of Normal Young Adults in Response to Power Wheelchair Trainer using EEG Coherence" (2020). *Masters Theses*. 982.
<https://scholarworks.gvsu.edu/theses/982>

This Thesis is brought to you for free and open access by the Graduate Research and Creative Practice at ScholarWorks@GVSU. It has been accepted for inclusion in Masters Theses by an authorized administrator of ScholarWorks@GVSU. For more information, please contact scholarworks@gvsu.edu.

Changes in Neural Network Connectivity of Normal Young Adults in Response to Power
Wheelchair Trainer using EEG Coherence

Ruby Phung

A Thesis Submitted to the Graduate Faculty of

GRAND VALLEY STATE UNIVERSITY

In

Partial Fulfillment of the Requirements

For the Degree of

Master of Science in Engineering – Biomedical Engineering

Padnos College of Engineering and Computing

August 2020

Acknowledgements

I would first like to thank my thesis advisor Dr. Samhita Rhodes of the School of Engineering in the Seymour and Esther Padnos College of Engineering and Computing of Grand Valley State University. Throughout my studies, she has offered tremendous support both personally and academically. Next, I would like to thank my committee members and experts who were involved in this research project: Dr. Lisa K. Kenyon, Dr. John Farris, and Dr. David Zeitler. Without their passionate participation and input, this study could not have been successfully conducted. I would also like to extend my sincere thanks to Dr. Shabbir Choudhuri of the School of Engineering and both the Graduate School and the College of Engineering at Grand Valley State University for all the wonderful resources, facilities, guidance, and assistance they provided to me throughout my graduate school journey.

Finally, I am forever grateful for all the support and continuous encouragement that my family and friends have provided to me throughout my entire academic career and through the process of researching and writing this thesis. They are the reason that I have come this far. This accomplishment would not have been possible without them.

Ruby Phung

Abstract

The ability to move and explore their surrounding environment plays a critical role in the development of cognitive function in children, especially during early childhood. The lack of independent and autonomous mobility is, therefore, a clear disadvantage for the overall development of children with multiple, severe disabilities. Limited number of studies have been conducted on the impact of power mobility device on this specific population. Previous exploratory and pilot studies showed promising results regarding quantifiable and consistent changes in the electroencephalogram (EEG) of children with multiple, severe disabilities when provided with power mobility training. This study aimed to further extend our understanding of the cognitive impact of power mobility training on a different population: healthy young adults aged 18 to 24 – a well-studied neurotypical control population. The study used Magnitude-Square Coherence (MSC) derived from the electroencephalogram (EEG) recorded at resting-yet-awake state before and after power mobility training to investigate changes in the functional connectivity in the brain of seven healthy young adults in the 18-to-24-year-old age range. Neural processes invoked between different functional lobes in the brain in: delta (1-4 Hz), theta (5-7 Hz), alpha (8-13 Hz), beta (14-30 Hz), and gamma (31-100 Hz) in response to power mobility training were examined and analyzed. Statistical analyses were then performed on the change, or difference in EEG coherence between the 5-minute rest with eyes closed before and after power mobility training. Results from both the paired t-test and the Wilcoxon-signed rank test with an alpha level of 0.05 ($p \leq 0.05$) on the change in EEG coherence after mobility training showed an overall decrease in EEG coherence between the parietal and temporal regions on healthy young adults after using the Trainer in all five frequency bands. Reduced interregional EEG coherence was found in the centro-parietal region for both the delta and beta frequency.

Lower EEG coherence was also noted between the frontal and temporal regions in alpha frequency. These findings help edify that power mobility training is responsible for objectively quantifiable changes in neural network connectivity that may be correlated with improvement in subjective measures of cognitive gains on children with multiple, severe disabilities.

Keywords: EEG coherence, brain functional lobes, brainwave frequencies, delta, theta, alpha, beta, gamma, power mobility training, young adults

Table of Contents

Acknowledgements.....	3
Abstract.....	4
Chapter 1 – Introduction.....	8
1.1 Introduction	12
1.2 Purpose	14
1.3 Scope	15
1.4 Assumptions	16
1.5 Hypothesis	16
Chapter 2 – Manuscript.....	18
Abstract	18
2.1 Introduction	18
2.2 Methods	23
2.2.1 EEG Data Collection.....	23
2.2.2 EEG Data Processing.....	30
2.2.3 Data Analysis	32
2.3 Results	36
2.4 Discussion	67
Chapter 3 – Extended Literature and Extended Methodology.....	77
3.1 Extended Literature Review.....	77
3.1.1 Brain Anatomy & Functional Lobes.....	77
3.1.2 Neuron & Nerve Impulse.....	79
3.1.3 EEG & Frequency Bands.....	81
3.1.4 Network Connectivity – MSC	83
3.2 Extended Methodology	84

3.2.1	Artifact Removal.....	84
3.2.2	EEG Cluster by Functional Lobes	87
3.2.3	Magnitude Square Coherence (MSC).....	89
3.2.4	Statistical Tests	93
Appendix A – Figures.....		95
Appendix B – Codes.....		116
	Function: RemoveStrongArtifact(.....)	116
	Function: STFTCoherence(.....)	117
	Function: MSC(.....)	118
	Function: FrequencyBandExtractMSC(.....)	119
	Function: swtest(.....)	119
	Main Script: YA_MSC_Analysis.m.....	123
	Main Script: YA_StatisticalAnalysis.m.....	131
Bibliography.....		135

List of Tables

Table 1. List of sequential testing conditions for each data collection session.....	29
Table 2. Topographic distribution of electrodes per brain region.....	31-32
Table 3. Frequency bands of interest and corresponding frequency ranges extracted for each band.....	34
Table 4. Summary of the MSC for all 7 participants in 2 test conditions (NI1 – 5-min before the Trainer and NI2 – 5-min after the Trainer) and the resulting difference in MSC (Δ MSC) across various brain regions in Delta frequency (1 – 4 Hz).....	37
Table 5. Paired t-test summary statistics on the change in MSC (Δ MSC) between NI1 and NI2 on the study sample size of seven typical developing young adults (n = 7) in Delta frequency (1 – 4 Hz)	39
Table 6. Summary of the MSC for all 7 participants in 2 test conditions (NI1 – 5-min before the Trainer and NI2 – 5-min after the Trainer) and the resulting difference in MSC (Δ MSC) across various brain regions in Theta frequency (5-7 Hz).....	42
Table 7. Paired t-test summary statistics on the change in MSC (Δ MSC) between NI1 and NI2 on the study sample size of seven typical developing young adults (n = 7) in Theta frequency (5 – 7 Hz)	44
Table 8. Summary of the MSC for all 7 participants in 2 test conditions (NI1 – 5-min before the Trainer and NI2 – 5-min after the Trainer) and the resulting difference in MSC (Δ MSC) across various brain regions in Alpha frequency (8 -13 Hz).....	47
Table 9. Paired t-test summary statistics on the change in MSC (Δ MSC) between NI1 and NI2 on the study sample size of seven typical developing young adults (n = 7) in Alpha frequency (8 – 13 Hz)	48
Table 10. Summary of the MSC for all 7 participants in 2 test conditions (NI1 – 5-min before the Trainer and NI2 – 5-min after the Trainer) and the resulting difference in MSC (Δ MSC) across various brain regions in Beta frequency (14-30 Hz).....	51
Table 11. Paired t-test summary statistics on the change in MSC (Δ MSC) between NI1 and NI2 on the study sample size of seven typical developing young adults (n = 7) in Beta frequency (14 – 30 Hz)	53
Table 12. Summary of the MSC for all 7 participants in 2 test conditions (NI1 – 5-min before the Trainer and NI2 – 5-min after the Trainer) and the resulting difference in MSC (Δ MSC) across various brain regions in Gamma frequency (31 -100 Hz)	56

Table 13. Paired t-test summary statistics on the change in MSC (Δ MSC) between NI1 and NI2 on the study sample size of seven typical developing young adults (n = 7) in Gamma frequency (31 – 100 Hz)	58
Table 14. Summary of the paired t-test on the changes in EEG inter-regional coherence between various regions in the brain with statistical significance ($p \leq 0.05$) on seven healthy young adults after operating the Trainer in five frequency bands of interest	60
Table 15. Wilk-Shapiro test of normality on the changes in EEG inter-regional coherence between various regions in the brain of seven healthy young adults after using the Trainer in five frequency bands of interest.....	61
Table 16. Overlaid results from the Wilk-Shapiro test of normality and the paired t-test on the changes in EEG inter-regional coherence between various regions in the brain of seven healthy young adults after the Trainer in five different frequency ranges	62
Table 17-1. Statistical p-values of the left-tailed Wilcoxon signed rank test on the changes in EEG inter-regional coherence in TD young adults after the Trainer in five frequency bands of interest	63
Table 17-2. Summary of the Wilcoxon-signed rank test with statistical significance ($p \leq 0.05$) on the changes in EEG inter-regional coherence in TD young adults after the Trainer in five frequency bands of interest	64
Table 18. Summary of all statistical tests used in the study with significant p-values ($p \leq 0.05$) on the changes in EEG inter-regional coherence in TD young adults after the Trainer in five frequency bands of interest	65
Table 19. Brain functional lobes and their corresponding functions.....	78

List of Figures

Figure 2-1. <i>eego</i> TM sports 64 pro ES-233 system.....	25
Figure 2-2. Graphic User Interface of the <i>eego</i> TM software.....	26-27
Figure 2-3 A) 64-channel Ag/AgCl surface electrodes EEG <i>waveguard</i> TM cap by ANT Neuro...26	
Figure 2-3 B) Position of the participant in a manual wheelchair on the Trainer during EEG data collection.....	27
Figure 2-4. The 10/20 system ANT Neuro 65-channel <i>waveguard</i> TM <i>original</i> electrode placement.....	30
Figure 2-5. Block diagram describes data processing and analysis of the study on EEG data recorded from No Interaction 1 (NI 1) and No Interaction 2 (NI 2) phase on each subject.....	34

Figure 2-6. An example of the overall time-frequency MSC before frequency band extraction A) MSC between the Frontal and Central region from No Interaction 1 (NI1) session on one young adult (YA), B) MSC between the Frontal and Central region from No Interaction 2 (NI2) on the same YA.....	36
Figure 2-7. Change in EEG coherence across different brain region combinations on 7 TD young adults after interaction with the Power Wheelchair Trainer in Delta (1- 4 Hz) frequency band. A “*” indicates brain regions in which the decrease in EEG coherence after the Trainer was found with significant p-values ($p \leq 0.05$).....	40
Figure 2-8. Change in EEG coherence across different brain region combinations on 7 TD young adults after interaction with Power Wheelchair Trainer in Theta (5-7 Hz) frequency band. A “*” indicates brain regions in which the decrease in EEG coherence after the Trainer was found with significant p-values ($p \leq 0.05$).....	45
Figure 2-9. Change in EEG coherence across different brain region combinations on 7 TD young adults after interaction with Power Wheelchair Trainer in Alpha frequency (8-13 Hz). A “*” indicates brain regions in which the decrease in EEG coherence after the Trainer was found with significant p-values ($p \leq 0.05$).....	50
Figure 2-10. Change in EEG coherence across different brain region combinations on 7 TD young adults after interaction with the Power Wheelchair Trainer in Beta (14-30 Hz) frequency band. A “*” indicates brain regions in which the decrease in EEG coherence after the Trainer was found with significant p-values ($p \leq 0.05$).....	54
Figure 2-11. Change in EEG coherence across different brain region combinations on 7 TD young adults after interaction with the Power Wheelchair Trainer in Gamma (31-100 Hz) frequency. A “*” indicates brain regions in which the decrease in EEG coherence was found with significant p-values ($p \leq 0.05$).....	59
Figure 3-1. Brain anatomy and major parts.....	77
Figure 3-2. EEG signals in five frequency bands.....	82
Figure 3-3. Block diagram describes data processing of the study on EEG data recorded from No Interaction 1 (NI 1) and No Interaction 2 (NI 2) phase on each subject.....	87
Figure 3-4. The 10/20 system ANT Neuro 65-channel <i>waveguardTM</i> original electrode placement scheme.....	88
Figure 3-5. The Empirical Rule (68-95-99.7%)	93
Figure A-1. Magnitude Square Coherence from NI1 – 5-min rest yet awake before the Trainer between various brain region combinations in subject 1 (YA004)	95

Figure A-2. Magnitude Square Coherence from NI2 – 5-min rest yet awake after the Trainer between various brain region combinations in subject 1 (YA004)	96
Figure A-3. Magnitude Square Coherence from NI1 – 5-min rest yet awake before the Trainer between various brain region combinations in subject 2 (YA005)	98
Figure A-4. Magnitude Square Coherence from NI2 – 5-min rest yet awake after the Trainer between various brain region combinations in subject 2 (YA005)	99
Figure A-5. Magnitude Square Coherence from NI1 – 5-min rest yet awake before the Trainer between various brain region combinations in subject 3 (YA006)	101
Figure A-6. Magnitude Square Coherence from NI2 – 5-min rest yet awake after the Trainer between various brain region combinations in subject 3 (YA006)	102
Figure A-7. Magnitude Square Coherence from NI1 – 5-min rest yet awake before the Trainer between various brain region combinations in subject 4 (YA007)	104
Figure A-8. Magnitude Square Coherence from NI2 – 5-min rest yet awake after the Trainer between various brain region combinations in subject 4 (YA007)	105
Figure A-9. Magnitude Square Coherence from NI1 – 5-min rest yet awake before the Trainer between various brain region combinations in subject 5 (YA008)	107
Figure A-10. Magnitude Square Coherence from NI2 – 5-min rest yet awake after the Trainer between various brain region combinations in subject 5 (YA008)	108
Figure A-11. Magnitude Square Coherence from NI1 – 5-min rest yet awake before the Trainer between various brain region combinations in subject 6 (YA009)	110
Figure A-12. Magnitude Square Coherence from NI2 – 5-min rest yet awake after the Trainer between various brain region combinations in subject 6 (YA009)	111
Figure A-13. Magnitude Square Coherence from NI1 – 5-min rest yet awake before the Trainer between various brain region combinations in subject 7 (YA010)	113
Figure A-14. Magnitude Square Coherence from NI2 – 5-min rest yet awake after the Trainer between various brain region combinations in subject 7 (YA010)	114

Chapter 1 – Introduction

1.1 Introduction

In typical developing children, the ability to move around and explore their surrounding environment is an integral component of growth and development. Literature has shown that these self-initiated mobilities play a critical role in the development of cognitive functions, motor skills, language, and visual perception during early childhood.¹⁻² However, children with multiple, severe physical disabilities exhibit very limited level of self-initiated locomotion thus, are at risk of having cognitive limitations during developmental stages. Thereby, having access to a power mobility device that could remedy the limitation in their locomotion and increase their independence is critical for these children to ensure a typical overall development in both mental health and quality of life. Due to limited number of studies have been done on the cognitive benefit of providing power mobility training for children with multiple, severe physical disabilities and the fact that most findings are based on subjective measures such as observational studies and parental reports, since 2015, the Department of Physical Therapy (Dr. Lisa Kenyon), the Department of Psychology (Dr. Naomi Aldrich), the School of Engineering (Dr. John Farris and Dr. Samhita Rhodes), and the Statistics Department (Dr. Paul Stephenson) of Grand Valley State University (GVSU) have worked collaboratively in a diligent effort to objectively quantify the effect of power mobility to improve the mobility, independence, quality of life, and general well-being of children with multiple, severe physical disabilities.³⁻⁶ In the attempt to provide these children with the opportunity to explore their surroundings with higher level of independence, the group designed and built a Power Wheelchair Trainer (the Trainer), which is a motorized platform on which any manual wheelchair can be mounted on easily so that individuals can practice using power mobility and explore their environment under safe and

controlled conditions.^{5,6} Thereafter, the group has been diligently working and conducting studies that utilize changes in the electroencephalogram (EEG) as an objective measure of improvements in cognitive function of children with multiple, severe disabilities with power mobility training.³⁻⁶ Those studies include the first exploratory study regarding the power spectral analysis of EEG data from a child with severe disabilities in alpha and theta power³ and a subsequent pilot study that investigated changes seen in the EEG power spectrum, coherence, and information theoretic within the brain of three children with severe disabilities after undergoing power mobility training.⁴

This thesis is an expansion of the work performed in two previous studies conducted by the group at GVSU.^{3,4} This current project sought to further extend our understanding of the cognitive impact of power mobility training on a different population: healthy young adults aged 18 to 24 – a well-studied neurotypical control population. The objective measure herein is changes in neural network connectivity between various brain regions of typical developing young adults in five different brainwave frequencies in response to the Trainer.

Neural network connectivity can be measured by a variety of signal processing techniques such as cross-power correlation and mutual information, among others. One such index is magnitude-square coherence (MSC) – a function of frequency with values ranging between 0 and 1 that indicate how well two signals in time domain correspond to each other at each frequency. In neuroscience, MSC has been used as a measure of synchronous co-activation between different EEG electrode channels to indicate functional connectivity between different areas of the brain⁷. High MSC indicates strong phase coupling or linear dependency between co-activated areas of

the brain during various cognitive activities. A change in coherence could show the changing relationship between the spectra of different EEG channels that may indicate communication between different areas of the brain. This study explored the differences in functional network connectivity of healthy young adults within the 18 to 24-year-old age range before and immediately after operating the Trainer by evaluating changes in EEG coherence between various functional regions in the brain and their behaviors in five different brainwave frequencies, including delta (1-4 Hz), theta (5-7 Hz), alpha (8-13 Hz), beta (14-30 Hz), and gamma (31-100 Hz) frequency.

1.2 Purpose

In children with multiple, severe disabilities, power mobility use has shown to increase number of subsequent self-initiated movements and positive peer initiations.⁸ While systematic analysis of the EEG spectral content of a single-subject study showed promising positive changes of power mobility training on one child with multiple, severe disabilities and the relationship of these changes to neural connectivity were further explored on more children with severe disabilities, there was no control group for comparison to be made regarding quantifiable changes observed in the brain due to power mobility training. Thus, the results of this study on the healthy young adult population may provide additional insights to the process of understanding and evaluating the cognitive impact of power mobility training on various population. The goal of the study is to further extend our understanding on the impact of power mobility training and perhaps to provide future studies with an additional objective method to quantify cognitive changes and improvements that the power mobility training invokes. Additionally, while conducting the study, we realized that there were very few papers concerned with EEG coherence in healthy young adults – a neurotypical control group that is presumably

thought to be a well-studied population, thus this study may help elucidate both region-specific and integrative perspectives on EEG coherence from various brain regions and their behaviors at different frequencies on typical developing young adults aged 18 to 24.

1.3 Scope

Coherence is a metric that examines the linear phase relationship between two signals in a frequency band.⁹ In short, it is a measure of synchronization between two EEG channels and an index of brain connectivity that shows how effectively two EEG sites between the brain regions accessed by chosen electrodes link and share information. High coherence represents a measure of strong connectivity while low coherence indicates a measure of weak connectivity. High coherence between two EEG signals has been interpreted as reflecting a strong structural or functional connection between the underlying cortical regions.¹⁰ A change in coherence shows the changing relationship in the spectra of different channels that may show the changes in communication between various areas of the brain. This study aims to investigate changes in the EEG coherence and how information is communicated within the brain of healthy young adults within the 18 to 24-year-old age range after undergoing power mobility training in five common brainwave frequencies, including delta (1-4 Hz) frequency, theta (5-7 Hz) frequency, alpha (8-13 Hz) frequency, beta (14-30 Hz) frequency, and gamma (31-100 Hz) frequency. Another aim of the study is to examine changes in EEG coherence between different functional lobes in the brain of typical developing young adults in response to the power mobility training. This study utilized a different EEG acquisition system from two previous studies thus, a new customized MATLAB program for EEG signal processing and coherence analysis was developed. Findings from the study may illuminate the impact of power mobility training on neural network connectivity in the brain of healthy young adults.

1.4 Assumptions

For this study, it is assumed that each subject's EEG is continuous, independent, and separate, non-connected from other subject's EEG. This independency assumption is important for the comparison among different subjects. It is also assumed that EEG data recorded in this study exhibits non-Gaussian and non-stationary characteristics. As different areas in the brain become active as the result of learning and using the Trainer, the resulting EEG changes over time thus explains the non-stationary characteristic. The changes in EEG magnitude over time tend to result in non-Gaussian behavior. All seven study participants were assumed to have no prior exposure to Power Wheelchair Trainer until on-site participation to the study to reduce any potential confounding factors in the study. The study follows a simple random sample study, which is composed of seven participants from the targeted population of healthy young adults aged between 18 and 24 years old. Each individual in the targeted population has an equal probability of being selected in the sample. This assumption is important for the paired t-test.

1.5 Hypothesis

Based on the results from two previous studies conducted by the GVSU research group, power mobility training seems to invoke a positive, short-term impact on cognitive performance of children with severe disabilities.^{3,4} Therefore, it is hypothesized that power mobility training would also have similar short-term cognitive impact on healthy young adults and the cognitive impact due to power mobility training, will result in a change in EEG coherence and communication between different areas in the brain of typical developing young adults.

Additionally, since different brainwave frequencies are associated with different cognitive functions and tasks, we hypothesize that different frequencies will invoke different regions in the

brain, which in turn will also result in a change in EEG coherence between different areas in the brain in response to the task of operating the Trainer. Changes in EEG coherence will be best reflected by evaluating the MSC derived from scalp EEG recorded before and immediately after using the Trainer.

Chapter 2 – Manuscript

Abstract

The ability to move and explore their surrounding environment plays a critical role in the development of cognitive function in children, especially during early childhood. The lack of independent and autonomous mobility is, therefore, a clear disadvantage for the overall development of children with multiple, severe disabilities. Limited number of studies have been conducted on the impact of power mobility device on this specific population. Previous exploratory and pilot studies showed promising results regarding quantifiable and consistent changes in the electroencephalogram (EEG) of children with multiple, severe disabilities when provided with power mobility training. This study aimed to further extend our understanding of the cognitive impact of power mobility training on a different population: healthy young adults aged 18 to 24 – a well-studied neurotypical control population. The study used Magnitude-Square Coherence (MSC) derived from the electroencephalogram (EEG) recorded at resting-yet-awake state before and after power mobility training to investigate changes in the functional connectivity in the brain of seven healthy young adults in the 18-to-24-year-old age range. Neural processes invoked between different functional lobes in the brain in: delta (1-4 Hz), theta (5-7 Hz), alpha (8-13 Hz), beta (14-30 Hz), and gamma (31-100 Hz) in response to power mobility training were examined and analyzed. Statistical analyses were then performed on the change, or difference in EEG coherence between the 5-minute rest with eyes closed before and after power mobility training. Results from both the paired t-test and the Wilcoxon-signed rank test with an alpha level of 0.05 ($p \leq 0.05$) on the change in EEG coherence after the Trainer showed an overall decrease in EEG coherence between the parietal and temporal regions on healthy young adults after using the Trainer in all five frequency bands. Reduced interregional

EEG coherence was found in the centro-parietal region for both the delta and beta frequency. Lower EEG coherence was also noted between the frontal and temporal regions in alpha frequency. These findings help edify that power mobility training is responsible for objectively quantifiable changes in neural network connectivity that may be correlated with improvement in subjective measures of cognitive gains on children with multiple, severe disabilities.

Keywords: EEG coherence, brain functional lobes, brainwave frequencies, delta, theta, alpha, beta, gamma, power mobility training, young adults

2.1 Introduction

The human brain is a vast network of connected pathways that communicate through synchronized electric brain activity along fiber tracts. The human brain is made of approximately 100 billion nerve cells called neurons.¹¹ Slow changes in the membrane potentials of these cortical neurons, especially the excitatory and inhibitory postsynaptic potentials can get detected by recording the electrical activity called Electroencephalogram, or EEG. The EEG recording captures the algebraic sum of the electrical potential charges contributed by each neuron. Thus, in time domain, the larger amplitude waves of EEG signal indicate the greater synchronous activity of these neurons. Since the EEG waveform contains component waves of different frequencies that can be extracted to provide information about different brain activities, it is also valuable to examine EEG signals in the frequency domain.

Five common frequency bands in the EEG brain waves are: delta (1-4 Hz), theta (4-8Hz), alpha (8-13Hz), beta (13-30Hz), and gamma (31-100 Hz). The frequencies of the brain can be noted in order of low to high by the order delta, theta, alpha, beta, and gamma. Different frequencies are

associated with different types of brain activity. In general, the more active the brain, the higher the frequency and the lower the amplitude of the EEG. Lower frequencies indicate the less responsive states, whereas higher frequencies indicate increased alertness, concentration, and perception. Delta waves - the slowest frequency in the five frequency bands, are composed of frequency ranging from 1 to 4 Hz and are present most frequently in young children and babies¹². In adults, delta waves are most prominent during deep sleep. These waves are also interconnected with proper digestion, regular heartbeat, and proper blood pressure. Theta waves with frequency in the range of 4 to 7 Hz, are the next slowest wave frequency and are associated with emotional connections, relaxation natural intuition, meditation, and creativity.^{12-15,21} Similar to the delta waves, it plays a role in restorative sleep, but not as deeply. Alpha waves include frequencies between 8 and 13 Hz and is found prominent in both the occipital and frontal cortex of the brain when the eyes are closed, and the participant is relaxed.^{4,12} Alpha rhythm is abolished by opening the eyes or mental effort that indicates the degree of cortical activation. The greater the activation, the lower the alpha activity. Meanwhile, beta waves - frequencies between 13 and 30 Hz - are present in alert participants with their eyes open. Beta waves are often associated with a strengthening of sensory feedback in static motor control and active concentration.¹⁶ Beta activity is increased with voluntarily suppressed movements.¹⁷ Lastly, gamma waves – frequency between 31 and 100 Hz – are believed to associate with mental activities that require a high level of concentration, perception, and consciousness.^{3,4}

Brain connectivity describes the networks of functional and anatomical connections across the brain. A large number of neuroimaging brain studies in the past have found that there are specific regions in the brain that are specialized for processing certain types of information. Thus,

functional connectivity between different regions of the brain in the resting state has been a topic of interest in neurophysiological research. Functional connectivity can be measured, using signal processing techniques, to determine the correlation between signals from different areas of the brain. One such technique is magnitude-square coherence (MSC) – a function of frequency with values ranging between 0 and 1 that indicate how two signals in time domain are linearly related. If the phase – rising and falling – of the two signals are more similar over time, then it suggests high functional connectivity and those two areas of the brain are working together. In neuroscience, MSC, or as often referred to as EEG coherence, has been used as a measure of synchronous co-activation between different EEG electrode channels to indicate functional connectivity between different areas of the brain that cannot be detected by simply measuring EEG amplitude or power spectra.⁷ High MSC indicates strong connectivity and linear dependency between co-activated areas of the brain during various cognitive activities while low coherence indicates a measure of weak connectivity. As a measure of synchronization between two EEG signals, EEG coherence has been widely used as an index of brain connectivity that shows how effectively two EEG sites between the brain regions accessed by chosen electrodes link and share information. High coherence between two EEG signals has been interpreted as reflecting a strong structural or functional connection between the underlying cortical regions.¹⁰

In typical developing children, the ability to move around and explore their surrounding environment is an integral component of growth and development. Literature has shown that these self-initiated mobilities play a critical role in the development of cognitive functions, motor skills, language, and visual perception during early childhood.^{1,2} However, children with multiple, severe physical disabilities exhibit very limited level of self-initiated locomotion thus,

are at risk of having cognitive limitations during developmental stages. Thereby, having access to a power mobility device that could remedy the limitation in their locomotion and increase their independence is critical for these children to ensure a normal overall development in both mental health and quality of life. Due to a limited number of studies have been done on the cognitive benefit of providing power mobility training for children with severe physical disabilities, and the fact that most findings are based on subjective measures such as observational studies and parental reports, since 2015, the Department of Physical Therapy (Dr. Lisa Kenyon), the Department of Psychology (Dr. Naomi Aldrich), the School of Engineering (Dr. John Farris and Dr. Samhita Rhodes), and the Statistics Department (Dr. Paul Stephenson) of Grand Valley State University (GVSU) have worked collaboratively in a diligent effort to objectively quantify the effect of power mobility to improve the mobility, independence, quality of life, and general well-being of children with multiple, severe physical disabilities.³⁻⁶ In the attempt to provide these children with the opportunity to explore their surroundings with a higher level of independence, the group designed and built a Power Wheelchair Trainer (the Trainer) which is a motorized platform on which any manual wheelchair can be mounted on easily so that individuals can practice using power mobility and explore their environment under safe and controlled conditions.^{5,6} Thereafter, the group has been diligently working and conducting studies that use changes in the electroencephalogram (EEG) as an objective measure of improvements in the cognitive function of children with severe disabilities with power mobility training.³⁻⁶ Those studies include the first exploratory study regarding the power spectral analysis of EEG data from a child with severe disabilities in alpha and theta power³ and a subsequent pilot study that investigated changes seen in the EEG power spectrum, coherence, and

information-theoretic within the brain of three children with severe disabilities after undergoing power mobility training.⁴

The current study is an expansion of the work performed in two previous studies conducted by the group at GVSU.^{3,4} This study sought to explore and investigate changes in the functional neural network connectivity of healthy young adults within the 18 to 24-year-old age range before and immediately after using the Trainer. The project uses a measure named Magnitude-Square Coherence (MSC) derived from scalp EEG as a means to examine neural processes invoked between various functional regions in the brain and their behaviors in five different brainwave frequencies, including delta (1-4 Hz), theta (5-7 Hz), alpha (8-13 Hz), beta (14-30 Hz), and gamma (31-100 Hz) frequency in response to the task of operating and controlling the Trainer. The goal is to further extend our understanding of the cognitive impact of power mobility training on a neurotypical population. While this is a well-studied population, coherence between EEG signals has not been explored extensively thus, our study may provide a valuable baseline for comparison. Additionally, the results of this study may help elucidate both region-specific and integrative perspectives on EEG coherence from various brain regions and their behaviors at different frequencies on typical developing young adults aged 18 to 24.

2.2 Methods

2.2.1 Data Collection

2.2.1.1 Human Subjects

This study was approved, authorized, and regulated by the Institutional Review Board (IRB) at Grand Valley State University (GVSU). EEG data was collected on seven healthy young adults

within the 18-to-24-year-old age range. The sample population for the study included both male and female participants. All participants were physically capable to use a traditional joystick as determined by the licensed physical therapist who led and provided oversight throughout the course of each data collection session. All seven participants met the age range requirement and were in good health with no known underlying health condition, or any other illnesses that would prohibit safe use of a power mobility device or use of the Trainer at the time of the experiment. None of the participants had diagnosis of developmental disability such as cerebral palsy, spina bifida, and autistic spectrum disorder. No history of diagnosed neurological disorders such as epilepsy, head injuries, stroke, or diabetes – a health condition in which extremes in blood sugar can potentially impact the individual’s EEGs was noted on any participant. Additionally, all participants were not under the use of medications that may impact the central nervous system such as anti-depressants or anti-convulsants. Prior to participating in the study, each participant was given a detailed explanation about the nature of the study, protocol, and test conditions. Informed consent was obtained from all participants before the start of data collection. Each data gathering session was conducted under strict supervision of a licensed physical therapist. At any point in the study, if the physical therapist determined that the participant was unable to operate the Trainer safely, the data acquisition would end, and the participant would be withdrawn from the study.

2.2.1.2 *Equipment Apparatus*

2.2.1.2.1 Hardware

The study used the eego™ sports 64 pro ES-233 (Advanced Neuro Technologies B.V., Enschede, Netherlands) for EEG data collection. The eego™ sports 64 pro ES-233 features a comprehensive EEG data acquisition system including both hardware and software, as well as

other system variants and components. The system is composed of an eegoTM amplifier, one 64-channel waveguardTM cap, an 8-inch Windows 8 tablet, an EEG starter kit, Trigger adapter DB25, Trigger adapter BNC, Sensebox, auxiliary kit, and one license of the ASA software, which is an advance EEG/ERP analysis software. Figure 2-1 illustrates the eegoTM sports 64 pro ES-233 system used to collect EEG data for the study.



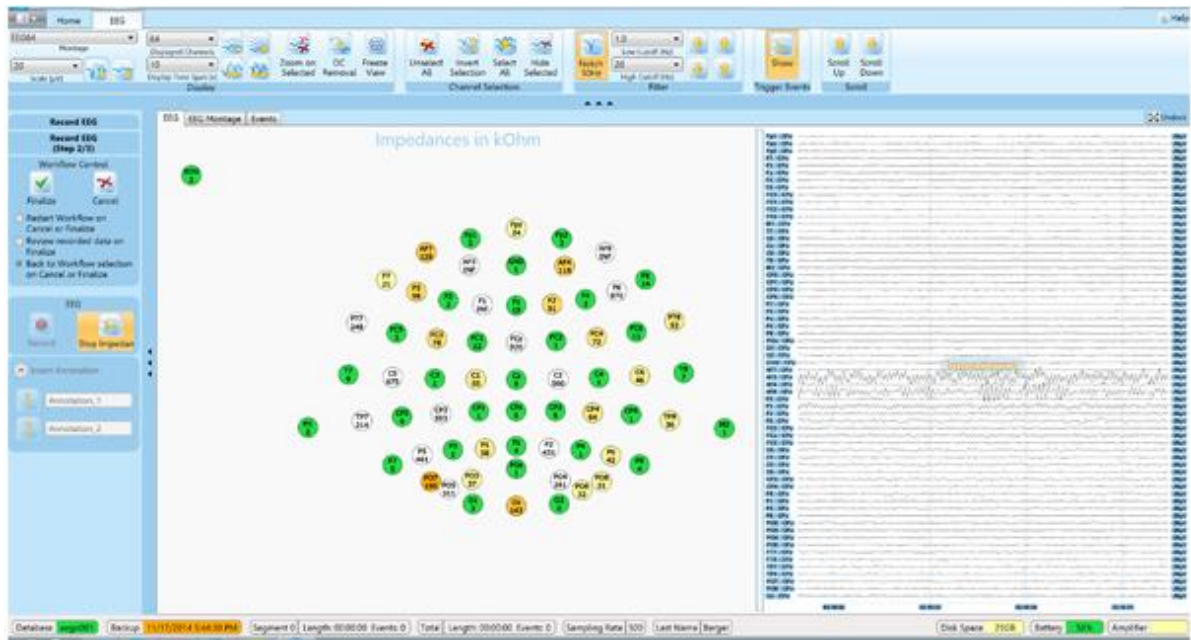
Figure 2-1. eegoTM sports 64 pro ES-233 system (Image retrieved from ANT Neuro website)

The amplifier offers a 64-referential channel and 24-bipolar channels, a 24-bit resolution, noise less than 1.0 uV root mean square (RMS), an input impedance greater than 1 giga-ohm (GOhm), a common mode rejection ratio (CMRR) greater than 100 dB, a 8-bit TTL trigger input, and a maximum sampling rate at 2048 Hz.

2.2.1.2.2 Software

The eegoTM sports 64 pro ES-233 comes with a proprietary real-time EEG recording and review software named *eegoTM* software (Advanced Neuro Technologies B.V., Enschede, Netherlands). The *eegoTM* software allows users to set up EEG recordings, manages new and existing subject entries, and reviews EEG data in real time. EEG recordings are stored in an MS-SQL server database and can be accessed and archived through standardized interfaces. The amplifier connection and status are detected automatically. The software also features a real-time

topographic map of 64-electrodes across the brain with different color codes indicating the connection between the surface electrode and the contacting point on the participant's scalp. Green color denotes good contact and the signal strength that warrant a high fidelity recording of EEG signal at the corresponding surface electrode while yellow indicates the acceptable level of connection that requires slight adjustment if better connection is desired. Figure 2-2 shows a screenshot of the *eego*TM software interface.



A)

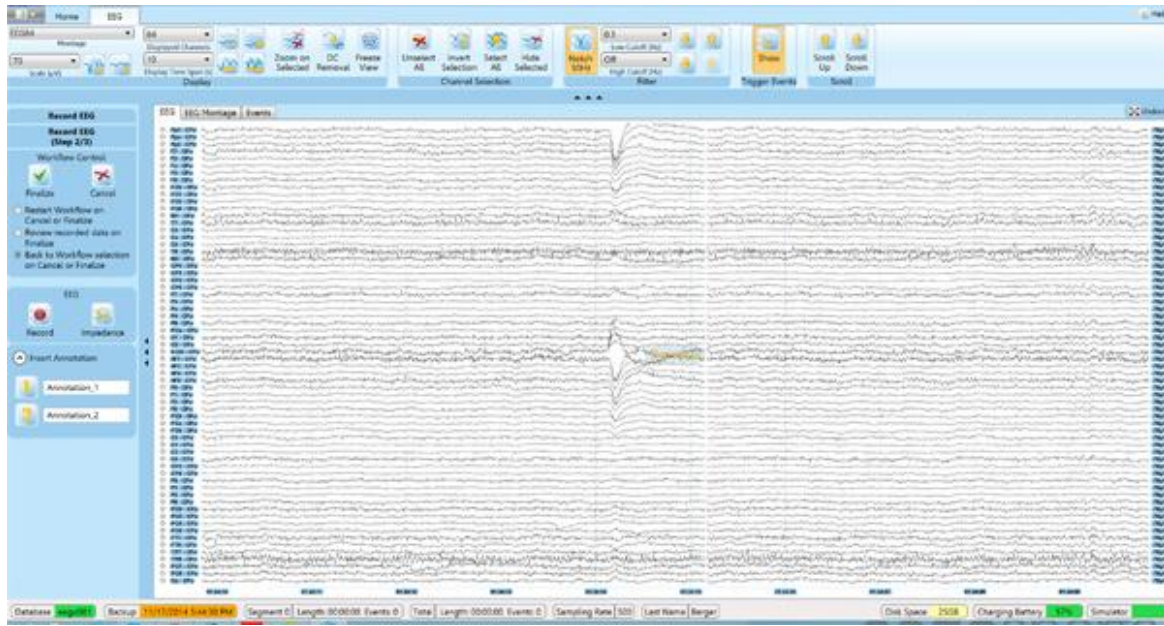


Figure 2-2. A-B) Graphic User Interface of the *eego*TM software (Image courtesy from ANT Neuro)

2.2.1.2.3 Power Wheelchair Trainer

In the attempt to accommodate all different types of custom-made manual wheelchairs that each child with multiple, severe disabilities uses for their special conditions and needs, the School of Engineering and the Department of Physical Therapy at GVSU designed and built a power mobility device named Power Wheelchair Trainer (the Trainer). The Trainer is a motorized platform on which any manual wheelchair can be mounted easily so that individuals can practice using power mobility and explore their environment using a joystick. The Trainer has two joysticks with one given to the individual to control and operate the Trainer and the other shared control joystick is given to the physical therapist leading the power mobility training session to intervene, correct, and override movement of the Trainer if necessary, for the operator's safety.

2.2.1.3 Procedure & Test Conditions

EEG signals were acquired at a sampling frequency of 2048 Hz. The 64-channel sintered Ag/AgCl electrode commercial wet cap (Waveguard™ original, Advanced Neuro Technologies B.V., Enschede, Netherlands) that features an equidistant electrodes layout for the 10/20 international system of electrode placement, was placed on the participant's head. A semi-viscous conductive gel was then applied to each electrode, or EEG channel to ensure good electrical connection between the surface electrode and the contacting point on the scalp of the young adult for high fidelity EEG recording. An additional pair of surface electrodes was placed above the eyebrow and under the eye of the participant for the purpose of eliminating the electrooculogram (EOG). A manual wheelchair was placed on the Trainer and secured using the tie down straps. The participant was asked to step onto the Trainer and sat inside the manual wheelchair. A seat belt was used to secure the participant to the manual wheelchair. Both placement of the EEG electrodes and positioning of the participant in a manual wheelchair on the Trainer are illustrated in Figure 2-3 below.

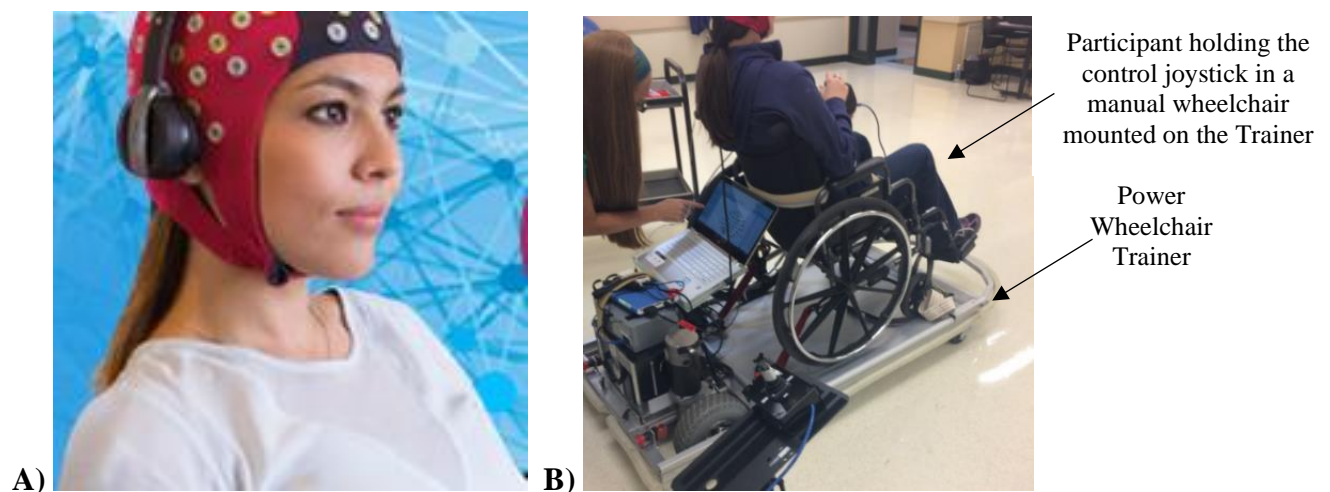


Figure 2-3. **A)** 64-channel Ag/AgCl surface electrodes EEG waveguard™ cap by ANT Neuro (Image courtesy from ANT Neuro); **B)** Position of the participant in a manual wheelchair on the Trainer during EEG data collection.

Once all contacts between every surface EEG channel and their points of contact on the participant’s scalp were inspected to be in good connection using the *eego*TM software (Figure 2-2), EEG data acquisition commenced when the participant was instructed to relax and sit comfortably with eyes closed for five minutes. EEG data collected during this 5-minute condition prior to the use and operation of the Trainer is called No Interaction 1 (NI1). Next, the participant was given brief verbal instructions on how to operate the Trainer before proceeding with active usage of the Trainer at their discretion for a total of 20 minutes. This phase was named Power Wheelchair Trainer. After 20 minutes of interaction with the Trainer, the onset of No Interaction 2 (NI2) phase began when the participant sat comfortably in resting condition with eyes closed for an additional five minutes. EEG data for each session was recorded separately and saved into a specified folder corresponding to each participant labeled Young Adult # (YA #) and the abbreviated naming convention NI1, Trainer, and NI2 accordingly. Table 1 summarizes three testing conditions for each data collection session conducted on every participant.

Table 1. List of sequential testing conditions for each data collection session

Conditions	Description
No Interaction 1 (NI1)	5 minutes of sitting and relaxing in a manual wheelchair mounted on the Trainer with eyes closed <i>prior to</i> the interaction phase
Power Wheelchair Trainer (Trainer)	20 minutes of sitting in a manual wheelchair mounted on the Trainer and actively use the Trainer (high level of interaction)
No Interaction 2 (NI2)	5 minutes of sitting and relaxing in a manual wheelchair mounted on the Trainer with eyes closed <i>after</i> the interaction phase

At the end of the experiment, the EEG cap was removed, and the participant was released from both the manual wheelchair and the Trainer. The procedure was then repeated following the same protocol on a different participant. The study conducted EEG data collection on seven healthy young adults in the 18 to 24-year-old range.

2.2.2 EEG Data Processing

Preprocessing, processing of raw EEG data, coherence analysis, and statistical analysis of the study was developed in MATLAB[®] (The Mathworks Inc., Natick, MA, USA). Import of raw EEG data collected from either No Interaction 1 (NI1) session or No Interaction 2 (NI2) session of each participant was first loaded into MATLAB using EEGLAB version 14.1.1b (Delorme and Makeig, 2004) – an open-source interactive MATLAB tool box for processing continuous and event-related EEG, and ANTeimport version 1.13 – a specific precompiled MATLAB plugin for EEGLAB to import continuous eeprobe (cnt/avr) data format. Raw EEG data from either NI1 or NI2 session was first preprocessed by removing the electrooculogram (EOG) channel and the 24-bipolar channels using the 10/20 standardized placement of scalp electrodes for EEG recording provided by ANT Neuro for the 64-channel *waveguardTM original* (Figure 2-4).

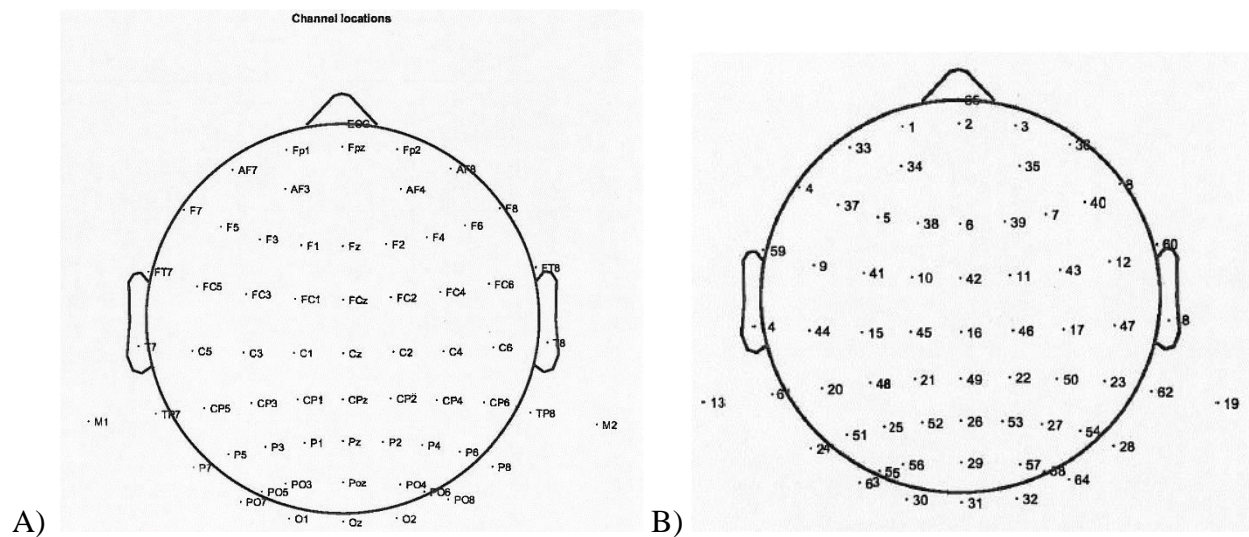


Figure 2-4. The 10/20 system ANT Neuro 65-channel *waveguardTM original* electrode placement

Next, the data was down sampled from the original sampling rate of 2048 Hz to 512 Hz to reduce the data size, save memory and disk storage, as well as to increase the general processing

speed. Reduced-sampling EEG data then went through a series of cascading steps for artifact removals including removal of the DC component i.e. 0 Hz noise and potential linear drifts, elimination of the 60 Hz power line interference with a digital 4th order Butterworth notch filter, re-referencing the data to overall average reference, and removal of the first and last 30 seconds of dataset to eliminate potential noises happened at the beginning and end of each data collection session. Additional noise source was identified and removed using the *runica* function, which is the default independent component analysis (ICA) algorithm in EEGLAB (Delorme and Makeig, 2004) developed based on the Infomax ICA for stable decompositions for multi-channels EEG recordings. Independent component analysis (ICA) attempts to reverse the superposition by separating the EEG into mutually independent scalp maps, or components.²⁰ ICA has proven to be an effective tool for artifact identification and extraction from EEG data.²¹ Independent components containing high amplitude artifacts such as ones stemmed from ocular muscle movements, breathing etc. were subsequently removed, prior to the reconstruction of EEG data. Cleaned artifact-free EEG data then were topographically divided into regional clusters as listed in Table 2 according to the electrode placement and its corresponding brain region as denoted by the letter in each electrode e.g. Frontal pole (Fp), Central (C), Parietal (P), Occipital (O), and Temporal (T) (Figure 2-4). Subsequently, EEG representative for each brain region was then determined by taking the average across all selected EEG channels.

Table 2. Topographic distribution of electrodes per brain region

EEG Clusters per brain region	Electrode placement on the brain	Electrode (Channel) #
Frontal	Fp1, Fpz, Fp2, F7, F3, Fz, F4, F8, FC5, FC1, FC2, FC6, AF7, AF3, AF4, AF8, F5, F1, F2, F6, FC3, FCz, FC4	23 channels – # 1, 2, 3, 4, 5, 6, 7, 8, 9, 10, 11, 12, 33, 34, 35, 36, 37, 38, 39, 40, 41, 42, 43
Central	C3, Cz, C4, C5, C1, C2, C6	7 channels – # 15, 16, 17, 44, 45, 46, 47

Parietal	CP5, CP1, CP2, CP6, P7, P3, Pz, P4, P8, Poz, CP3, CPz, CP4, P5, P1, P2, P6	17 channels – # 20, 21, 22, 23, 24, 25, 26, 27, 28, 29, 48, 49, 50, 51, 52, 53, 54
Parietal-Occipital	PO5, PO3, PO4, PO6, PO7, PO8	6 channels – # 55, 56, 57, 58, 63, 64
Occipital	O1, Oz, O2	3 channels – # 30, 31, 32
Temporal	T7, T8, FT7, FT8, TP7, TP8	6 channels – # 14, 18, 59, 60, 61, 62

2.2.3 Data Analysis

2.2.3.1 Magnitude-Square Coherence (MSC)

The method to derive the time-frequency coherence was implemented in MATLAB following equations presented in the Lovett and Ropella paper²². Magnitude-squared coherence (MSC) is defined as the squared absolute value (i.e., magnitude) of the cross-spectrum divided by the product of the power spectra of X and Y signal in the frequency domain:

$$MSC(f) = \frac{|S_{XY}(f)|^2}{S_{XX}(f) * S_{YY}(f)} \quad (1)$$

Fourier Transform $X_l[k]$ and $Y_l[k]$ of the two temporal signals, $x_l[n]$ and $y_l[n]$ over L overlapping, equal-length segments is the base of the cross-power spectrum. To obtain an unbiased estimation of coherence, ensemble averaging over a window function $w[n]$ can be used. Thereby, the discrete MSC can be described as:

$$MSC = \frac{|\sum_{l=0}^{L-1} X_l[k] Y_l^*[k]|^2}{\sum_{l=0}^{L-1} |X_{l[k]}|^2 \sum_{l=0}^{L-1} |Y_{l[k]}|^2} \quad (2)$$

In which, L is the number of windows used and is given by l and k , the frequency index.

Equation 2 serves as the base for further development of the MSC time-frequency analysis by Lovett and Ropella. The Fourier Transform of each signal is replaced in Equation 2 with the Short-Term Fourier Transform (STFT). The STFT is a time-frequency analog of the Fourier

Transform. A l th order Discrete Prolate Spheroidal Sequences (DPSS) window is then used to obtain the short-term minimum bias eigen transform:

$$X_l[n, k] = \sum_{m=0}^{M-1} x[n + m - \frac{M}{2}] v_l[m] e^{-j2\pi mk/M} \quad (3)$$

with n is the time index, k is the frequency index, M is the window length, and m is a variable of summation. The l^{th} window is given as v_l . Equation 3 is then substituted for the Fourier Transform in Equation 2 to obtain MSC in both the temporal and spectral domain as described in Equation 4.

$$MSC[n, k] = \frac{|\sum_{l=0}^{L-1} X_l[n, k] Y_l^*[n, k]|^2}{\sum_{l=0}^{L-1} |X_l[n, k]|^2 \sum_{l=0}^{L-1} |Y_l[n, k]|^2} \quad (4)$$

Equation 4 was implemented in MATLAB using a window length $M = 1024$, $L = 7$, and $fs = 512$ Hz to obtain the time-frequency coherence between two representative EEG signals from different brain regions e.g. Frontal and Central, Parietal and Occipital, and so forth for each session i.e. No Interaction 1 - NI1 and No Interaction 2 - NI2 on each participant. Six brain regions as identified from the 10/20 system 64-channel *waveguardTM original* (as shown in Table 2) results to a total of fifteen brain region combinations for MSC per session for each participant.

2.2.3.2 MSC in 5 Dominant Frequency bands

Since the study was not only interested in the changes in EEG coherence among different regions in the brain due to the Trainer, but also in EEG coherence characteristics in different frequencies, the MSC for each frequency band of interest including the delta, theta, alpha, beta, and gamma band was extracted from the overall time-frequency MSC collected from each pair of regional EEG. Table 3 presents five frequency bands of focus and the corresponding frequency ranges

used for extracting frequency-band MSC from the overall MSC. Subsequently, MSC representative for each frequency band was calculated by averaging across all frequency sub-bands.

Table 3. Frequency bands of interest and corresponding frequency ranges extracted for each band

Frequency bands	Corresponding frequency range (Hz)
Delta	1 - 4
Theta	5 - 7
Alpha	8 - 13
Beta	14 - 30
Gamma	31 - 100

The complete sequence of EEG data processing, artifact reduction, and coherence analysis of the study was summarized in Figure 2-5 below.

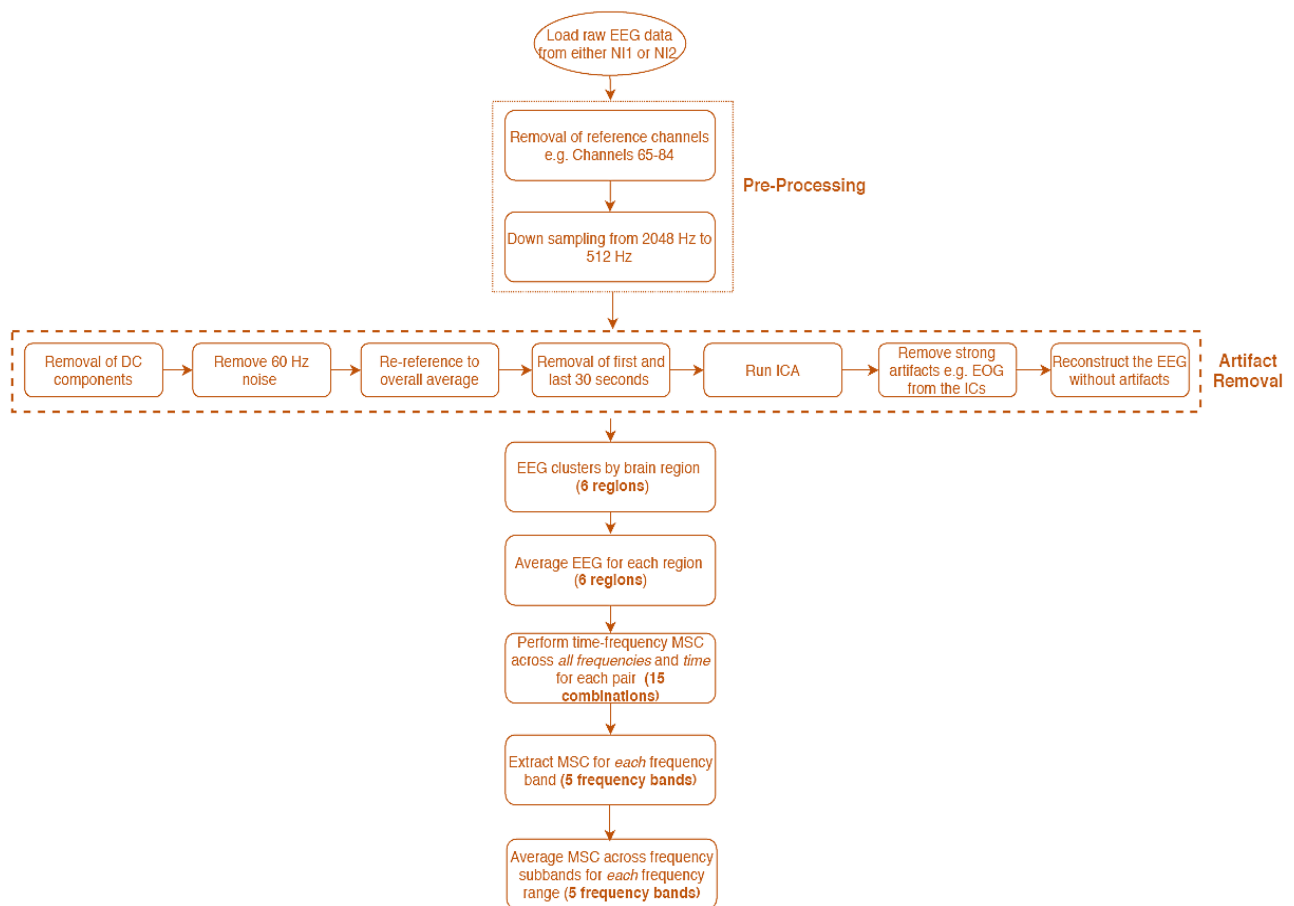


Figure 2-5. Block diagram illustrates data processing of the study on EEG data recorded from No Interaction 1 (NI 1) and No Interaction 2 (NI 2) phase on each participant

2.2.3.3 Statistical Analyses

All statistical analyses of the study were developed in MATLAB[®] (The Mathworks Inc., Natick, MA, USA). Verification of the statistical results obtained in MATLAB and graphic illustrations of the study were performed in Excel 2006. A paired sample t-test accompanied with a 95% confidence interval (CI) for the difference, or change in EEG coherence between the MSC before interacting with the Trainer (No Interaction 1 – NI1) and the MSC after interacting with the Trainer (No Interaction 2 – NI2) on the study sample size of seven participants ($n = 7$, $df = 6$) was used to determine the statistical evidence on the impact of the Trainer on the functional connectivity across different brain regions in five different frequency bands in typical developing (TD) young adults. Change in EEG coherence, or as often abbreviated herein as Δ MSC, is calculated by subtracting the MSC from NI1 session from the MSC from NI2 session for each participant as illustrated in the equation below.

$$\Delta MSC = MSC\ NI2\ (after\ the\ Trainer) - MSC\ NI1\ (before\ the\ Trainer)$$

A negative Δ MSC indicates a decrease in EEG coherence after the Trainer while a positive Δ MSC denotes an increase in EEG coherence after the Trainer. A p-value equal or less than the alpha level of 0.05 ($p \leq 0.05$) was considered statistically significant in rejecting the null hypothesis, which states that there is no change in EEG coherence before the Trainer and after the Trainer. Additionally, the Wilk-Shapiro test on the changes, or differences in EEG coherence was conducted to examine the normality assumption on the data that is fundamental to the validity of the paired t-test. The Wilcoxon signed rank test – a non-parametric equivalence of the paired sample t-test that does not assume normality in the data, was also conducted on Δ MSC to ultimately assess the statistical evidence on the results as compared to the results yielded from the paired t-test.

2.3 Results

Figure 2-6 shows an example of the overall time-frequency MSC between the Frontal and Central (FC) region from No Interaction 1 session (NI1 – 5-minute sitting relaxed with eyes closed before operating the Trainer) and No Interaction 2 session (NI2 – 5-minute sitting relaxed with eyes closed after active usage of the Trainer) in one participant before frequency band extraction.

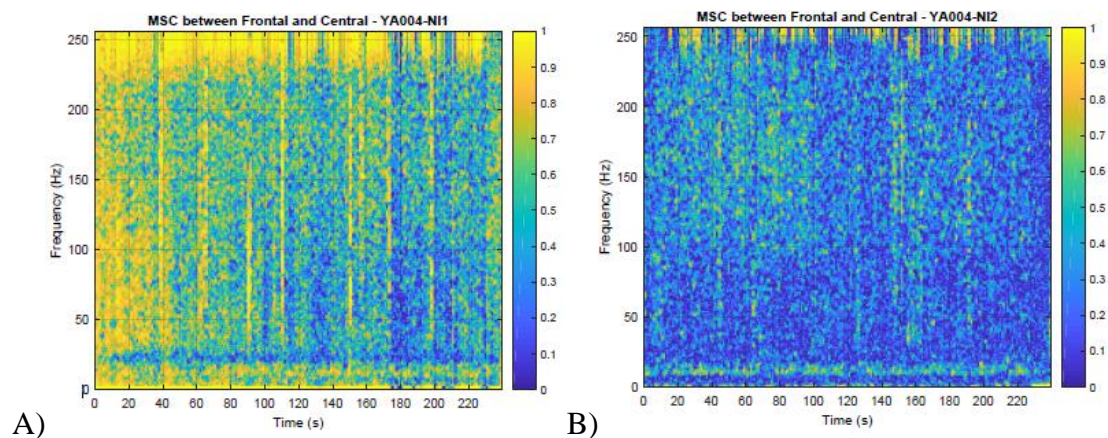


Figure 2-6. An example of overall time-frequency MSC before frequency band extraction **A)** MSC between the Frontal and Central region from No Interaction 1 (NI1) session on one young adult (YA), **B)** MSC between the Frontal and Central region from No Interaction 2 (NI2) on the same YA

Since coherence is a measure of correlation coefficient, MSC values range from 0 to 1 with 1 meaning perfect agreement in phase difference and 0 meaning completely random phase differences. In this context, a MSC of 0 indicates complete independency of the frequency between two EEG signals i.e. there is absolutely no synchronization between the two EEG sites, whereas a coherence of 1 indicates the phase coupling or linear dependency of the frequency between two EEG signals. In Figure 2-6, high coherence is denoted by the yellow color shading and the dark blue shading indicates low level of coherence between two example EEG signals.

1. Delta (1-4 Hz) Frequency

MSC in Delta frequency, which was derived from averaging MSC values from 1 Hz to 4 Hz range, was extracted from the overall time-frequency MSC between each combination of the regional EEG for each session i.e. NI1 or NI2. Average MSC in Delta frequency for both test conditions (NI1 and NI2) and the changes in MSC (Δ MSC) after the Trainer, which was calculated by subtracting the MSC from NI1 from the MSC NI2, across fifteen brain region combinations for all seven healthy young adults participated in the study were calculated and summarized in Table 4.

Table 4. Summary of the MSC for all 7 participants in 2 test conditions (NI1 – 5-min before the Trainer and NI2 – 5-min after the Trainer) and the resulting difference in MSC (Δ MSC) across various brain regions in Delta frequency (1 – 4 Hz)

Young Adult (YA) subject # - Condition	Brain Region														
	FC	FP	FPO	FO	FT	CP	CPO	CO	CT	PPO	PO	PT	POO	POT	OT
YA1 - NI1	0.817	0.913	0.390	0.696	0.788	0.919	0.370	0.554	0.881	0.361	0.585	0.939	0.567	0.381	0.527
YA1 - NI2	0.351	0.398	0.737	0.791	0.477	0.437	0.501	0.461	0.523	0.344	0.375	0.381	0.742	0.615	0.465
YA1 - Δ MSC	-0.466	-0.515	0.348	0.095	-0.311	-0.482	0.131	-0.092	-0.357	-0.017	-0.210	-0.558	0.175	0.233	-0.063
YA2 - NI1	0.981	0.998	0.999	0.992	0.995	0.984	0.984	0.968	0.979	0.998	0.985	0.989	0.992	0.995	0.996
YA2 - NI2	0.453	0.911	0.385	0.517	0.687	0.459	0.280	0.476	0.418	0.359	0.525	0.617	0.424	0.337	0.616
YA2 - Δ MSC	-0.529	-0.087	-0.615	-0.475	-0.308	-0.525	-0.704	-0.492	-0.561	-0.639	-0.460	-0.372	-0.568	-0.657	-0.380
YA3 - NI1	0.464	0.434	0.662	0.440	0.437	0.488	0.511	0.487	0.498	0.546	0.970	0.839	0.552	0.467	0.837
YA3 - NI2	0.421	0.937	0.847	0.485	0.674	0.398	0.525	0.212	0.514	0.789	0.564	0.549	0.352	0.741	0.225
YA3 - Δ MSC	-0.043	0.503	0.185	0.045	0.237	-0.089	0.014	-0.275	0.016	0.243	-0.407	-0.290	-0.200	0.274	-0.611
YA4 - NI1	0.698	0.686	0.675	0.684	0.714	0.789	0.796	0.808	0.939	0.972	0.991	0.839	0.969	0.833	0.855
YA4 - NI2	0.898	0.863	0.865	0.822	0.902	0.870	0.973	0.823	0.935	0.891	0.985	0.927	0.846	0.949	0.883
YA4 - Δ MSC	0.200	0.176	0.189	0.138	0.187	0.081	0.177	0.014	-0.004	-0.081	-0.006	0.088	-0.123	0.116	0.028
YA5 - NI1	0.825	0.978	0.601	0.882	0.821	0.822	0.807	0.952	0.992	0.607	0.868	0.823	0.717	0.795	0.961
YA5 - NI2	0.367	0.494	0.409	0.428	0.415	0.596	0.774	0.614	0.617	0.793	0.531	0.617	0.609	0.615	0.607
YA5 - Δ MSC	-0.458	-0.485	-0.193	-0.454	-0.405	-0.226	-0.033	-0.338	-0.375	0.186	-0.337	-0.206	-0.108	-0.180	-0.355
YA6 - NI1	0.857	0.968	0.833	0.705	0.912	0.839	0.711	0.631	0.771	0.871	0.661	0.824	0.516	0.681	0.772
YA6 - NI2	0.893	0.978	0.851	0.900	0.953	0.878	0.879	0.890	0.875	0.834	0.872	0.919	0.970	0.928	0.968
YA6 - Δ MSC	0.036	0.010	0.018	0.195	0.041	0.040	0.168	0.259	0.104	-0.037	0.211	0.095	0.454	0.248	0.197
YA7 - NI1	0.774	0.994	0.953	0.530	0.858	0.764	0.722	0.467	0.707	0.963	0.525	0.887	0.542	0.902	0.497
YA7 - NI2	0.415	0.869	0.723	0.482	0.527	0.417	0.469	0.419	0.419	0.855	0.528	0.558	0.641	0.652	0.802
YA7 - Δ MSC	-0.360	-0.125	-0.230	-0.048	-0.331	-0.347	-0.253	-0.049	-0.287	-0.108	0.002	-0.329	0.099	-0.249	0.305

In Table 4, the difference in MSC (Δ MSC) values per different brain regions on the same participant seems to demonstrate that different brain regions exhibit different cortical characteristics thus resulted in different MSC values. For instance, young adult #1 (YA1) showed a decrease in EEG coherence after the Trainer as indicated by negative values in Δ MSC in the frontal – central (FC), frontal – parietal (FP), frontal – temporal (FT), central – parietal (CP), central – occipital (CO), central – temporal (CT), parietal – parietal occipital (PPO), parietal – occipital (PO), parietal – temporal (PT), and the occipital – temporal (OT) regions, but

an increase in EEG coherence after the Trainer in the frontal - parietal occipital (FPO), frontal - occipital (FO), central-parietal occipital (CPO), parietal occipital - occipital (POO) and the parietal occipital - temporal (POT) regions. The erratic, non-deterministic behaviors of Δ MSC observed from fifteen communication channels across different pairs of brain regions in Delta frequency (1 – 4 Hz) confirm that due to the difference in their functions and attributes, different brain regions exhibit different neural synchronization, which resulted in different MSC values and Δ MSC values across 15 pairs of brain region combination per participant. Biological variation between participants was also demonstrated in Table 4 through a mixture of both positive and negative Δ MSC for the same brain region combination, but on different young adults. For example, a reduction in EEG coherence between the frontal and central (FC) area in the brain after the Trainer was observed in four young adults (YA1, YA2, YA3, YA5, and YA7) while an increase in EEG coherence in the FC area was noted in YA4 and YA6 as indicated by the positive Δ MSC values.

A paired-sample t-test on the change, or difference in EEG coherence (Δ MSC) between No Interaction 1 (NI1 - before using the Trainer) and No Interaction 2 (NI2 - after using the Trainer) session was conducted to evaluate if the decline in EEG coherence after using the trainer in Delta frequency (1-4 Hz) range is valid and in which brain regions, despite the physiological variation between participants. Table 5 presents the statistical results of the paired sample t-test on seven TD young adults across 15 pairs of brain region combinations. Other relevant statistics including the average (mean) Δ MSC, standard deviation (STD), and the 95% confidence interval range in which the population mean Δ MSC is projected to fall between, were also summarized in Table 5.

Table 5. Paired t-test summary statistics on the change in MSC (Δ MSC) between NI1 and NI2 on the study sample size of seven typical developing young adults ($n = 7$) in Delta frequency (1 – 4 Hz)

Young Adult (YA) subject # - Change in MSC (Δ MSC)	Brain Region														
	FC	FP	FPO	FO	FT	CP	CPO	CO	CT	PPO	PO	PT	POO	POT	OT
YA1 - Δ MSC	-0.466	-0.515	0.348	0.095	-0.311	-0.482	0.131	-0.092	-0.357	-0.017	-0.210	-0.558	0.175	0.233	-0.063
YA2 - Δ MSC	-0.529	-0.087	-0.615	-0.475	-0.308	-0.525	-0.704	-0.492	-0.561	-0.639	-0.460	-0.372	-0.568	-0.657	-0.380
YA3 - Δ MSC	-0.043	0.503	0.185	0.045	0.237	-0.089	0.014	-0.275	0.016	0.243	-0.407	-0.290	-0.200	0.274	-0.611
YA4 - Δ MSC	0.200	0.176	0.189	0.138	0.187	0.081	0.177	0.014	-0.004	-0.081	-0.006	0.088	-0.123	0.116	0.028
YA5 - Δ MSC	-0.458	-0.485	-0.193	-0.454	-0.405	-0.226	-0.033	-0.338	-0.375	0.186	-0.337	-0.206	-0.108	-0.180	-0.355
YA6 - Δ MSC	0.036	0.010	0.018	0.195	0.041	0.040	0.168	0.259	0.104	-0.037	0.211	0.095	0.454	0.248	0.197
YA7 - Δ MSC	-0.360	-0.125	-0.230	-0.048	-0.331	-0.347	-0.253	-0.049	-0.287	-0.108	0.002	-0.329	0.099	-0.249	0.305
Mean Δ MSC	-0.231	-0.075	-0.042	-0.072	-0.127	-0.221	-0.071	-0.139	-0.209	-0.065	-0.172	-0.225	-0.039	-0.031	-0.126
Standard Deviation (STD)	0.290	0.358	0.328	0.279	0.272	0.243	0.317	0.250	0.248	0.287	0.249	0.241	0.323	0.348	0.334
T-statistic	-2.110	-0.552	-0.342	-0.682	-1.233	-2.414	-0.596	-1.470	-2.230	-0.597	-1.833	-2.464	-0.319	-0.235	-0.994
p-value	0.040	0.300	0.372	0.260	0.132	0.026	0.287	0.096	0.034	0.286	0.058	0.024	0.380	0.411	0.179
95% Confidence Interval (CI) for the population mean	0.268	0.331	0.304	0.258	0.252	0.224	0.293	0.231	0.230	0.265	0.230	0.223	0.299	0.321	0.309
Lower bound CI	-0.500	-0.400	-0.300	-0.300	-0.400	-0.400	-0.400	-0.400	-0.400	-0.300	-0.400	-0.400	-0.300	-0.400	-0.400
Upper bound CI	0.037	0.256	0.261	0.186	0.125	0.003	0.222	0.092	0.020	0.200	0.058	-0.002	0.260	0.291	0.183

Table 5 shows that four out of fifteen pairs of brain region combinations in which a decrease in EEG coherence after the Trainer in Delta frequency were found to be statistically significant ($p \leq 0.05$). Those regions are the frontal - central (FC), central - parietal (CP), central - temporal (CT), and the parietal – temporal (PT) areas. There is sufficient statistical evidence to believe that there is a change in the functional neural network connectivity of typical developing young adults after interacting with the Trainer, specifically there is a decrease in EEG coherence between the frontal and central (FC), central and parietal (CP), central and temporal (CT), and between the parietal and temporal (PT) regions in the brain of healthy young adults after operating the Trainer in the Delta rhythm.

Changes in EEG coherence (Δ MSC) after the Trainer in the brains of seven typical developing young adults in Delta frequency (1-4 Hz) were graphically illustrated in Figure 2-7 below. A decrease in EEG coherence is indicated by negative bars while positive bars signal an increase in coherence after the Trainer. For each brain region, the change, or Δ MSC from each young adult (YA) participated in the study was represented by a different color bar, and the overall mean (average) Δ MSC across seven participants was presented by the cross sign. A cross sign enlisted

within a circle indicates brain regions in which a reduction in EEG coherence was found with significant p-value ($p \leq 0.05$). Both the lower and upper boundary of 95% confidence interval (CI) for each brain region combination were also graphically presented to show the range in which the predicted average Δ MSC of the healthy young adult population would fall after active usage of the Trainer.

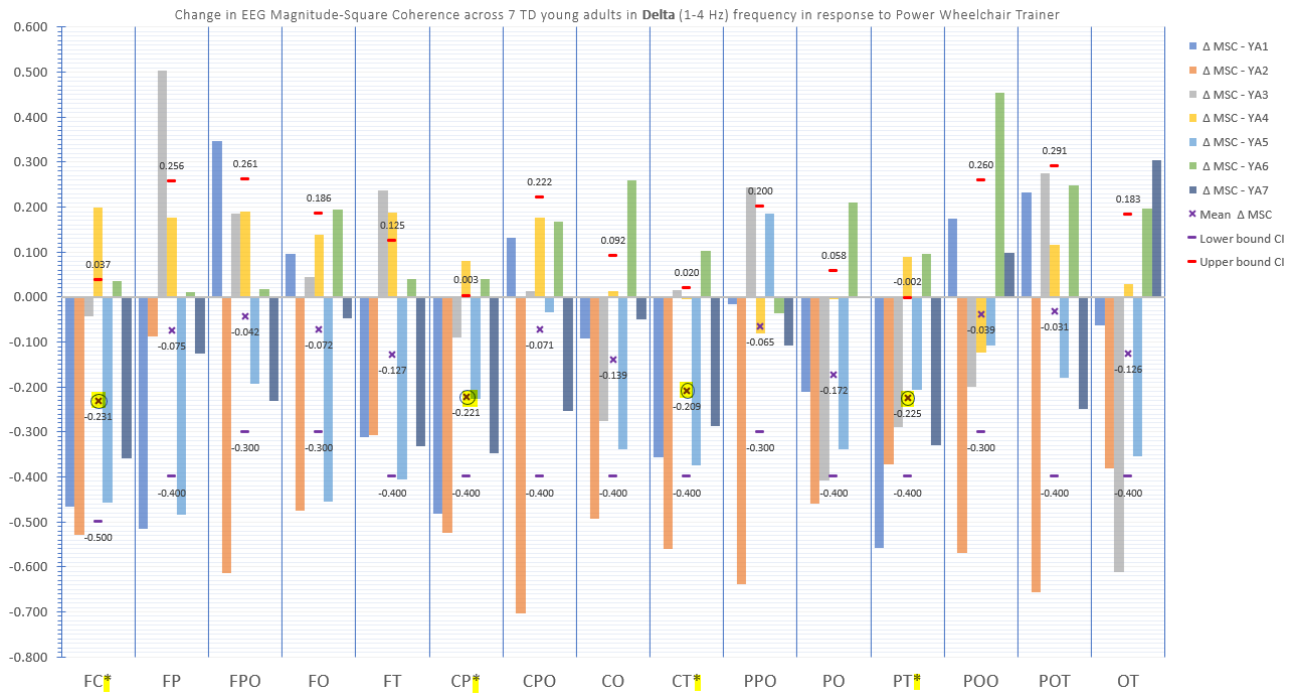


Figure 2-7. Change in EEG coherence across different brain regions on 7 TD young adults after interaction with the Power Wheelchair Trainer in Delta (1- 4 Hz) frequency band. A “*” indicates brain regions in which the decrease in EEG coherence after the Trainer was found with significant p-values ($p \leq 0.05$)

The dominant presence of negative bars that outnumbered positive bars in Δ MSC (change in MSC after the Trainer) seems to suggest an overall decrease in EEG coherence across 15 pairs of brain region combinations on TD young adults in Delta frequency (1-4 Hz). Negative population mean Δ MSC (Mean Δ MSC) across all fifteen pairs of brain region combinations in Delta frequency also seems to confirm the observed pattern. Four areas in which the decrease in EEG coherence in Delta frequency (1-4 Hz) were found to be statistically significant include the

frontal - central (FC), central - parietal (CP), central - temporal (CT), and the parietal – temporal (PT) regions. These four brain regions were highlighted in yellow with a superscripted asterisk to distinguish from other brain regions, where statistical evidence on the impact of the Trainer on EEG coherence of TD young adults was lacking. Both the lower and upper boundary of 95% confidence interval (CI) were shown to project the range in which the population mean Δ MSC would be. For example, based on the sample size of seven typical developing young adults, there is sufficient statistical evidence to believe that there is an average decrease of 0.231 in mean Δ MSC in the frontal – central (FC) brain region and we are 95% confident that the mean Δ MSC on the typical developing young adult population will fall between -0.5 and 0.037, as projected by the lower and upper boundary of 95% confidence interval. Zero was included in this confidence interval implies that the Power Wheelchair Trainer (the Trainer) could have either a positive or negative effect on the mean Δ MSC, or EEG coherence of the typical developing young adult population in Delta frequency (1-4 Hz). Similar interpretations regarding a decrease in EEG coherence in young adults after interacting with the Power Wheelchair Trainer in Delta frequency could be applied for the central – parietal (CP), central – temporal (CT), and the parietal – temporal (PT) regions.

2. Theta (5-7 Hz) Frequency

Similar to the process of extracting and averaging MSC values from the overall time-frequency MSC between each combination of the regional EEG in Delta frequency range, MSC in Theta frequency ranging between 5 Hz and 7 Hz were extracted and then averaged across the number of frequency sub-bands to obtain the representative MSC in Theta range for each test condition i.e. No Interaction 1 (NI1) or No Interaction 2 (NI2). Average MSC in Theta frequency for both test conditions (NI1 and NI2) and the changes in MSC (Δ MSC) after the Trainer across various

regions in the brain for all seven healthy young adults participated in the study were calculated and summarized in Table 6.

Table 6. Summary of the MSC for all 7 participants in 2 test conditions (NI1 – 5-min before the Trainer and NI2 – 5-min after the Trainer) and the resulting difference in MSC (Δ MSC) across various brain regions in Theta frequency (5-7 Hz)

Young Adult (YA) subject # - Condition	Brain Region														
	FC	FP	FPO	FO	FT	CP	CPO	CO	CT	PPO	PO	PT	POO	POT	OT
YA1 - NI1	0.583	0.739	0.328	0.517	0.409	0.763	0.179	0.217	0.568	0.173	0.261	0.803	0.675	0.268	0.194
YA1 - NI2	0.156	0.672	0.754	0.753	0.265	0.183	0.179	0.190	0.216	0.395	0.567	0.183	0.666	0.318	0.188
YA1 - Δ MSC	-0.427	-0.067	0.426	0.236	-0.144	-0.579	0.000	-0.027	-0.352	0.222	0.306	-0.620	-0.010	0.050	-0.006
YA2 - NI1	0.933	0.998	0.998	0.991	0.990	0.935	0.947	0.919	0.946	0.995	0.983	0.983	0.990	0.990	0.987
YA2 - NI2	0.186	0.853	0.556	0.411	0.375	0.209	0.202	0.168	0.195	0.416	0.427	0.250	0.485	0.194	0.250
YA2 - Δ MSC	-0.747	-0.144	-0.442	-0.581	-0.615	-0.726	-0.745	-0.751	-0.752	-0.579	-0.557	-0.732	-0.505	-0.796	-0.737
YA3 - NI1	0.256	0.348	0.756	0.321	0.240	0.217	0.328	0.218	0.274	0.560	0.946	0.608	0.530	0.253	0.618
YA3 - NI2	0.207	0.929	0.840	0.738	0.385	0.185	0.344	0.163	0.357	0.766	0.841	0.258	0.568	0.406	0.183
YA3 - Δ MSC	-0.049	0.580	0.084	0.417	0.145	-0.032	0.016	-0.055	0.084	0.206	-0.106	-0.350	0.038	0.153	-0.434
YA4 - NI1	0.476	0.591	0.522	0.573	0.536	0.678	0.726	0.719	0.813	0.969	0.990	0.805	0.977	0.837	0.838
YA4 - NI2	0.689	0.582	0.528	0.555	0.634	0.771	0.824	0.712	0.759	0.865	0.986	0.826	0.816	0.841	0.777
YA4 - Δ MSC	0.213	-0.009	0.006	-0.019	0.098	0.093	0.098	-0.007	-0.054	-0.104	-0.004	0.021	-0.161	0.004	-0.061
YA5 - NI1	0.561	0.947	0.293	0.745	0.550	0.578	0.692	0.867	0.977	0.297	0.739	0.578	0.471	0.672	0.879
YA5 - NI2	0.181	0.692	0.502	0.522	0.273	0.217	0.516	0.164	0.199	0.641	0.308	0.252	0.232	0.235	0.277
YA5 - Δ MSC	-0.380	-0.255	0.209	-0.222	-0.278	-0.361	-0.176	-0.703	-0.779	0.344	-0.432	-0.326	-0.239	-0.437	-0.602
YA6 - NI1	0.609	0.973	0.702	0.208	0.823	0.606	0.315	0.202	0.476	0.692	0.209	0.720	0.237	0.483	0.289
YA6 - NI2	0.604	0.955	0.479	0.576	0.857	0.581	0.750	0.701	0.642	0.461	0.516	0.765	0.902	0.687	0.837
YA6 - Δ MSC	-0.005	-0.019	-0.223	0.368	0.034	-0.025	0.435	0.499	0.165	-0.231	0.307	0.045	0.664	0.204	0.548
YA7 - NI1	0.542	0.985	0.938	0.411	0.652	0.543	0.498	0.247	0.552	0.959	0.393	0.719	0.398	0.733	0.310
YA7 - NI2	0.263	0.915	0.738	0.305	0.403	0.249	0.328	0.209	0.249	0.796	0.305	0.420	0.373	0.587	0.514
YA7 - Δ MSC	-0.279	-0.070	-0.200	-0.106	-0.249	-0.294	-0.170	-0.038	-0.303	-0.162	-0.088	-0.299	-0.025	-0.146	0.204

Again, the erratic, non-deterministic behaviors of EEG coherence, as illustrated by different MSC values and Δ MSC values across 15 pairs of regional brain combinations per participant in Theta frequency (5-7 Hz) in Table 6 seem to confirm the differences in EEG coherence between different brain regions, as each brain region is attributed to different function and cognitive tasks. In young adult #1 (YA1), nine out of fifteen brain region combinations exhibited a decrease in EEG coherence after Trainer while five other brain regions showed an increase in phase coupling of the underlying EEG signals as demonstrated by positive Δ MSC in the frontal - parietal occipital (FPO), frontal - occipital (FO), parietal - parietal occipital (PPO), parietal - occipital (PO), parietal occipital - temporal (POT) regions, and no change in EEG coherence in the central-parietal occipital (CPO) area as denoted by zero Δ MSC value.

Similar observation on the physiological variation in EEG coherence between participants in Delta frequency was also noted in Theta frequency. For instance, using the example listed above,

when young adult #1 (YA1) showed a decrease in EEG coherence after the Trainer in nine brain regions including the frontal – central (FC), frontal – parietal (FP), frontal – temporal (FT), central – parietal (CP), central – occipital (CO), central – temporal (CT), parietal – temporal (PT), parietal occipital – occipital (POO), occipital – temporal (OT), and an increase in EEG coherence in the frontal - parietal occipital (FPO), frontal - occipital (FO), parietal - parietal occipital (PPO), parietal - occipital (PO), parietal occipital - temporal (POT) region, and no change in coherence in the central-parietal occipital (CPO) area. Young adult #2 (YA2 – Δ MSC) seemed to defy the observed pattern with an overall reduction in EEG coherence in all 15 brain region combinations, as observed in Table 6.

A paired-sample t-test on the change, or difference in EEG Coherence (Δ MSC) due to the Trainer was conducted to evaluate the change in EEG coherence on typical developing (TD) young adults in Theta frequency (5-7 Hz) range across various brain regions, in spite of physiological variation between participants. Table 7 presents the statistical results of the paired sample t-test on 7 TD young adults across 15 brain region combinations. Other important statistics including standard deviation (STD) of the average Δ MSC and 95% confidence interval range in which the population mean Δ MSC would fall between, were also presented in Table 7.

Table 7. Paired t-test summary statistics on the change in MSC (Δ MSC) between NI1 and NI2 on the study sample size of seven typical developing young adults ($n = 7$) in Theta frequency (5-7 Hz)

Young Adult (YA) subject # - Change in MSC (Δ MSC)	Brain Region														
	FC	FP	FPO	FO	FT	CP	CPO	CO	CT	PPO	PO	PT	POO	POT	OT
YA1 - Δ MSC	-0.427	-0.067	0.426	0.236	-0.144	-0.579	0.000	-0.027	-0.352	0.222	0.306	-0.620	-0.010	0.050	-0.006
YA2 - Δ MSC	-0.747	-0.144	-0.442	-0.581	-0.615	-0.726	-0.745	-0.751	-0.752	-0.579	-0.557	-0.732	-0.505	-0.796	-0.737
YA3 - Δ MSC	-0.049	0.580	0.084	0.417	0.145	-0.032	0.016	-0.055	0.084	0.206	-0.106	-0.350	0.038	0.153	-0.434
YA4 - Δ MSC	0.213	-0.009	0.006	-0.019	0.098	0.093	0.098	-0.007	-0.054	-0.104	-0.004	0.021	-0.161	0.004	-0.061
YA5 - Δ MSC	-0.380	-0.255	0.209	-0.222	-0.278	-0.361	-0.176	-0.703	-0.779	0.344	-0.432	-0.326	-0.239	-0.437	-0.602
YA6 - Δ MSC	-0.005	-0.019	-0.223	0.368	0.034	-0.025	0.435	0.499	0.165	-0.231	0.307	0.045	0.664	0.204	0.548
YA7 - Δ MSC	-0.279	-0.070	-0.200	-0.106	-0.249	-0.294	-0.170	-0.038	-0.303	-0.162	-0.088	-0.299	-0.025	-0.146	0.204
Mean Δ MSC	-0.239	0.002	-0.020	0.013	-0.144	-0.275	-0.077	-0.155	-0.284	-0.043	-0.082	-0.323	-0.034	-0.138	-0.155
Standard Deviation (STD)	0.319	0.268	0.293	0.356	0.266	0.306	0.359	0.437	0.378	0.322	0.331	0.292	0.359	0.360	0.460
T-statistic	-1.985	0.024	-0.180	0.099	-1.433	-2.380	-0.571	-0.936	-1.990	-0.357	-0.655	-2.929	-0.250	-1.016	-0.894
p-value	0.047	0.509	0.431	0.538	0.101	0.027	0.294	0.193	0.047	0.367	0.268	0.013	0.406	0.174	0.203
95% Confidence Interval (CI) for the population mean	0.295	0.248	0.271	0.330	0.246	0.283	0.332	0.404	0.350	0.298	0.306	0.270	0.332	0.333	0.426
Lower bound CI	-0.500	-0.200	-0.300	-0.300	-0.400	-0.600	-0.400	-0.600	-0.600	-0.300	-0.400	-0.600	-0.400	-0.500	-0.600
Upper bound CI	0.056	0.251	0.251	0.343	0.102	0.008	0.254	0.250	0.065	0.254	0.224	-0.053	0.298	0.195	0.270

The change, or difference in EEG coherence (Δ MSC) on TD young adults after interaction with the Trainer in Theta band (5-7 Hz) shows similar behavior to the change in EEG coherence found in Delta (1-4 Hz) frequency with exactly the same four brain regions in which a decrease in EEG coherence after Trainer were found to be statistically significant ($p \leq 0.05$). Those include the frontal - central (FC), central - parietal (CP), central - temporal (CT), and the parietal – temporal (PT) regions.

Figure 2-8 illustrates the changes in EEG coherence (Δ MSC) after the Trainer in the brain of seven healthy young adults in Theta (1-4 Hz) frequency. Negative Δ MSC as represented by negative bars in the graph indicates a decrease in EEG coherence after the Trainer while positive bars signal an increase in EEG coherence after the Trainer.

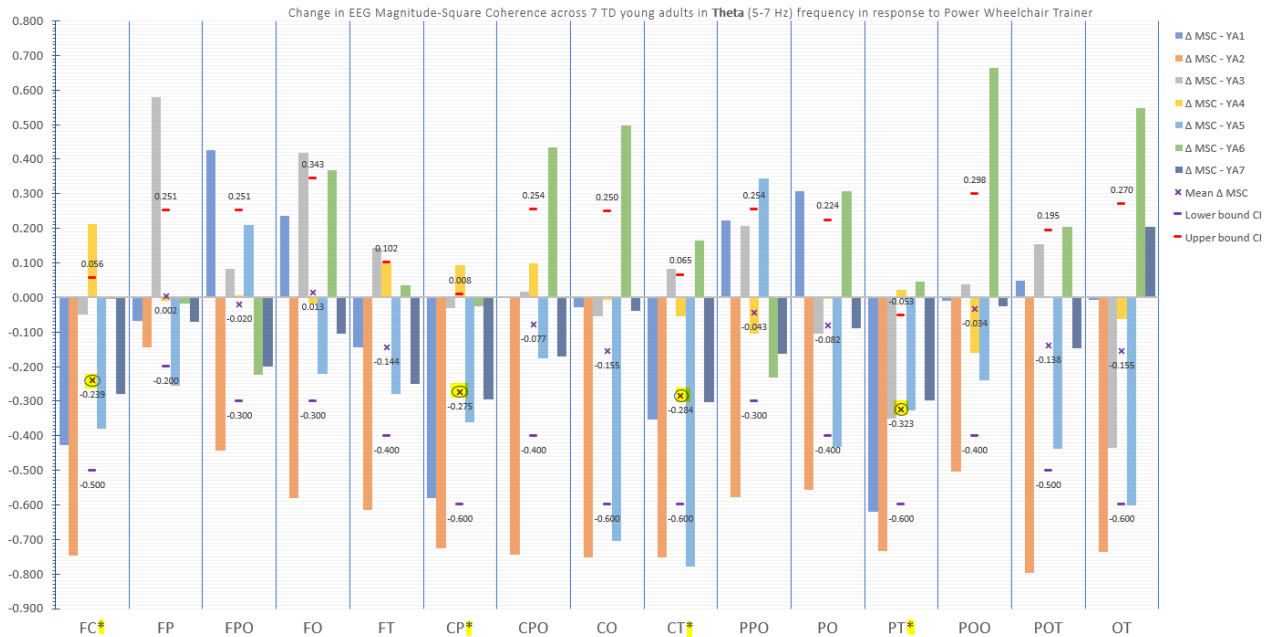


Figure 2-8. Change in EEG coherence across different brain regions on 7 TD young adults after interaction with Power Wheelchair Trainer in Theta (5-7 Hz) frequency band. A “*” indicates brain regions in which the decrease in EEG coherence after the Trainer was found with significant p-values ($p \leq 0.05$)

Figure 2-8 shows a strong presence of negative Δ MSC in most brain regions over the positive Δ MSC, with a few exceptions in the frontal – parietal occipital (FPO), frontal – occipital (FO), parietal – parietal occipital (PPO), parietal occipital – temporal (POT) among others where a combination of both positive and negative bars is shown. Physiological variation between participants was also demonstrated in Figure 2-8. Similar to findings discovered in Δ MSC, or changes in EEG coherence on healthy young adults due to the Trainer in Delta (1-4 Hz) frequency, four areas in which the decrease in EEG coherence was found to be statistically significant ($p \leq 0.05$) in Theta band (5-7 Hz) include the frontal - central (FC), central - parietal (CP), central - temporal (CT), and the parietal – temporal (PT) regions as highlighted in yellow with a superscripted asterisk in Figure 2-8. Both the lower and upper boundary of 95% confidence interval (CI) were used to show the projected range in which the population mean Δ

MSC would fall. For example, based on the sample size of seven typical developing young adults, there is enough statistical evidence to believe that there is an average decrease of 0.239 in EEG coherence (mean Δ MSC = -0.239) in the frontal – central (FC) brain region in Theta (5-7 Hz) frequency and we are 95% confident that the population mean Δ MSC in Theta band will fall between -0.5 and 0.056 as projected by the lower and upper boundary of 95% confidence interval. The fact that zero was included in this confidence interval range implies that the Trainer could have either a positive or negative effect on the outcome of interest, which is the mean Δ MSC, or EEG coherence of the healthy young adult population in Theta (5-7 Hz) frequency. Similar interpretations regarding the results of the paired-sample t-test on the effect of the Trainer on TD young adults could also be applied for the central - parietal (CP), central - temporal (CT), and the parietal – temporal (PT) regions.

3. Alpha (8-13 Hz) Frequency

For each test condition i.e. No Interaction 1 (NI1) or No Interaction 2 (NI2), MSC values within the 8-to-13 Hz (Alpha) frequency range were extracted from the overall time-frequency MSC between each combination of the regional EEG, then averaged across the number of frequency sub-bands to obtain the representative MSC in the Alpha frequency. For each brain region combination, changes in MSC after the Trainer, or as often referred to as Δ MSC, was calculated by subtracting the MSC from NI1 from the MSC from NI2. MSC values between each pair of brain region combinations for both NI1 and NI2, and changes in MSC after the Trainer (Δ MSC) in Alpha frequency for all seven typical developing (TD) young adults were summarized in Table 8.

Table 8. Summary of the MSC for all 7 participants in 2 test conditions (NI1 – 5-min before the Trainer and NI2 – 5-min after the Trainer) and the resulting difference in MSC (Δ MSC) across various brain regions in Alpha frequency (8 -13 Hz)

Young Adult (YA) subject # - Condition	Brain Region														
	FC	FP	FPO	FO	FT	CP	CPO	CO	CT	PPO	PO	PT	POO	POT	OT
YA1 - NI1	0.685	0.7584	0.567	0.6624	0.302	0.6987	0.3901	0.3954	0.3573	0.2663	0.3785	0.6565	0.8163	0.1765	0.1772
YA1 - NI2	0.4065	0.8231	0.8257	0.8047	0.1648	0.3834	0.5095	0.3342	0.2402	0.6265	0.7351	0.2136	0.7795	0.1686	0.1944
YA1 - Δ MSC	-0.279	0.065	0.259	0.142	-0.137	-0.315	0.119	-0.061	-0.117	0.360	0.357	-0.443	-0.037	-0.008	0.017
YA2 - NI1	0.8865	0.9957	0.9865	0.9875	0.9606	0.8762	0.9089	0.8778	0.8928	0.975	0.9761	0.9536	0.985	0.9325	0.9367
YA2 - NI2	0.2802	0.8803	0.7409	0.6805	0.2504	0.2412	0.4081	0.318	0.1878	0.6025	0.6809	0.1902	0.67	0.1823	0.1935
YA2 - Δ MSC	-0.606	-0.115	-0.246	-0.307	-0.710	-0.635	-0.501	-0.560	-0.705	-0.373	-0.295	-0.763	-0.315	-0.750	-0.743
YA3 - NI1	0.4067	0.7598	0.9189	0.6681	0.3457	0.3523	0.4668	0.3206	0.3049	0.8354	0.9433	0.2839	0.7476	0.2842	0.3097
YA3 - NI2	0.3528	0.9711	0.9053	0.8722	0.4026	0.3321	0.4467	0.3151	0.5355	0.8528	0.9312	0.3399	0.7496	0.4448	0.3136
YA3 - Δ MSC	-0.054	0.211	-0.014	0.204	0.057	-0.020	-0.020	-0.006	0.231	0.017	-0.012	0.056	0.002	0.161	0.004
YA4 - NI1	0.4463	0.6955	0.5855	0.6702	0.4747	0.5969	0.6515	0.6371	0.6474	0.9437	0.9853	0.6904	0.9401	0.78	0.7083
YA4 - NI2	0.6642	0.2963	0.2421	0.2675	0.4488	0.5072	0.431	0.423	0.4846	0.8336	0.9527	0.5218	0.8285	0.5158	0.4446
YA4 - Δ MSC	0.218	-0.399	-0.343	-0.403	-0.026	-0.090	-0.221	-0.214	-0.163	-0.110	-0.033	-0.169	-0.112	-0.264	-0.264
YA5 - NI1	0.3585	0.9474	0.3854	0.6597	0.3541	0.3631	0.5197	0.6743	0.9435	0.3643	0.6462	0.3665	0.2997	0.4671	0.7235
YA5 - NI2	0.3615	0.8775	0.7026	0.6476	0.291	0.3386	0.5791	0.3341	0.2458	0.6628	0.5172	0.2263	0.5494	0.2196	0.2339
YA5 - Δ MSC	0.003	-0.070	0.317	-0.012	-0.063	-0.025	0.059	-0.340	-0.698	0.299	-0.129	-0.140	0.250	-0.248	-0.490
YA6 - NI1	0.4177	0.9798	0.7171	0.36	0.6992	0.4333	0.2074	0.2242	0.2858	0.6869	0.367	0.6211	0.5528	0.4058	0.1856
YA6 - NI2	0.4409	0.9357	0.2554	0.2869	0.5803	0.4373	0.5402	0.3783	0.3651	0.2429	0.2634	0.438	0.7935	0.4981	0.6849
YA6 - Δ MSC	0.023	-0.044	-0.462	-0.073	-0.119	0.004	0.333	0.154	0.079	-0.444	-0.104	-0.183	0.241	0.092	0.499
YA7 - NI1	0.2624	0.9844	0.9417	0.5644	0.4652	0.2671	0.2605	0.3071	0.3943	0.9544	0.5375	0.5285	0.5129	0.5164	0.2919
YA7 - NI2	0.5643	0.9654	0.8691	0.566	0.2878	0.5246	0.5905	0.4602	0.2987	0.8645	0.5325	0.2784	0.4646	0.3488	0.3278
YA7 - Δ MSC	0.302	-0.019	-0.073	0.002	-0.177	0.258	0.330	0.153	-0.096	-0.090	-0.005	-0.250	-0.048	-0.168	0.036

There are more positive Δ MSC values, which indicate an increase in EEG coherence after the Trainer in Alpha frequency (8-13 Hz), as compared to what was observed in Δ MSC after the Trainer in both Delta (1-4 Hz) frequency and Theta (5-7 Hz) frequency. For example, in the frontal – central (FC) bregion, four young adults (YA4, YA5, YA6, and YA7) exhibited an increase in EEG coherence after the Trainer in Alpha frequency as compared to only one young adult (YA4) in the Theta frequency and two young adults (YA4 and YA6) in the Delta frequency showed an increase in EEG coherence after active usage of the power wheelchair trainer.

Again, physiological variation between subjects seems to explain the variability in EEG coherence, specifically Δ MSC. In the example mentioned above, four young adults (YA4, YA5, YA6, and YA7) showed an increase in coherence after interaction with the Trainer while the opposite behavior was noted on three other young adults (YA1, YA2, and YA3) in the frontal – central (FC) brain region. Thus, a paired-sample t-test on the change, or difference in EEG coherence (Δ MSC) between NI1 and NI2 was conducted to determine the changes in EEG coherence on TD young adults after the Trainer in Alpha (8-13 Hz) frequency across 15 brain

region combinations. Table 9 presents statistical results of the paired sample t-test on seven TD young adults across 15 brain region combinations.

Table 9. Paired t-test summary statistics on the change in MSC (Δ MSC) between NI1 and NI2 on the study sample size of seven typical developing young adults ($n = 7$) in Alpha frequency (8-13 Hz)

Young Adult (YA) subject #	Brain Region														
Change in MSC (Δ MSC)	FC	FP	FPO	FO	FT	CP	CPO	CO	CT	PPO	PO	PT	POO	POT	OT
YA1 - Δ MSC	-0.279	0.065	0.259	0.142	-0.137	-0.315	0.119	-0.061	-0.117	0.360	0.357	-0.443	-0.037	-0.008	0.017
YA2 - Δ MSC	-0.606	-0.115	-0.246	-0.307	-0.710	-0.635	-0.501	-0.560	-0.705	-0.373	-0.295	-0.763	-0.315	-0.750	-0.743
YA3 - Δ MSC	-0.054	0.211	-0.014	0.204	0.057	-0.020	-0.020	-0.006	0.231	0.017	-0.012	0.056	0.002	0.161	0.004
YA4 - Δ MSC	0.218	-0.399	-0.343	-0.403	-0.026	-0.090	-0.221	-0.214	-0.163	-0.110	-0.033	-0.169	-0.112	-0.264	-0.264
YA5 - Δ MSC	0.003	-0.070	0.317	-0.012	-0.063	-0.025	0.059	-0.340	-0.698	0.299	-0.129	-0.140	0.250	-0.248	-0.490
YA6 - Δ MSC	0.023	-0.044	-0.462	-0.073	-0.119	0.004	0.333	0.154	0.079	-0.444	-0.104	-0.183	0.241	0.092	0.499
YA7 - Δ MSC	0.302	-0.019	-0.073	0.002	-0.177	0.258	0.330	0.153	-0.096	-0.090	-0.005	-0.250	-0.048	-0.168	0.036
Mean Δ MSC	-0.056	-0.053	-0.080	-0.064	-0.168	-0.118	0.014	-0.125	-0.210	-0.049	-0.032	-0.270	-0.003	-0.169	-0.134
Standard Deviation (STD)	0.307	0.187	0.294	0.222	0.251	0.283	0.299	0.264	0.362	0.305	0.198	0.263	0.198	0.304	0.405
T-statistic	-0.484	-0.753	-0.721	-0.761	-1.768	-1.099	0.127	-1.253	-1.535	-0.422	-0.421	-2.721	-0.037	-1.471	-0.877
p-value	0.323	0.240	0.249	0.238	0.064	0.157	0.548	0.128	0.088	0.344	0.344	0.017	0.486	0.096	0.207
95% Confidence Interval (CI) for the population mean	0.284	0.173	0.272	0.205	0.233	0.262	0.276	0.244	0.334	0.282	0.183	0.243	0.183	0.282	0.375
Lower bound CI	-0.300	-0.200	-0.400	-0.300	-0.400	-0.400	-0.300	-0.400	-0.500	-0.300	-0.200	-0.500	-0.200	-0.500	-0.500
Upper bound CI	0.228	0.120	0.192	0.141	0.065	0.144	0.291	0.119	0.125	0.234	0.152	-0.027	0.181	0.112	0.241

Table 9 shows that based on the study sample size composed of seven healthy young adults, there is sufficient statistical evidence ($p \leq 0.05$) to believe that there was a reduction in EEG coherence of neurotypical, medical-healthy young adults between the parietal and temporal (PT) regions after the Trainer in Alpha frequency (8-13 Hz). However, there is a lack of statistical significance to draw any conclusion on findings with regard to the effect of the Trainer on EEG coherence in other brain regions on healthy young adults in Alpha frequency band (8-13 Hz) including a decrease in EEG coherence in the frontal - central (FC), central - parietal (CP), and the central – temporal (CT) regions as previously found in both the Delta (1-4 Hz) and Theta (5-7 Hz) frequency. The average Δ MSC (Mean Δ MSC) presents the average change in EEG coherence across seven participants in each pair of regional brain combinations while the standard deviation (STD) of the paired differences shows the amount of variation or dispersion of the Δ MSC set from the mean. The standard deviation indicates how tightly the data is clustered around the study-population mean Δ MSC. A small STD indicates the data is tightly clustered with a taller bell curve while a large STD implies the data is more spread apart. Other

relevant statistic includes a 95% confidence interval (CI) – the interval estimates in which we are 95% confident that might contain the true value of the population parameter, in this case, the healthy young adult population mean Δ MSC. For example, given the parietal – temporal (PT) region and based on the sample size of seven typical developing young adults in the study, there is statistical significance to infer that on average, there is a drop of precisely 0.270 in coherence (mean Δ MSC = -0.270) between the EEG signals recorded from the parietal region and the EEG signals recorded from the temporal region, due to the Trainer. A relatively high STD of 0.263 indicates a wider variation in Δ MSC values across 7 participants between the parietal and temporal region in the Alpha (8-13 Hz) frequency. Meanwhile, a 95% confidence interval (CI) ranging from -0.5 (lower CI boundary) to -0.027 (upper CI boundary) projects the estimated range where the true population mean Δ MSC in Alpha frequency will fall. The fact that zero was not included in this confidence interval range seems to confirm that the Trainer would result to a decrease in the mean Δ MSC, or EEG coherence of the typical developing young adult population in Alpha (8-13 Hz) frequency.

Figure 2-9 provides a visual illustration on findings with respect to changes in EEG coherence after the Trainer (Δ MSC) in various brain regions of seven typical developing young adults (YA) in Alpha frequency, along with other important statistical results such as population mean Δ MSC, lower and upper 95% confidence interval (CI), and highlighted brain regions in which the change in EEG coherence after Trainer were found to be statistical significant ($p \leq 0.05$).

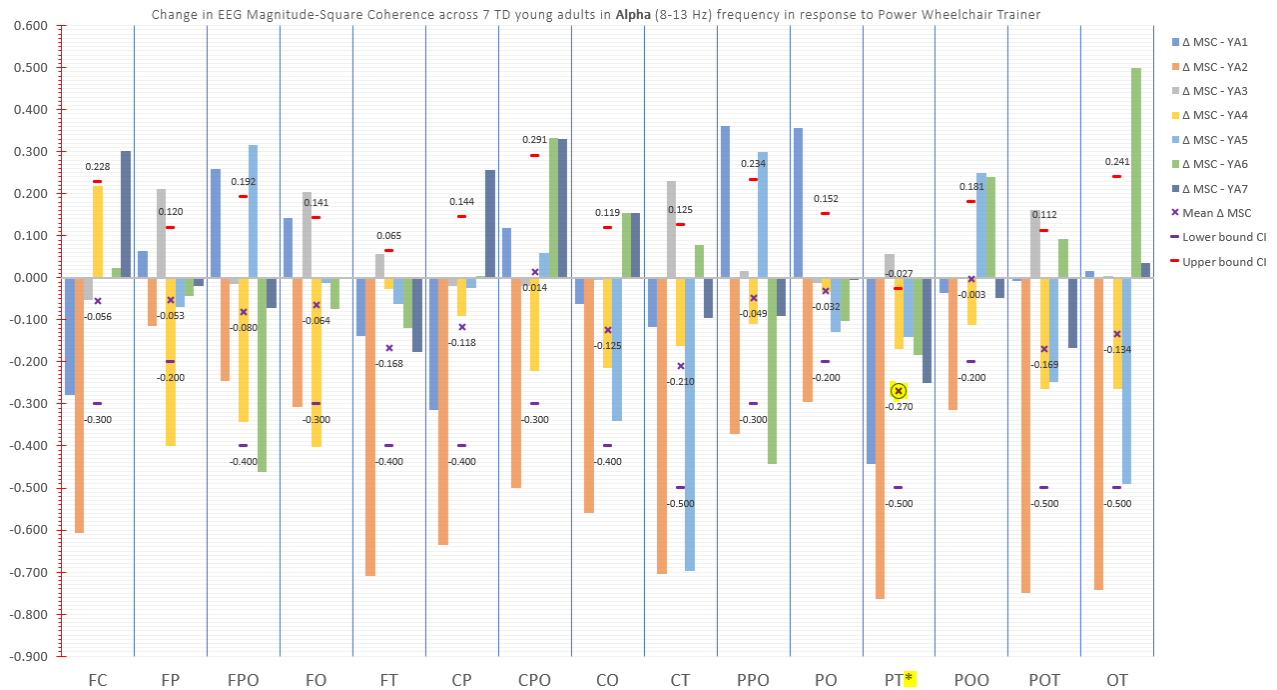


Figure 2-9. Change in EEG coherence across different brain regions on 7 TD young adults after interaction with Power Wheelchair Trainer in Alpha frequency (8-13 Hz). A "*" indicates brain regions in which the decrease in EEG coherence after the Trainer was found with significant p-values ($p \leq 0.05$)

4. Beta (14-30 Hz) Frequency

Following the same methodology as established above, for each test condition i.e. No Interaction 1 (NI1) and No Interaction (NI2), the magnitude square coherences (MSC) in Beta frequency ranging from 14 Hz to 30 Hz were extracted from the overall time-frequency MSC between each combination of different brain regions, then averaged across the number of frequency sub-bands to obtain the representative MSC in Beta frequency. Table 10 summarizes the MSC between each combination of different brain regions for a total of 15 regional brain combinations on each young adult (YA) for both test conditions (NI1 and NI2), and changes in MSC after the Trainer (Δ MSC), which was calculated by subtracting the NI1-derived MSC values from the NI2-derived MSC values in Beta frequency, for all seven healthy young adults participated in the study.

Table 10. Summary of the MSC for all 7 participants in 2 test conditions (NI1 – 5-min before the Trainer and NI2 – 5-min after the Trainer) and the resulting difference in MSC (Δ MSC) across various brain regions in Beta frequency (14-30 Hz)

Young Adult (YA) subject # - Condition	Brain Region														
	FC	FP	FPO	FO	FT	CP	CPO	CO	CT	PPO	PO	PT	POO	POT	OT
YA1 - NI1	0.451	0.751	0.426	0.602	0.297	0.536	0.250	0.242	0.298	0.213	0.332	0.625	0.668	0.161	0.177
YA1 - NI2	0.226	0.794	0.638	0.731	0.202	0.220	0.310	0.201	0.277	0.484	0.628	0.186	0.648	0.168	0.175
YA1 - Δ MSC	-0.224	0.043	0.212	0.129	-0.095	-0.316	0.060	-0.041	-0.021	0.271	0.295	-0.439	-0.020	0.008	-0.002
YA2 - NI1	0.799	0.995	0.989	0.984	0.918	0.788	0.823	0.773	0.860	0.982	0.977	0.900	0.981	0.897	0.876
YA2 - NI2	0.192	0.813	0.632	0.583	0.259	0.172	0.307	0.221	0.252	0.489	0.578	0.168	0.588	0.164	0.177
YA2 - Δ MSC	-0.607	-0.182	-0.357	-0.401	-0.659	-0.616	-0.516	-0.552	-0.607	-0.493	-0.398	-0.732	-0.393	-0.733	-0.699
YA3 - NI1	0.196	0.541	0.799	0.498	0.195	0.189	0.234	0.192	0.206	0.664	0.934	0.386	0.640	0.185	0.394
YA3 - NI2	0.223	0.940	0.851	0.779	0.342	0.204	0.316	0.183	0.362	0.833	0.873	0.239	0.714	0.288	0.171
YA3 - Δ MSC	0.027	0.399	0.052	0.282	0.147	0.015	0.082	-0.009	0.155	0.169	-0.062	-0.146	0.074	0.102	-0.223
YA4 - NI1	0.414	0.695	0.578	0.658	0.432	0.587	0.640	0.632	0.627	0.935	0.981	0.688	0.936	0.782	0.717
YA4 - NI2	0.491	0.268	0.216	0.255	0.309	0.477	0.394	0.407	0.347	0.773	0.946	0.517	0.743	0.497	0.450
YA4 - Δ MSC	0.078	-0.427	-0.362	-0.403	-0.123	-0.109	-0.246	-0.224	-0.280	-0.162	-0.035	-0.171	-0.193	-0.286	-0.268
YA5 - NI1	0.401	0.909	0.311	0.700	0.374	0.400	0.532	0.698	0.898	0.291	0.656	0.401	0.297	0.459	0.696
YA5 - NI2	0.239	0.751	0.576	0.624	0.218	0.232	0.455	0.239	0.225	0.600	0.458	0.193	0.427	0.185	0.180
YA5 - Δ MSC	-0.162	-0.158	0.264	-0.076	-0.156	-0.168	-0.076	-0.460	-0.672	0.309	-0.197	-0.208	0.130	-0.275	-0.516
YA6 - NI1	0.368	0.949	0.503	0.273	0.657	0.415	0.217	0.196	0.242	0.431	0.270	0.541	0.576	0.279	0.198
YA6 - NI2	0.434	0.938	0.334	0.344	0.585	0.400	0.599	0.464	0.444	0.297	0.308	0.442	0.876	0.521	0.636
YA6 - Δ MSC	0.066	-0.011	-0.169	0.071	-0.072	-0.015	0.383	0.268	0.203	-0.134	0.039	-0.099	0.300	0.243	0.438
YA7 - NI1	0.271	0.968	0.906	0.418	0.350	0.286	0.263	0.178	0.469	0.941	0.355	0.418	0.357	0.430	0.185
YA7 - NI2	0.226	0.938	0.769	0.424	0.374	0.217	0.342	0.191	0.319	0.786	0.381	0.360	0.381	0.436	0.278
YA7 - Δ MSC	-0.045	-0.030	-0.137	0.006	0.024	-0.070	0.078	0.013	-0.151	-0.155	0.026	-0.057	0.024	0.006	0.094

Again, different characteristics in EEG coherence due to the differences in underlying cortical functions per brain region, was observed by the non-deterministic changes in Δ MSC values across 15 pairs of brain region combinations on the same participant in Beta frequency (14-30 Hz). With young adult #1 (YA1), eight out of the fifteen brain region combinations showed a decrease in EEG coherence after the Trainer including the frontal – central (FC), frontal – temporal (FT), central – parietal (CP), central – occipital (CO), central – temporal (CT), parietal – temporal (PT), parietal occipital – occipital (POO), and occipital – temporal (OT) areas while seven other brain region combinations showed an increase in EEG coherence, which indicates high synchronization between the underlying EEG signals between the frontal and parietal (FP), frontal and parietal occipital (FPO), frontal and occipital (FO), central and parietal occipital (CPO), parietal and parietal occipital (PPO), parietal and occipital (PO), parietal occipital and temporal (POT) regions, as demonstrated by positive Δ MSC values.

Similar observation on the physiological variation in brain activities between different participants in Delta, Theta and Alpha frequency was also noted in Beta frequency as the pattern

in EEG coherence observed on one young adult does not apply to the behavior of EEG coherence on another young adult. For instance, while young adult #1 (YA1) showed a decrease in EEG coherence after the Trainer between the FC, FT, CP, CO, CT, PT, POO, and OT areas of the brain and an increase in EEG coherence in the FP, FPT, FO, CPO, PPO, and PO areas as listed in the example above; young adult #2 (YA2) showed an overall reduction in EEG coherence in all fifteen brain region combinations as shown in Table 10 with all negative Δ MSC values recorded across fifteen brain region combinations.

A paired-sample t-test on the change, or difference (Δ) in EEG coherence between NI1 and NI2 was conducted to evaluate if the decline in EEG coherence on TD young adults after interacting with the Trainer in Beta frequency is valid and between which areas in the brain, despite the physiological variation between seven participants. Table 11 presents the statistical results of the paired sample t-test on seven TD young adults across 15 brain region combinations. Other relevant statistics including the average mean Δ MSC, standard deviation (STD), and the 95% confidence interval range in which a population mean Δ MSC would fall between were also summarized in Table 11.

Table 11. Paired t-test summary statistics on the change in MSC (Δ MSC) between NI1 and NI2 on the study sample size of seven typical developing young adults ($n = 7$) in Beta frequency (14-30 Hz)

Young Adult (YA) subject # Change in MSC (Δ MSC)	Brain Region														
	FC	FP	FPO	FO	FT	CP	CPO	CO	CT	PPO	PO	PT	POO	POT	OT
YA1 - Δ MSC	-0.224	0.043	0.212	0.129	-0.095	-0.316	0.060	-0.041	-0.021	0.271	0.295	-0.439	-0.020	0.008	-0.002
YA2 - Δ MSC	-0.607	-0.182	-0.357	-0.401	-0.659	-0.616	-0.516	-0.552	-0.607	-0.493	-0.398	-0.732	-0.393	-0.733	-0.699
YA3 - Δ MSC	0.027	0.399	0.052	0.282	0.147	0.015	0.082	-0.009	0.155	0.169	-0.062	-0.146	0.074	0.102	-0.223
YA4 - Δ MSC	0.078	-0.427	-0.362	-0.403	-0.123	-0.109	-0.246	-0.224	-0.280	-0.162	-0.035	-0.171	-0.193	-0.286	-0.268
YA5 - Δ MSC	-0.162	-0.158	0.264	-0.076	-0.156	-0.168	-0.076	-0.460	-0.672	0.309	-0.197	-0.208	0.130	-0.275	-0.516
YA6 - Δ MSC	0.066	-0.011	-0.169	0.071	-0.072	-0.015	0.383	0.268	0.203	-0.134	0.039	-0.099	0.300	0.243	0.438
YA7 - Δ MSC	-0.045	-0.030	-0.137	0.006	0.024	-0.070	0.078	0.013	-0.151	-0.155	0.026	-0.057	0.024	0.006	0.094
Mean Δ MSC	-0.124	-0.052	-0.071	-0.056	-0.133	-0.183	-0.034	-0.144	-0.196	-0.028	-0.047	-0.265	-0.011	-0.134	-0.168
Standard Deviation (STD)	0.242	0.253	0.254	0.261	0.254	0.220	0.285	0.287	0.346	0.290	0.215	0.240	0.225	0.326	0.383
T-statistic	-1.357	-0.545	-0.738	-0.568	-1.392	-2.194	-0.312	-1.324	-1.501	-0.255	-0.585	-2.919	-0.131	-1.082	-1.161
p-value	0.112	0.303	0.244	0.295	0.107	0.035	0.383	0.117	0.092	0.404	0.290	0.013	0.450	0.160	0.145
95% Confidence Interval (CI) for the population mean	0.224	0.234	0.235	0.241	0.234	0.204	0.264	0.266	0.320	0.268	0.198	0.222	0.208	0.302	0.354
Lower bound CI	-0.300	-0.300	-0.300	-0.300	-0.400	-0.400	-0.300	-0.400	-0.500	-0.300	-0.200	-0.500	-0.200	-0.400	-0.500
Upper bound CI	0.100	0.182	0.164	0.185	0.101	0.021	0.230	0.122	0.124	0.240	0.151	-0.043	0.197	0.168	0.186

Table 11 shows that there is sufficient statistical evidence to believe that there is a change in the brain functional connectivity of typical developing young adults after interacting with the Trainer in Beta frequency, specifically there is a decrease in EEG coherence between the central and parietal (CP) and between the parietal and temporal (PT) areas in the brain of healthy young adults in Beta frequency due to the Trainer. Otherwise, there is a lack of statistical evidence to confirm findings with regard to EEG coherence in other brain regions including a decrease in EEG coherence between the frontal and central (FC) regions and between the central and temporal (CT) areas in Beta frequency as previously discovered from the paired t-test in both the Delta and Theta frequency. Compared to findings found from the paired t-test in Alpha frequency, which confirms only the reduction in EEG coherence after the Trainer in the parietal – temporal (PT) region of TD young adults, the decrease in EEG coherence in both the central – parietal (CP) regions and the parietal – temporal (PT) regions of healthy young adults after interaction with the Trainer was found to be statistically significant in Beta frequency.

Changes in EEG coherence after the Trainer in the brain of seven typical developing young adults in Beta frequency (14-30 Hz) as shown via Δ MSC values, were illustrated in Figure 2-10

below. A decrease in EEG coherence is indicated by negative bars. Likewise, positive bars signal an increase in EEG coherence after the Trainer.

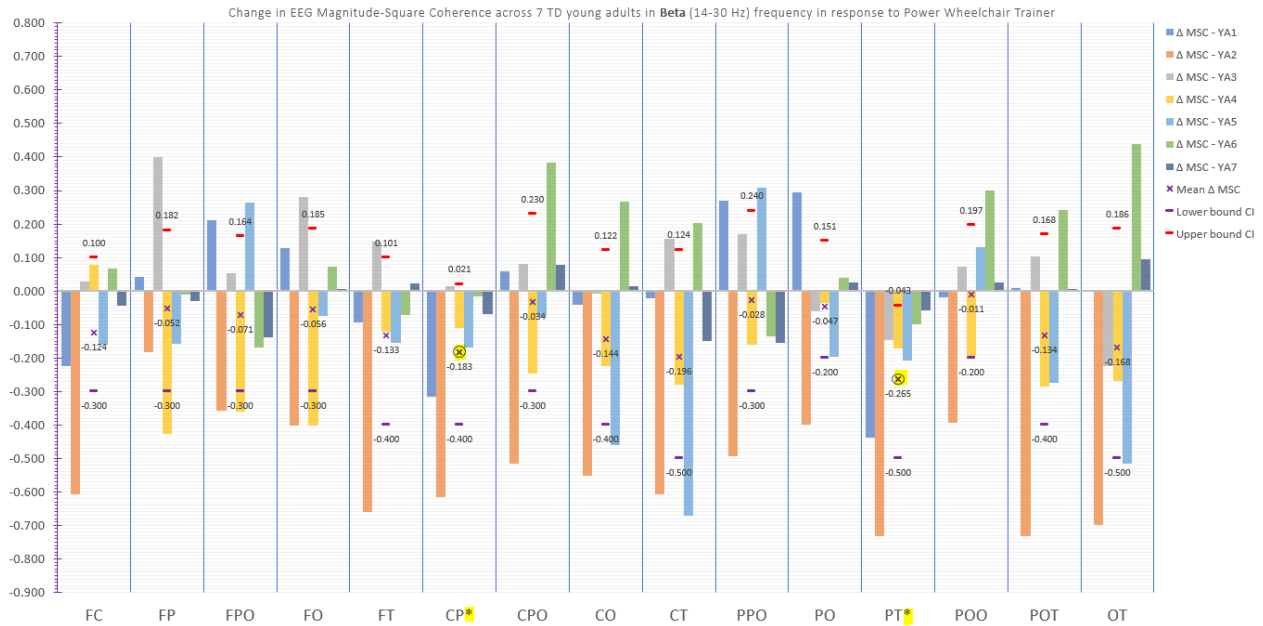


Figure 2-10. Change in EEG coherence across different brain regions on 7 TD young adults after interaction with the Power Wheelchair Trainer in Beta (14-30 Hz) frequency band. A “*” indicates brain regions in which the decrease in EEG coherence after the Trainer was found with significant p-values ($p \leq 0.05$)

Figure 2-10 shows a strong presence of negative bars that seems to signal an overall decrease in EEG coherence across fifteen brain region combinations on TD young adults in Beta frequency. Negative population mean Δ MSC (Mean Δ MSC) across all fifteen brain region combinations in Beta frequency also seems to confirm the observed pattern. Additionally, lower amplitude in Δ MSC in Beta frequency was also noted in Figure 2-10. The central - parietal (CP) and the parietal – temporal (PT) regions in which the decrease in EEG coherence in Beta frequency (14-30 Hz) was found to be statistically significant ($p \leq 0.05$), were highlighted in yellow with an asterisk to distinguish from other brain regions where the changes in EEG coherence lack statistical evidence on the impact of the Trainer on the functional connectivity in TD young adults. Both the lower and upper boundary of 95% confidence interval (CI) were shown to project the range

in which the mean Δ MSC for the young adult population would fall. For example, based on the sample size of seven TD young adults in our study, there is sufficient statistical evidence to believe that there is an average decrease of 0.183 in the EEG coherence between the central and parietal (CP) brain regions in Beta frequency (14 -30 Hz) on healthy young adults after interacting with the Trainer and the population mean Δ MSC will fall between -0.4 and 0.021 as projected by the lower and upper boundary of 95% confidence interval. Zero was included in this confidence interval implies that the Trainer could have either a positive or negative effect on the mean Δ MSC, or EEG coherence of the TD young adult population. Similar interpretation could be drawn for the parietal – temporal (PT) region regarding the effect of Trainer on TD young adults in Beta frequency (14-30 Hz). There is an average decrease of 0.265 in EEG coherence (mean Δ MSC = -0.265) between the parietal and temporal (PT) region of young adults in Beta frequency after using the Trainer, and we are 95% confident that the average decrease in EEG coherence for the TD adult population in Beta frequency will fall between -0.5 and -0.043, as estimated by the lower and upper 95% confidence interval boundary.

5. Gamma (31 – 100 Hz) Frequency

MSC values in Gamma frequency ranging from 31 Hz to 100 Hz were extracted from the overall time-frequency MSC between each combination of different brain regions, then averaged across the number of frequency sub-bands to obtain the representative MSC in Gamma band for each test condition i.e. No Interaction 1 (NI1) and No Interaction 2 (NI2). Table 12 summarizes the MSC between each pair of brain regions for a total of 15 inter-regional brain combinations on each young adult (YA) for the two test conditions (NI1 and NI2), and changes in MSC (Δ MSC) after the Trainer, which was calculated by subtracting the representative NI1 MSC value from

the representative NI2 MSC value in Gamma frequency, for all seven typical developing (TD) young adults participated in the study.

Table 12. Summary of the MSC for all 7 participants in 2 test conditions (NI1 – 5-min before the Trainer and NI2 – 5-min after the Trainer) and the resulting difference in MSC (Δ MSC) across various brain regions in *Gamma* frequency (31 -100 Hz)

Young Adult (YA) subject # - Condition	Brain Region														
	FC	FP	FPO	FO	FT	CP	CPO	CO	CT	PPO	PO	PT	POO	POT	OT
YA1 - NI1	0.514	0.749	0.301	0.503	0.322	0.543	0.189	0.252	0.295	0.214	0.337	0.565	0.535	0.223	0.234
YA1 - NI2	0.224	0.676	0.485	0.576	0.200	0.217	0.217	0.232	0.258	0.400	0.501	0.230	0.519	0.209	0.170
YA1 - Δ MSC	-0.290	-0.073	0.184	0.073	-0.123	-0.327	0.029	-0.020	-0.037	0.187	0.164	-0.335	-0.016	-0.014	-0.064
YA2 - NI1	0.632	0.989	0.976	0.966	0.795	0.618	0.664	0.602	0.725	0.970	0.963	0.746	0.967	0.748	0.706
YA2 - NI2	0.174	0.779	0.550	0.556	0.247	0.200	0.215	0.188	0.226	0.459	0.559	0.167	0.615	0.166	0.172
YA2 - Δ MSC	-0.457	-0.210	-0.426	-0.410	-0.547	-0.418	-0.448	-0.414	-0.499	-0.512	-0.404	-0.579	-0.352	-0.582	-0.534
YA3 - NI1	0.168	0.449	0.573	0.417	0.201	0.178	0.165	0.174	0.208	0.493	0.896	0.413	0.513	0.193	0.399
YA3 - NI2	0.174	0.839	0.687	0.688	0.308	0.171	0.187	0.160	0.349	0.737	0.822	0.189	0.683	0.198	0.161
YA3 - Δ MSC	0.006	0.390	0.114	0.271	0.107	-0.007	0.022	-0.014	0.141	0.244	-0.074	-0.224	0.170	0.005	-0.238
YA4 - NI1	0.442	0.754	0.625	0.714	0.453	0.630	0.704	0.670	0.660	0.908	0.957	0.710	0.896	0.795	0.702
YA4 - NI2	0.412	0.281	0.226	0.249	0.267	0.465	0.349	0.333	0.300	0.655	0.883	0.431	0.668	0.330	0.348
YA4 - Δ MSC	-0.029	-0.474	-0.399	-0.466	-0.186	-0.165	-0.355	-0.337	-0.360	-0.253	-0.074	-0.279	-0.228	-0.465	-0.354
YA5 - NI1	0.370	0.818	0.357	0.671	0.313	0.445	0.537	0.603	0.771	0.368	0.701	0.400	0.338	0.460	0.520
YA5 - NI2	0.243	0.692	0.528	0.528	0.264	0.276	0.394	0.235	0.196	0.679	0.389	0.193	0.326	0.204	0.188
YA5 - Δ MSC	-0.127	-0.126	0.171	-0.143	-0.048	-0.169	-0.144	-0.369	-0.575	0.311	-0.312	-0.207	-0.013	-0.257	-0.332
YA6 - NI1	0.484	0.939	0.481	0.240	0.683	0.479	0.225	0.210	0.272	0.410	0.231	0.581	0.522	0.241	0.208
YA6 - NI2	0.668	0.930	0.391	0.401	0.644	0.627	0.448	0.418	0.519	0.360	0.371	0.522	0.873	0.585	0.651
YA6 - Δ MSC	0.184	-0.010	-0.089	0.161	-0.040	0.148	0.224	0.208	0.247	-0.050	0.140	-0.059	0.351	0.344	0.443
YA7 - NI1	0.229	0.951	0.880	0.424	0.292	0.243	0.217	0.226	0.328	0.914	0.346	0.368	0.399	0.382	0.162
YA7 - NI2	0.262	0.928	0.760	0.507	0.331	0.253	0.379	0.291	0.219	0.784	0.453	0.307	0.458	0.280	0.226
YA7 - Δ MSC	0.033	-0.023	-0.119	0.083	0.039	0.010	0.161	0.065	-0.109	-0.129	0.107	-0.060	0.060	-0.102	0.064

The non-deterministic behaviors of EEG coherence as illustrated by different MSC values and Δ MSC values across 15 inter-regional brain combinations per participant in Gamma frequency (31-100 Hz) in Table 12 again, suggests the differences in EEG coherence between different brain regions. For example, young adult #1 (YA1) showed a decrease in EEG coherence after the Trainer, which is denoted by negative values in Δ MSC in the frontal – central (FC), frontal – parietal (FP), frontal – temporal (FT), central – parietal (CP), central – occipital (CO), central – temporal (CT), parietal – temporal (PT), parietal occipital – occipital (POO), parietal occipital – temporal (POT), and in the occipital – temporal (OT) regions. However, the frontal - parietal occipital (FPO), frontal - occipital (FO), central-parietal occipital (CPO), parietal – parietal occipital (PPO), and the parietal – occipital (PO) regions of YA1 showed an increase in EEG coherence after the Trainer. Biological variation in EEG coherence between participants was also demonstrated in Table 12 with a combination of both positive and negative Δ MSC for the same brain region combination, but on different young adults. For instance, a reduction in EEG

coherence between the frontal and central (FC) area in the brain after the Trainer was observed in four young adults (YA1, YA2, YA4, YA5) while an increase in EEG coherence in the FC area was noted in YA3, YA6, and YA7 by the positive Δ MSC values.

A paired-sample t-test on the changes, or difference in EEG coherence (Δ MSC) between NI1 and NI2 was conducted to evaluate if the decline in EEG coherence on TD young adults after interacting with the Trainer in Gamma frequency is statistically sound and between which brain regions, despite the physiological variation between participants. Table 13 presents the statistical results of the paired sample t-test on 7 TD young adults across 15 inter-regional brain combinations. Other relevant statistics including the average mean Δ MSC, standard deviation (STD), and the 95% confidence interval range in which a population mean Δ MSC would fall between were also summarized in Table 13.

Table 13. Paired t-test summary statistics on the change in MSC (Δ MSC) between NI1 and NI2 on the study sample size of seven typical developing young adults ($n = 7$) in *Gamma* frequency (31-100 Hz)

Young Adult (YA) subject # Change in MSC (Δ MSC)	Brain Region														
	FC	FP	FPO	FO	FT	CP	CPO	CO	CT	PPO	PO	PT	POO	POT	OT
YA1 - Δ MSC	-0.290	-0.073	0.184	0.073	-0.123	-0.327	0.029	-0.020	-0.037	0.187	0.164	-0.335	-0.016	-0.014	-0.064
YA2 - Δ MSC	-0.457	-0.210	-0.426	-0.410	-0.547	-0.418	-0.448	-0.414	-0.499	-0.512	-0.404	-0.579	-0.352	-0.582	-0.534
YA3 - Δ MSC	0.006	0.390	0.114	0.271	0.107	-0.007	0.022	-0.014	0.141	0.244	-0.074	-0.224	0.170	0.005	-0.238
YA4 - Δ MSC	-0.029	-0.474	-0.399	-0.466	-0.186	-0.165	-0.355	-0.337	-0.360	-0.253	-0.074	-0.279	-0.228	-0.465	-0.354
YA5 - Δ MSC	-0.127	-0.126	0.171	-0.143	-0.048	-0.169	-0.144	-0.369	-0.575	0.311	-0.312	-0.207	-0.013	-0.257	-0.332
YA6 - Δ MSC	0.184	-0.010	-0.089	0.161	-0.040	0.148	0.224	0.208	0.247	-0.050	0.140	-0.059	0.351	0.344	0.443
YA7 - Δ MSC	0.033	-0.023	-0.119	0.083	0.039	0.010	0.161	0.065	-0.109	-0.129	0.107	-0.060	0.060	-0.102	0.064
Mean Δ MSC	-0.097	-0.075	-0.081	-0.061	-0.114	-0.133	-0.073	-0.126	-0.170	-0.029	-0.065	-0.249	-0.004	-0.153	-0.145
Standard Deviation (STD)	0.216	0.259	0.256	0.286	0.214	0.198	0.254	0.244	0.316	0.297	0.224	0.179	0.235	0.313	0.325
T-statistic	-1.194	-0.766	-0.832	-0.568	-1.409	-1.769	-0.760	-1.363	-1.423	-0.258	-0.767	-3.690	-0.046	-1.293	-1.178
p-value	0.139	0.236	0.219	0.295	0.104	0.064	0.238	0.111	0.102	0.402	0.236	0.005	0.482	0.122	0.142
95% Confidence Interval (CI) for the population mean	0.199	0.240	0.237	0.264	0.198	0.184	0.235	0.226	0.293	0.275	0.207	0.165	0.217	0.289	0.301
Lower bound CI	-0.300	-0.300	-0.300	-0.300	-0.300	-0.300	-0.300	-0.400	-0.500	-0.300	-0.300	-0.400	-0.200	-0.400	-0.400
Upper bound CI	0.102	0.165	0.156	0.203	0.084	0.051	0.162	0.100	0.122	0.246	0.142	-0.084	0.213	0.136	0.156

Similar to findings found from the paired t-test in Alpha frequency, which confirms only the reduction in EEG coherence after the Trainer in the parietal – temporal (PT) region of TD young adults, only the decrease in EEG coherence between the parietal and temporal (PT) regions in the brain of seven TD young adults after the Trainer was found to be statistically significant ($p \leq 0.05$) in Gamma frequency. Otherwise, there is a lack of statistical evidence to draw any conclusion on findings with regard to a decrease in EEG coherence in other brain regions on healthy young adults after interacting with the Trainer including the decrease in EEG coherence between the central and parietal (CP) region as previously discovered in Beta frequency and a decrease in EEG coherence in the frontal - central (FC), central - parietal (CP), and the central – temporal (CT) regions as previously found in both the Delta (1-4 Hz) and Theta (5-7 Hz) frequency.

Changes in EEG coherence after the Trainer, as illustrated by Δ MSC in the brain of seven TD young adults in Gamma (31-100 Hz) frequency were summarized in Figure 2-11. A decrease in EEG coherence is indicated by negative bars while positive bars signal an increase in coherence after the Trainer.

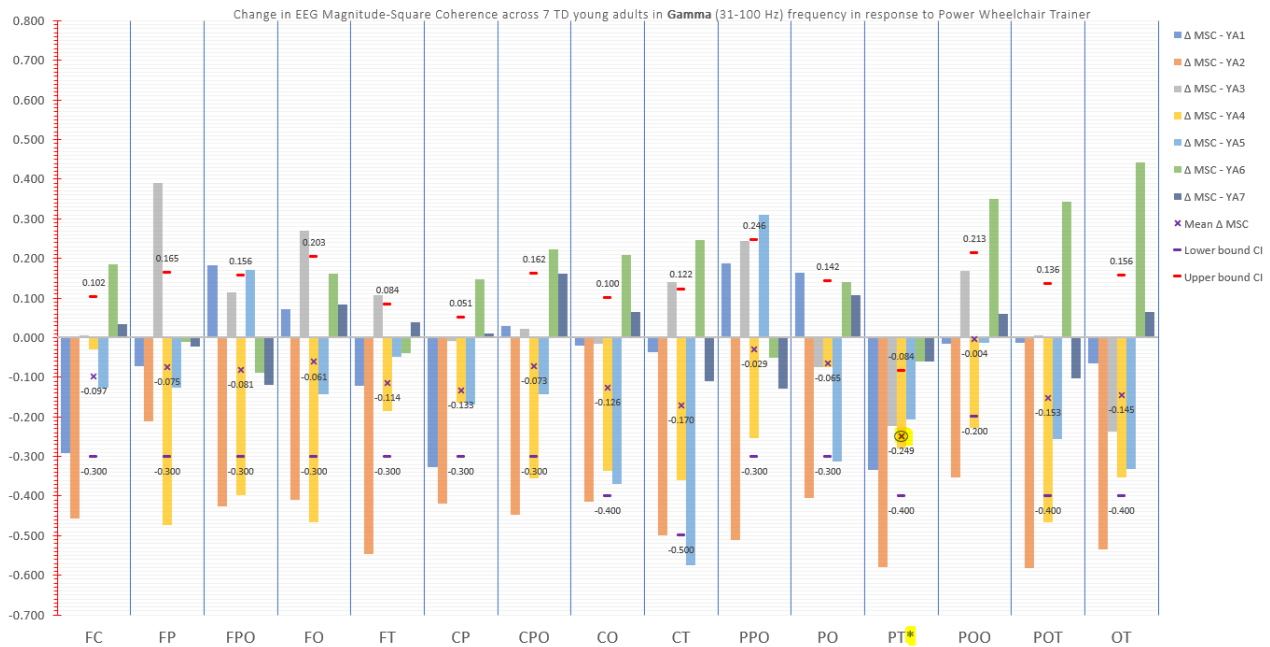


Figure 2-11. Change in EEG coherence across different brain regions on 7 TD young adults after interaction with the Power Wheelchair Trainer in *Gamma* frequency (31-100 Hz). A”*” indicates brain regions in which the decrease in EEG coherence was found with significant p-values ($p \leq 0.05$)

A reduction in amplitude of Δ MSC in *Gamma* frequency as compared to the amplitude of Δ MSC in other frequency bands, particularly in the *Delta* and *Theta* frequency, was observed in Figure 2-11. Δ MSC represents the changes in EEG coherence after the Trainer thus, a lower amplitude in Δ MSC indicates less changes in the EEG coherence in *Gamma* frequency.

Additionally, the strong presence of negative bars that outnumbered positive bars in Δ MSC (change in EEG coherence after the Trainer) in Figure 2-11 seems to suggest an overall decrease in EEG coherence across fifteen inter-regional brain combinations on TD young adults in

Gamma frequency. Negative population mean Δ MSC (Mean Δ MSC) across all fifteen inter-regional brain combinations in *Gamma* frequency also seems to confirm the observed pattern.

The parietal – temporal (PT) regions in which the decrease in EEG coherence was found to be statistically significant in *gamma* frequency was highlighted in yellow with a superscripted asterisk to distinguish from other brain regions where there was a lack of statistical evidence to

draw any conclusion regarding the decrease in EEG coherence after the Trainer. Both the lower and upper boundary of 95% confidence interval (CI) showed the range in which the population mean Δ MSC is projected to fall between. Based on the sample size of seven healthy young adults, there is statistical evidence to believe that there is an average decrease of 0.249 in EEG coherence (mean Δ MSC = -0.249) in the parietal – temporal brain region and we are 95% confident that the population mean Δ MSC will fall between -0.084 and -0.4 as projected by the lower and upper boundary of 95% confidence interval accordingly. The fact that zero was not included in this confidence interval suggests that the average change in EEG coherence (mean Δ MSC) in the typical developing young adult population would be negative, which translates to a decrease in coherence between the parietal and temporal regions in the brain after interacting with the Power Wheelchair Trainer in Gamma frequency.

Table 14 summarizes the decrease in EEG coherence in brain regions found with statistical significance ($p \leq 0.05$) from the paired t-test on the changes, or differences in the EEG inter-regional coherence after operating the Power Wheelchair Trainer on seven typical developing young adults aged 18 to 24 in five frequency bands of interest.

Table 14. Summary of the paired t-test on the changes in EEG inter-regional coherence between various regions in the brain with statistical significance ($p \leq 0.05$) on seven healthy young adults after operating the Trainer in five frequency bands of interest.

Frequency Bands	Brain Region															▼ Decrease in coherence ▲ Increase in coherence	
	FC	FP	FPO	FO	FT	CP	CPO	CO	CT	PPO	PO	PT	POO	POT	OT		
Delta (1-4 Hz)	▼					▼			▼			▼					
Theta (5-7 Hz)	▼					▼			▼			▼					
Alpha (8-13 Hz)												▼					
Beta (14-30 Hz)						▼						▼					
Gamma (31-100 Hz)												▼					

Since the key assumption for the paired t-test is the normality of the data, the Wilk-Shapiro test was conducted to examine the normality assumption of the data, which is the differences, or changes in EEG coherence after the Trainer (Δ MSC) in this context. Table 15 shows the results from the Shapiro-Wilk test to determine whether the changes in EEG coherence on the study sample size of seven healthy young adults randomly drawn from the typical developing 18-to-24-year-old young adult population, follow a normal probability distribution.

Table 15. Wilk-Shapiro test of normality on the changes, or differences in EEG inter-regional coherence between various regions in the brain of seven healthy young adults after using the Trainer in five frequency bands of interest. A cell highlighted in yellow indicates violation to the normality assumption in the Wilk-Shapiro test

Frequency Bands	Brain Region														
	FC	FP	FPO	FO	FT	CP	CPO	CO	CT	PPO	PO	PT	POO	POT	OT
Delta (1-4 Hz)	0.198	0.714	0.665	0.035	0.079	0.500	0.045	0.971	0.496	0.076	0.536	0.461	0.941	0.151	0.790
Theta (5-7 Hz)	0.937	0.010	0.976	0.764	0.663	0.560	0.209	0.140	0.419	0.658	0.636	0.599	0.114	0.440	0.830
Alpha (8-13 Hz)	0.615	0.367	0.611	0.535	0.028	0.347	0.611	0.751	0.181	0.509	0.105	0.599	0.663	0.581	0.794
Beta (14-30 Hz)	0.071	0.734	0.387	0.366	0.038	0.100	0.746	0.687	0.469	0.394	0.854	0.053	0.892	0.443	0.981
Gamma (31-100 Hz)	0.777	0.323	0.193	0.324	0.100	0.861	0.525	0.274	0.651	0.681	0.269	0.402	0.943	0.892	0.660

The null hypothesis (H_0) in the Wilk-Shapiro test assumes that the data, i.e., Δ MSC values (changes in EEG coherence after the Trainer) obtained for each pair of brain region combinations from the seven participants participated in the study, is not normally distributed while the alternative hypothesis (H_A) assumes the opposite. At the significance level alpha of 0.05 (a 95% confidence interval), a small p-value ($p \leq 0.05$) indicates strong evidence against the null hypothesis thus, the null hypothesis can be rejected. Results from the Wilk-Shapiro test in Table 15 indicate that per frequency band, there are areas in the brain where the changes in EEG coherence after the Trainer (Δ MSC) from our study sample size do not meet the normally distributed assumption. For example, in Delta frequency which ranges from 1 Hz to 4 Hz, the changes in EEG coherence after the Trainer between the frontal and occipital (FO) regions and between the central and parietal occipital (CPO) regions on our study sample size of seven, are not normally distributed. In Theta frequency, it is the changes in EEG coherence after the Trainer

(Δ MSC) between the frontal and parietal (FP) regions failed to meet the normal distribution assumption. Non-conformity to the normality assumption of the data i.e. Δ MSC (changes in EEG coherence after the Trainer) was also found between the frontal and temporal (FT) areas in both the Alpha and Beta frequency.

Results from the Wilk-Shapiro test were superimposed over the summary findings from the paired t-test on the changes in EEG coherence between fifteen inter-regional brain combinations in five frequency bands of interest in Table 16.

Table 16. Overlaid results from the Wilk-Shapiro test of normality and the paired t-test on the changes in EEG inter-regional coherence between various regions in the brain of seven healthy young adults after the Trainer in five different frequency ranges

Frequency Bands	Brain Region														
	FC	FP	FPO	FO	FT	CP	CPO	CO	CT	PPO	PO	PT	POO	POT	OT
Delta (1-4 Hz)	▼			✘		▼	✘		▼			▼			
Theta (5-7 Hz)	▼	✘				▼			▼			▼			
Alpha (8-13 Hz)					✘							▼			
Beta (14-30 Hz)					✘	▼						▼			
Gamma (31-100 Hz)												▼			

▼ Decrease in coherence
 ▲ Increase in coherence
 ✘ Failed to meet the normality assumption

Based on the results from the Wilk-Shapiro test, brain regions in which the changes in EEG coherence (Δ MSC) per frequency range were found coming from a non-normally distributed pool, are highlighted in yellow with a cross mark. Table 16 shows that the results from the Wilk-Shapiro test endorse findings from the paired t-test on the brain region combinations with statistical significance (as illustrated by the red downward triangle) since they uphold to the assumption of normality in the data. It could be seen that violation to the normality assumption occurs in brain region combinations where the decrease in EEG coherence after the Trainer lack of statistical power from the paired t-test. The assumption of normality in the data is critical to the validity of the paired t-test thus a violation to the normally-distributed assumption would impact the results from the paired t-test on the changes, or differences in EEG coherence after

the Trainer obtained in five frequency bands of interest. This translates to our findings regarding changes in EEG coherence in these brain regions are inconclusive, due to unmet assumption regarding normality of the data.

Since violation to the normality assumption was found in several brain region combinations, the Wilcoxon signed rank test – a non-parametric equivalence of the paired sample t-test that does not make any assumption about the underlying distribution, was conducted to verify statistical evidence regarding the impact of the Trainer on EEG coherence of typical developing young adults. Table 17 shows the results from the Wilcoxon signed-rank test on the changes in EEG coherence after the Trainer (Δ MSC) across various regions in the brain of healthy young adults in five frequency bands of interest. Keen observations and preliminary results thus far indicate a decrease in EEG coherence after the Trainer thus a left-tailed Wilcoxon signed rank at the 5% significance level, or 95% confidence level was selected, in place of a two-tailed test.

Table 17. Left-tailed Wilcoxon signed rank test at the 5% significance level on the changes in EEG inter-regional coherence between various regions in the brain of seven healthy young adults after the Trainer in five different frequency ranges

Table 17-1. Statistical p-values of the left-tailed Wilcoxon signed rank test on the changes in EEG inter-regional coherence in TD young adults after the Trainer in five frequency bands of interest

Frequency Bands	Brain Region														
	FC	FP	FPO	FO	FT	CP	CPO	CO	CT	PPO	PO	PT	POO	POT	OT
Delta (1-4 Hz)	0.078	0.344	0.406	0.469	0.109	0.039	0.469	0.078	0.078	0.344	0.055	0.039	0.344	0.531	0.188
Theta (5-7 Hz)	0.078	0.148	0.531	0.594	0.109	0.055	0.344	0.078	0.078	0.469	0.234	0.016	0.289	0.406	0.188
Alpha (8-13 Hz)	0.469	0.234	0.234	0.289	0.023	0.078	0.656	0.148	0.188	0.289	0.148	0.016	0.469	0.109	0.406
Beta (14-30 Hz)	0.188	0.234	0.289	0.406	0.109	0.023	0.531	0.148	0.148	0.594	0.289	0.008	0.594	0.289	0.148
Gamma (31-100 Hz)	0.234	0.109	0.344	0.406	0.078	0.078	0.406	0.148	0.148	0.469	0.406	0.008	0.469	0.109	0.188

Table 17-2. Summary of the Wilcoxon-signed rank test with statistical significance ($p \leq 0.05$) on the changes in EEG inter-regional coherence in TD young adults after the Trainer in five frequency bands of interest

Frequency Bands	Brain Region															
	FC	FP	FPO	FO	FT	CP	CPO	CO	CT	PPO	PO	PT	POO	POT	OT	
Delta (1-4 Hz)						↓						↓				
Theta (5-7 Hz)												↓				
Alpha (8-13 Hz)					↓							↓				
Beta (14-30 Hz)						↓						↓				
Gamma (31-100 Hz)												↓				

↓ Decrease in coherence
↑ Increase in coherence

Similar to the null hypothesis set out for the paired t-test, the null hypothesis (H_0) in the Wilcoxon-signed rank test assumes that there is no change in the EEG coherence of healthy young adults after operating the trainer (Δ MSC) against the alternative hypothesis (H_A) for the left-tailed test that the change in EEG coherence will be less than 0, i.e. there is a decrease in coherence after the Trainer. At the 5% significance level alpha, a small p-value ($p \leq 0.05$) casts doubt on the validity of the null hypothesis thus the null hypothesis can be rejected.

For ease of visualization and comparison of results obtained from different tests, the results from all three statistical tests conducted on the change in EEG coherence after the Trainer (Δ MSC) including the paired t-test, the Wilk-Shapiro test, and the Wilcoxon signed-rank test were summarized in Table 18. Note that the table only illustrates the brain region combinations in which the decrease in EEG inter-regional coherence on TD young adults after the Trainer was found with statistical significance per frequency band of interest.

Table 18. Summary of all statistical tests used in the study with significant p-values ($p \leq 0.05$) on the changes in EEG inter-regional coherence in TD young adults after the Trainer in five frequency bands of interest

Frequency Bands	Brain Region														
	FC	FP	FPO	FO	FT	CP	CPO	CO	CT	PPO	PO	PT	POO	POT	OT
Delta (1-4 Hz)	▼			*		▼↓	*		▼			▼↓			
Theta (5-7 Hz)	▼	*				▼			▼			▼↓			
Alpha (8-13 Hz)					*↓							▼↓			
Beta (14-30 Hz)					*↓	▼↓						▼↓			
Gamma (31-100 Hz)												▼↓			

▼ Decrease in coherence from the paired t-test

↓ Decrease in coherence from the Wilcoxon signed-rank test

* Violation to normality assumption from the Wilk-Shapiro test

Results from the Wilcoxon-signed rank test in both Table 17 and Table 18 show that there are areas in the brain where the decrease in coherence between two EEG regions after the Trainer is statistically significant per frequency band of interest; however, there are also brain region combinations in which the decrease in coherence was previously found to be statistically significant from the paired t-test, yet appear to lack statistical significance from the Wilcoxon-signed-rank test. For example, in the Delta frequency, the Wilcoxon-signed rank test confirms the decrease in EEG coherence between the central and parietal (CP) regions and between the parietal and temporal (PT) regions yet negates the decrease in EEG coherence between the frontal and central (FC) regions and between the central and temporal (CT) regions, as previously found from the paired t-test. In Theta frequency, contrary to findings resulted from the paired t-test, there is not sufficient statistical evidence from the Wilcoxon signed-rank test to draw any conclusion regarding the reduction in EEG coherence between the frontal-central (FC) regions, central-parietal (CP) regions, and central-temporal (CT) regions. However, the Wilcoxon signed-rank test does confirm the decrease in EEG coherence between the central-parietal (CP) regions and the parietal-temporal (PT) lobes in the brain of healthy young adults after the Trainer. Another contrast difference between the paired t-test and the Wilcoxon signed-

rank test can be observed in the Alpha rhythm. The decrease in EEG coherence in healthy young adults after the Trainer between the frontal and temporal regions was found with statistical significance from the Wilcoxon signed-ranked test whereas the findings were found not to be significant by the paired t-test. Additionally, result from the Wilk-Shapiro test on Δ MSC between the frontal and temporal regions in the Alpha frequency indicates a violation to the normal distribution assumption necessary for the paired t-test. Beside significant differences in the results obtained from the changes in EEG coherence after the Trainer in the Delta, Theta, and Alpha frequency bands, results from the Wilcoxon signed-rank test regarding the decrease in EEG coherence after the Trainer align with the results obtained from the paired t-test in both the Beta and Gamma frequency. The reduction in EEG coherence in Beta frequency between the central-parietal (CP) regions and between the parietal-temporal (PT) lobes in the brain of healthy young adults after active usage of the Trainer was confirmed by both the paired t-test and the Wilcoxon signed-rank test. Similarly, the decrease in EEG coherence in Gamma frequency between the parietal and temporal (PT) lobes in the brain of TD young adults after operating the Trainer was first discovered by the paired t-test then corroborated with the results from the Wilcoxon signed-rank.

Since results from the Wilk-Shapiro test indicated violation to the normality assumption that is fundamental for the paired t-test to uphold its validity, findings from the paired t-test should be interpreted with caution. Due to its independence from the normality assumption, the Wilcoxon signed-rank test yields more definitive and unassailable results with regard to the decrease in EEG coherence between different brain regions and in five different frequency ranges on healthy young adults (aged 18-24) after operating the Trainer.

2.4 Discussion

The goal of this study was to examine neural processes invoked between different functional lobes in the brain of healthy young adults and how this neural network connectivity behaves at different frequencies in response to power mobility training. The study used a measure named Magnitude-Square Coherence (MSC) derived from the scalp EEG as a means to explore the functional connectivity in the brain of healthy young adults after active usage of the power mobility trainer (the Trainer) in five frequency rhythms: delta (1-4 Hz), theta (4-7 Hz), alpha (8-13 Hz), beta (13-30 Hz), and gamma (31 -100 Hz) frequency. As the dependent variable of interest, EEG coherence was obtained from systematically-cleaned EEG data across six functional regions in the brain, including the frontal, central, parietal, parietal-occipital, and temporal areas from NI1 and NI2 conditions when participants were in resting states, awake yet immobile with eyes closed. Changes in EEG coherence due to interaction with the Trainer were reflected by delta coherence between NI1 and NI2 (Δ MSC). A negative Δ MSC indicates a decrease in coherence after the Trainer while a positive Δ MSC denotes an increase in coherence after the Trainer.

Our results demonstrated that the systematic exchange of information established between various regions in the brain of healthy young adults aged from 18 to 24 after using the Trainer was evident, particularly an overall decrease in EEG coherence from a group of seven healthy young adults after the task of operating the power mobility trainer was recorded in all five frequency bands of interest. High coherence between two EEG sites indicates high level of excitability between two regions thus, an elevated level of excitability when the participant is in relaxing state with eyes closed and minimal-to-no stimuli may associate with abnormal neural

oscillations and synchrony. In fact, high coherence in the brain of young adults in relaxing state has been negatively correlated to attention deficit hyperactivity disorder (ADHD), seizure, schizophrenia, and depression. There is a growing body of evidence suggesting that altered brain connectivity may be a defining feature of disorders such as ADHD, depression, general anxiety disorder, Asperger syndrome, and headaches. From many of the psychiatric disorders, EEG coherence is the most researched in ADHD. Many studies utilizing EEG coherence have shown significant differences between the neurotypical control and ADHD subjects. Markovska-Simoska et al.⁴¹ found that in eyes opened condition, ADHD patients expressed an increased coherence in central regions in theta frequency and an increased coherence in posterior regions in delta frequency. The study also found an increased intra-hemispheric coherence for patients with headaches in the anterior regions for delta band and in the posterior regions for theta band. Song et al. showed a pattern of strong EEG coherence centered on temporal lobe structures in several patients with epilepsy.⁴⁶ Bowyer et al. used Magnetoencephalography Coherence Source Imaging (MEG-CSI), which had been applied successfully for detecting coherent areas in the cortical networks of patients with epilepsy⁴⁷, to investigate brain imaging with biomarkers of schizophrenia⁴⁸. The study found increased regions of coherence across a large frequency range (3–50Hz) in schizophrenia patients compared to controls in the medial and ventrolateral prefrontal cortex and anterior cingulate cortex. These areas are involved in language, memory, decision making, empathy, executive and higher cognitive functioning. Using the same technique (MEG-CSI), Boutros et al. looked at the connectivity in patients with panic disorder⁴⁹; where they found coherence imaging values were significantly higher in panic patients compared to controls during a 10-minute, eyes open, resting state scan. The strong pattern in the elevated coherence observed in the panic patient group led to their proposal of using the increased

coherence i.e. increased excitability as a promising biomarker for favorable responses to medications that limit excitatory transmission, such as antiseizure drugs. Another research group – Lajiness-O’Neil et al. have also applied the same technique to study the neural synchrony during eye gaze in patients with autism spectrum disorder (ASD).⁵⁰ Significantly higher coherence and synchronization in posterior brain regions including the temporal, parietal, and occipital areas across all frequencies was evident in ASD patients, particularly within the low 0 to 15 Hz frequency range. However, EEG coherence studies in patients with depression showed a mixture of different results. Some studies for patients with depressive disorder reported reduced coherence values compared to healthy controls⁵¹⁻⁵² while other studies showed significantly higher overall or partial coherence in patients with major depressive disorder as compared to controls.⁵³⁻⁵⁵ Findings of Leuchter et al.^{38,53} claimed that patients with depression had significantly higher overall coherence as compared to controls in delta, theta, alpha, and beta frequency bands. The overall greater coherence observed in depressed subjects establishes a new context for the interpretation of previous studies showing differences in delta, theta, alpha, and beta frequency and synchrony between subjects with depression and normal controls. However, contrary to these results, the experiments of Suhhova et al.⁴⁰ demonstrated no significant changes in the EEG coherence between healthy subjects and patients with depression or reduced coherence values compared to healthy control in alpha, theta, and beta rhythms. Li et al.⁵⁴ explained that the increase in theta, alpha and beta in the frontal/prefrontal sites might reflect the overcompensatory mechanism to maintain normal cognitive performance. Thus, it is reasonable to suggest that typical developing young adults exhibit lower coherence in the delta, theta, alpha and beta bands, which was confirmed by our findings regarding an overall decrease in EEG coherence on healthy young adults after operating the Trainer and sitting in relaxing state with

eyes closed. The decrease in coherence from our study group of seven neurotypical young adults after interacting with the Trainer in the frequency bands that are associated with deep sleeps and meditation such as delta and theta frequency might serve as an indicator that all participants were not engaged in deep-relaxing states and the brain perhaps is more active in higher ordered cognitive functions.

Specific regions in the brain are specialized for processing certain types of information. The frontal lobe is important for cognitive functions such as thinking, planning, and control of voluntary movement or activity. The parietal lobe processes information about perception, temperature, taste, touch, and movement while the occipital lobe is primarily responsible for vision. The temporal lobe processes memories, integrating them with sensations of taste, touch, sight, and sound. However, it is imperative to note the level of harmony in the brain i.e. each lobe in the brain does not function alone. There are complex relationships and frequent communication exchanges between the lobes of the brain and between the right and left hemispheres. Operating the power wheelchair trainer is a motor task that requires a high level of coordination between various regions in the brain for purposefully skilled movements. Results from both the paired t-test and the Wilcoxon-signed rank test provided a striking statistical evidence on the diminished coherence between the parietal and temporal regions in the brain of healthy young adults in all five frequency bands. Since the parietal lobe plays a large role in visuomotor tasks including the understanding of intention, spatial attention, episodic memory retrieval, movement⁶⁰⁻⁶² and the temporal lobe is heavily associated with the formation of memories, the reduced coherence between these two regions suggests the brain might be active

in higher order cognitive functions such as the visuomotor, attention, formation as well as consolidation of memory required for operating and controlling of the power mobility trainer.

Intrinsic activity of the brain typically measured when an individual is awake and immobile (i.e., in a “resting state”), has proven effective at identifying various functional brain networks.

Decades of research on this activity have led to the fact that some rhythms are robustly characteristic of particular brain regions, functions, and states. Delta frequency is found to be prevalent in frontal areas and in superior temporal and inferior parietal regions. In healthy adults, delta frequency is broadly distributed at the scalp, being largest over frontal and medial centroparietal sites.^{12,44} This aligns with our findings with regard to the presence of delta coherence in the centro-parietal regions. In delta frequency, our study showed a decrease in coherence between the central and parietal (CP) regions as well as between the parietal and temporal (PT) regions. Theta waves, which is most prominently seen over frontal midline locations in EEG scalp recordings, has been found to be modulated by multiple cognitive demands such as working memory and error monitoring. Theta has been associated with the temporal lobe in human intracranial recordings, though various tasks including navigation, speech comprehension, and working memory have been shown to modulate theta in occipital, frontal, pericentral, and orbitofrontal areas. Markovska-Simoska et al.⁴¹ found that in theta frequency, lower coherence was observed in the group with Asperger syndrome compared to the control group, ADHD, and headaches in parietal region. Meanwhile, Xing et al.⁵⁶ found increased oscillatory midline coherence in the theta frequency band indicating higher connectivity in the generalized social anxiety disorder relative to healthy control group during rest. In our study, the decrease in coherence between the central and parietal (CP) regions found

in delta frequency and between the parietal-temporal (PT) regions in theta rhythm may reflect a state of relaxed alertness by guarding against extremes of arousal stimuli.

Alpha frequency is increased by the lack of attention and visual input. Some interpret alpha as an idling rhythm that self-organizes when cortical areas are disengaged. However, there is a growing evidence that the presence of alpha frequency may modulate local cortical activity suggests that it serves an active role in attention and sensory processing and mediates communication between different cortical areas. Alpha is predominantly generated by the occipital cortex and is found to a lesser extent in the parietal and temporal lobes. Our result aligns with the findings since there was significantly lower inter-regional coherence between the parietal and temporal lobes in alpha frequency on young adults in waking resting state (eyes closed yet awake and immobile). Thus, it is suggested that a decrease in alpha coherence found in our study can be attributed to the brain was mediating communication across various lobes and regions. The decrease in coherence in both alpha and theta rhythm can be interpreted as signifiers of an elevated level of attention with alpha specifically representing the level of internalized attention as well as indexing states of relaxation.⁶³

The beta rhythm - the frequency ranges from 14 Hz to 30 Hz, is normally present during a waking state. They allow for logical thought processes, and therefore are instrumental in problem-solving and decision-making activities. Normal presence of beta frequency is heavily associated with the engagement in conscious thought and logical reasoning such as difficult work tasks or schoolwork. The optimal level of beta wave action allows people to focus consciously on tasks, perform problem-solving and remember things since an elevated level of beta waves is

affiliated with anxiety, inability to relax, and stress. Beta oscillations are prominent in the pre- and postcentral gyri and are reduced at the onset of movement. This has led some to speculate that beta acts to suppress the function of motor cortex by synchronizing its activity. Curiously, following movement onset, beta amplitude rebounds if the movement is sustained, and is enhanced when movements are suppressed. Thus, others have argued that beta functions to promote tonic motor activity at the expense of voluntary movement. Although beta activity has been described as being generally characteristic of the frontal lobe frontal beta may simply reflect its role in areas involving motor networks. There are reports of intrinsic beta oscillations being found over other areas of the frontal lobe as well as the medial temporal lobe. Beta activity in these regions has also been associated with other cognitive functions such as speech comprehension, visual perception, and executive functions. Thus, this activity may reflect a more general role for beta in mediating long distance communication between these areas and other brain regions, language processing, or maintaining cognitive states. Uchida et al. have speculated that it is the human analog of “rhythmic slow activity” in animal models of memory and involved in memory consolidation.⁵⁸ Gross et al. found frontal, parietal and temporal coherence in Beta frequency was relevant for the processing of stimuli in working memory.⁵⁹ We believe that the decline in beta coherence between the parietal and temporal (PT) region may play a role in maintaining cognitive states and memory consolidation on healthy young adults at rest yet in a waking state after the motor task of using the Trainer. Markovska-Simoska et al.⁴¹ found that depressive patients showed significantly greater interhemispheric coherence in both the alpha and beta frequency, especially at central sites compared to control group, anxiety, and ADHD. Thus, our findings regarding a decrease in coherence between the central-parietal (CP) regions in

the brain of healthy young adults after operating the Trainer in beta frequency is consistent with their findings.

The gamma wave is a higher frequency ranging between 31 Hz to 100 Hz and is needed for high order cognitive function. It plays an important part in processing information, learning, and memory. Using senses to understand, memorize and process new materials is evidence of gamma wave presence. Lowered gamma wave activity is believed to associate with learning difficulty while strong gamma presence is believed to be highly dominant during performance of complex cognitive actions. The optimal level of gamma wave action allows people to think clearly, process information, use problem-solving, and ration logics easily. Gamma and high gamma modulations by tasks or the phase of low frequency oscillations have been demonstrated across multiple cortical areas. Indeed, regions exhibiting particularly elevated levels of intrinsic gamma or high gamma activity (indicative of true oscillations) have not been established, though there is some evidence of gamma/high gamma activity in medial temporal cortical areas during both wake and sleep states. When gamma peaks were present, they tended to be in the temporal lobe. Uchida et al. previously reported gamma peaks in the intrinsic activity of the medial temporal lobe.⁵⁸ However, it is not clear from their analyses if these peaks were reliably observed across participants, and they note that the anatomical focus of this activity varied across individuals. Their results may be compatible with ours regarding the presence of gamma frequency in the temporal region.

Overall, the statistical indication from our study demonstrated significant changes in EEG coherence, particularly a decrease in EEG coherence on young adults from active interaction

with the Trainer. This finding may help edify that power mobility training via the use of a power mobility trainer is responsible for consistent and objectively quantifiable changes in neural network connectivity that may be correlated with improvement in subjective measures of cognitive gains on children with multiple, severe disabilities. However, there are limitations in the current study that are worth mentioning. The first limitation was our small sample size of seven typical developing young adults aged between 18 and 24. A larger scale study would increase the power of our statistical tests with regard to EEG coherence on the neurotypical control group. Additionally, our combination or clustering of EEG channels per brain region could have also influenced the observed pattern. Finally, since there was substantial variability in the dominant frequencies within each region, this suggests a low degree of regional specificity for oscillations across the cortical parcellations used here. There are several reasons why we are likely underestimating the degree of regional specificity. We suspect that individual differences participants' neurophysiological state and characteristics could account for a lot of this variability. Even though care and caution were taken to ensure study participants were alert and immobile during data collection, there may have been significant differences in the state of alertness and restedness across participants that would affect our results. Shortcomings of the parcellation used to define brain regions and the fact that several clusters combined electrodes across hemispheres may also have contributed to the high within-area variability in dominant frequencies. These shortcomings could have biased our analyses because some areas contributed disproportionately to the clustering results, and because there may be some significant hemispheric asymmetries in intrinsic oscillations. Although these methodological limitations complicate making generalizations about normal brain function, they do not limit the potential clinical utility of these data since they should be representative of EEG data collected from

young healthy adults aged 18 to 24. Our results, however, are corroborated in many ways by other similarly non-invasive EEG coherence studies in healthy young adults as the neurotypical control group.

Chapter 3 – Extended Literature and Extended Methodology

3.1 Extended Literature Review

3.1.1 Brain Anatomy & Functional Lobes

Human brain – the marvelous organ that stores, organizes, retrieves, interprets information from the outside world, controls senses, regulates bodily functions, and embodies the essence of the mind and soul, is composed of three major components: the cerebrum, cerebellum, and brainstem¹³. Figure 3-1 provides an illustrative diagram of major components in the brain.

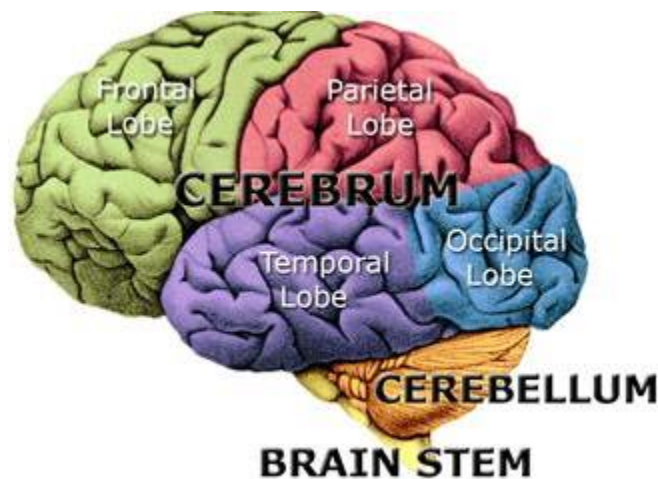


Figure 3-1. Brain anatomy and major parts (Brain diagram compliments of University of Washington - Department of Neurosurgery, Janet Schukar)

Balance, muscle coordination and fine movement are regulated in the cerebellum, which is located under the cerebrum¹⁵. The brainstem is located at the back of the brain and serves as a relay center connecting the cerebrum and cerebellum to the spinal cord. The brainstem performs

and regulates involuntary movements such as breathing, digestion, blood circulation, and other automatic functions for survival. Cerebrum is the largest part of the brain and is divided into left and right hemispheres. Each hemisphere controls the opposite side of the body and has different functions. The left hemisphere is dominant for language and hand use, while the right hemisphere is dominant for visual information, spatial attention and processing. The left hemisphere controls speech, comprehension, arithmetic calculation, and writing while creativity, spatial attention, artistic, and musical skills are attributed to the right hemisphere^{14,15}. Each hemisphere is separated into four main lobes: frontal, temporal, parietal, and occipital by distinct fissures. Each lobe is then associated with different functions. The frontal lobe is important for cognitive functions and control of voluntary movement or activity. The parietal lobe processes information about temperature, taste, touch and movement, while the occipital lobe is primarily responsible for vision. The temporal lobe processes memories, integrating them with sensations of taste, touch, sight and sound. Table 19 summarizes the four main functional lobes and their respective functions in the brain.

Table 19. Brain functional lobes and corresponding functions³

<i>Lobe</i>	<i>Function</i>
<i>Frontal</i>	Motor system Language production (left) Motor prosody (right) Comportment Executive function Motivation
<i>Temporal</i>	Audition Language comprehension (left) Sensory prosody (right) Memory Emotion
<i>Parietal</i>	Tactile sensation Visuospatial function (right) Reading (left) Calculation (left)
<i>Occipital</i>	Vision Visual perception

It is important to note the level of harmony in the brain i.e. each lobe in the brain does not function alone. There are complex relationships between the lobes of the brain and between the right and left hemispheres, which is commonly referred to as brain lateralization. The lateralization of brain function is beyond the scope and focus of this study.

3.1.2 Neuron & Nerve Impulse

The brain is made up of hundreds of millions nerve cells, called neurons. Neurons are information-processing units of the brain responsible for communicating messages throughout the body. The neuron conveys information through electrical and chemical signals called action potential and chemical neurotransmitters at the junction between two neurons called synapse. There are many sizes and shapes of neurons, but all neurons consist of a cell body, dendrites and an axon. Dendrites are tree-like extension at the beginning of a neuron that helps increase the surface area of the cell body, or soma. Dendrites are also covered with synapses. These tiny protrusions receive information from other neurons and transmit electrical stimulation to the soma. The soma, or cell body, is where the signals from the dendrites are joined and passed on. The soma and the nucleus do not play an active role in the transmission of the neural signal. Instead, these two structures serve to maintain the cell and keep neuron functional. The axon is the elongated fiber that extends from the cell body to the terminal endings and transmits the neural signal. The larger the diameter of the axon, the faster the information is transmitted. Some axons are covered with a fatty substance called myelin sheath that acts as an insulator. The myelin sheath is broken up by points known as the nodes of Ranvier or myelin sheath gaps where nerve impulses, or action potentials, jump from one node to the next, which plays a role in speeding up the transmission of the signal.

Nerve impulses, or action potentials, occur when the electrical potential across a cellular membrane rapidly rises, then falls, in response to an event, or stimulus. When a neuron is not sending signals i.e., the cell is at rest, the inside of the neuron has a negative charge relative to the positive charge outside the cell. The electrical potential of neurons at the resting membrane potential is typically measured to be around -70 mV ¹⁶. The resting membrane potential is maintained due to ion channels that allow ions to flow into and out of cells and sodium/potassium pumps which can pump ions in and out of the cell. Electrically charged chemicals – ions, maintain the positive and negative charge balance. Calcium (Ca^{2+}) contains two positive charges, sodium (Na^+) and potassium (K^+) contain one positive charge and chloride (Cl^-) contains a negative charge. When at rest, the cell membrane of the neuron allows certain ions to pass through while preventing or restricting other ions from moving, specifically the cell membrane is permeable to potassium (K^+) ions and impermeable to negative ion inside the cell, i.e. potassium (K^+) ions are able to freely cross the membrane while negative ions inside of the cell are unable to cross the barrier. Sodium (Na^+) ion pump is the cell membrane's active transport mechanism in which three sodium ions are pumped out for every two potassium ions pass through the membrane to maintain its polarized state. In response to a signal, or stimulus, the sodium channels open allowing the positive sodium (Na^+) ions surge into the cell. The membrane potential depolarizes - becoming more positive. Once the cell reaches a threshold value- usually around -55 mV , an action potential will fire, sending the electrical signal down the axon. If the potential is not reached, the action potential does not happen, and the cell will go back to its resting membrane potential. Neurons always fire at their full strength as action potential is an all-or-none response and there is no such thing as a partial firing of a neuron. This full intensity of the signal is carried down the nerve fiber and transferred to the next cell and the

signal does not weaken or become lost the further it travels from the source. After reaching the threshold value, voltage-gated Na⁺ channels open, and Na⁺ ions flood into the cell. The membrane potential flips from negative to positive because the inside of the cell is now more positive relative to the outside. As the membrane potential reaches +30 mV – the peak of the action potential – voltage-gated potassium channels open, and K⁺ leaves the cell due to the concentration gradient. The membrane potential repolarizes or moves back towards the negative resting membrane potential. The neuron becomes temporarily hyperpolarized as the K⁺ ions cause the membrane potential to become a little more negative than the resting potential. The neuron enters a refractory period, in which the sodium/potassium pump returns the neuron to its resting membrane potential.

3.1.3 EEG & Frequency Bands

These electrical activities, or action potentials can be detected and recorded by an electroencephalogram (EEG) test, which is a non-invasive method using multiple electrodes placed along the scalp to monitor and measure voltage potential fluctuations within the nerve cells - neurons of the brain. The EEG recording shows the algebraic sum of the electrical potential charges contributed by each nerve cell. Each nerve cell may have a small contribution but due to the large population of the cells present in the cerebral cortex, the resulting signal is able to be recorded. However, in comparison to the signal measured is weaker since the brain's surface and the electrodes are separated by a layer of cerebrospinal fluid, the skull, and the scalp. The measured signal is typically 50 μ V peak-to-peak. Recorded signals larger than this are typically due to head muscle movement. Such signals are called artifacts.

When examining EEG signals, it is useful to examine the signal in the frequency domain. The larger amplitude waves require the synchronous activity of many neurons. Depending on the type of brain activity, different frequencies are present. Alpha waves (frequencies between 8 and 12 Hz) are seen when the eyes are closed, and the participant is relaxed. Mental effort diminishes the presents of alpha waves indicating the degree of cortical activation. The greater the activation, the lower the activity. Beta waves (frequencies between 12 and 30 Hz) are present in alert participants with their eyes open. Theta waves (frequencies between 4 and 7 Hz) are seen in children when awake and in everyone during sleep. Delta waves (frequencies between 0 and 4 Hz) are present in sleep stages. These frequencies can also be present if there is movement in the jaw or neck muscles. Gamma waves (frequencies between 30 and 100 Hz) are present during higher mental activity. Figure 3-2 illustrates the oscillation pattern for each brainwave frequency.

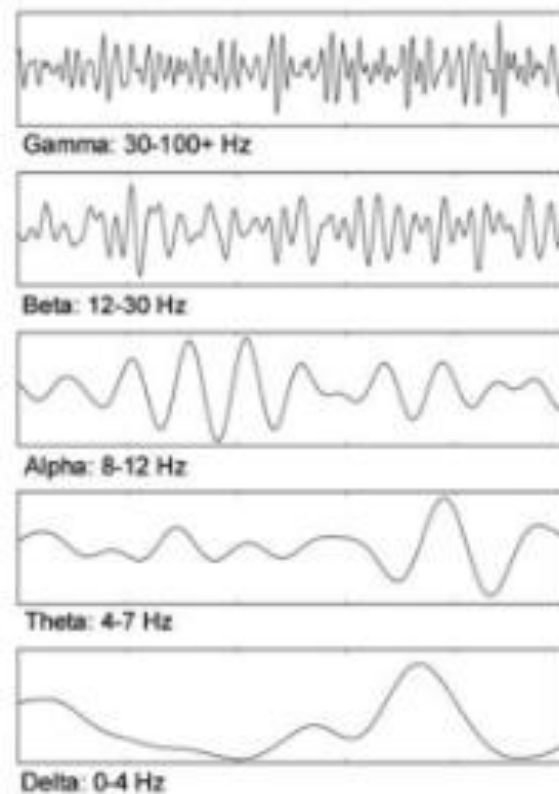


Figure 3-2. EEG signals in five most common frequency bands

3.1.4 Network Connectivity – MSC

Network connectivity, when applied to signals measured from the brain, is an area of study that seeks to measure interactions between areas in the brain. Neural network connectivity techniques for quantifying the brain networks use signal processing techniques that have been around for many decades.²⁸ Network connectivity can be subdivided into three categories: structural, functional, and effective²⁸. Structural connectivity is how individual neurons and groups of neurons are physically connected throughout the brain. This type of connectivity is hard to assess because synaptic connections are dynamic in that new connections are constantly formed, and others are eliminated. These structural connections are difficult to visualize. For this reason, functional and effective connectivity are examined through different measures of activity in the brain, such as the EEG.

Functional connectivity is the measure of the "temporal correlation among the activity of different neural assemblies."²⁸ This type of connectivity can be measured, using signal processing techniques, to determine the correlation between signals from different areas of the brain. The important thing to note with functional connectivity is that it is only a measure of the strength of a connection between two signals. There is no information about the direction of the communication. Functional connectivity can be further broken down into linear coupling and nonlinear coupling. Linear based techniques of functional connectivity are based on coherence, typically Magnitude Squared Coherence (MSC) and Wavelet Coherence.²⁸ Nonlinear techniques are often used because processes within the brain have nonlinear characteristics. These techniques are based on phase synchronization. A third group of techniques, outside of linear and

nonlinear, can also be used to assess connectivity. These techniques are based on information theory, which is sensitive to both linear and nonlinear models.

The third measure of network connectivity is effective connectivity, which is "the direct or indirect influence that one neural system exerts over another."²⁸ This category differs from functional connectivity in two ways. An effective connectivity measure provides information about the direction of the coupling, unlike functional connectivity. The second difference is that effective connectivity measures indirect, as well as direct, coupling between two signals. There are two main categories that measures of effective connectivity falls under. One is a data-driven estimate which is a direct estimate of the connectivity based on signals recorded from different areas in the brain. The other category is a model-based approach, which uses a combination of structural and functional connectivity. The model-based approach requires knowledge, or a hypothesis, about an existing neurobiological model based on the structural connectivity. The model is then tested using functional connectivity. The data-driven techniques use signals measured from the brain. Techniques include partial directed coherence, the directed transfer function, and transfer entropy. Transfer entropy is an information-based technique, so it does not require the assumption of a linear or nonlinear model.²⁸

3.2 Extended Methodology

3.2.1 Artifact Removal

The biggest challenge with monitoring EEG is artifact recognition and elimination. There are first the human-test-subject related artifacts (e.g. movement, sweating, ECG, eye movements) and technical artifacts (50/60 Hz artifact, cable movements, electrode paste-related), which must be handled differently. Electrodes used in EEG recording do not discriminate the electrical

signals they receive. The recorded activity which is not of cerebral origin is termed artifact and can be divided into physiologic (generated from the subject from sources other than the brain) and extra-physiologic artifacts arise from outside the body (equipment including the electrodes and the environment). Electromyogram (EMG) activity are common artifacts: the myogenic potentials generated in the frontalis muscles (raising eyebrows) and the temporalis muscles (clenching of jaw muscles) are of shorter duration than those generated in the brain. These artifacts can be identified on the basis of duration, morphology and rate of firing (frequency). Particular patterns of EMG artifacts can occur in some movement disorders: essential tremor and Parkinson disease can produce rhythmic 4 to 6 Hz sinusoidal waveforms. Another common artifact comes from eye movements. The eyeball acts as a dipole with a positive pole oriented anteriorly (cornea) and a negative pole oriented posteriorly (retina). When the globe rotates about its axis, it generates a large amplitude alternate current field detectable by any of the electrodes positioned near the eye. A blink causes the positive pole (the cornea) to move closer to frontopolar FP1, FP2 electrodes, producing symmetric downward deflections. A further difficulty arises due to properties of certain layers of the skin. A significant DC potential exists between the outer most layer of the skin (stratum corneum) and the thin granular layer of cells in the epidermis (stratum granulosum) and any local deformation of the skin will alter this potential. The only reliable way to eliminate the source of artifact is to create a low resistance pathway through the layers of skin by skin cleaning (alcohol swab). Also, sodium chloride (electrolyte) from sweating reacting with metals of the electrodes may produce a slow baseline drift. Surface electrodes such as the ones used in EEG must create an interface between an ionic solution (the subject) and a metallic conductor (the electrode). This leads to a half-cell potential which can be quite large relative to the signal being recorded. To minimize this problem of

polarization of the electrode, some electrodes are coated with silver chloride, but all are maintained away from the skin through an intermediate layer of conductive paste. Touching the electrodes during recording can produce artifacts. An electrode which is not contacting the skin very well acts like an antenna with resulting 60-cycle interference. The study utilized the electrodes coated with silver chloride and a conductive paste (gel), thus the system is considered relatively robust in comparison to other existing methods. Additionally, since the study focused on analyzing EEG data collected from NI1 and NI2 in which participant sat with eyes closed in a relaxing state and immobile, thus is not prone to artifacts from both EMG and EOG as compared to the EEG data collected from the Trainer session. Artifact removal for processing EEG data is composed of removal of DC components (0 Hz noise and potential linear drifts), elimination of the 60 Hz power line interference, reference to the overall average, removal of the first and last 30 seconds due to assumption of noise at the beginning and end of each session, ICA execution, and removal of EOG from ocular movements. Figure 3-3 summarized the complete sequence of data processing, artifact reduction, and data analysis procedure of the study.

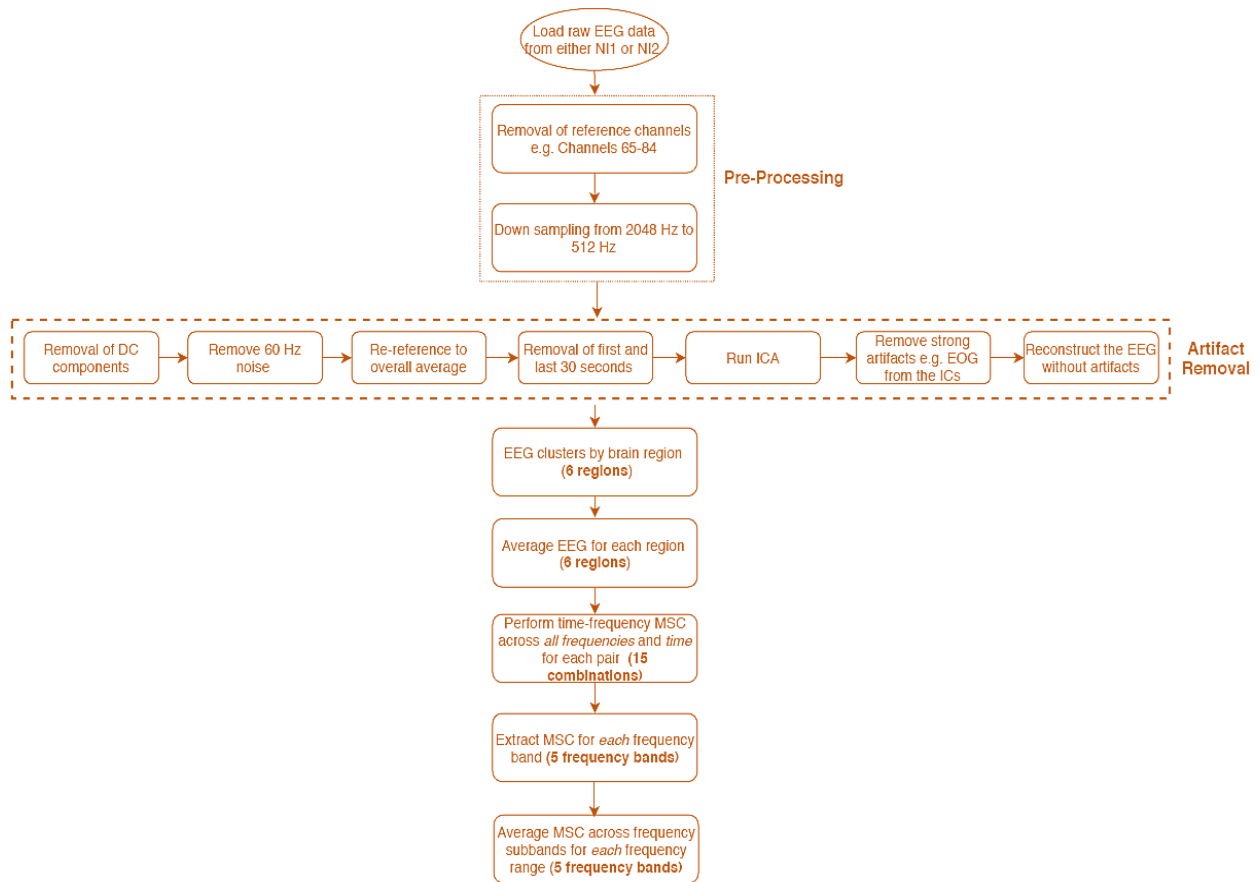
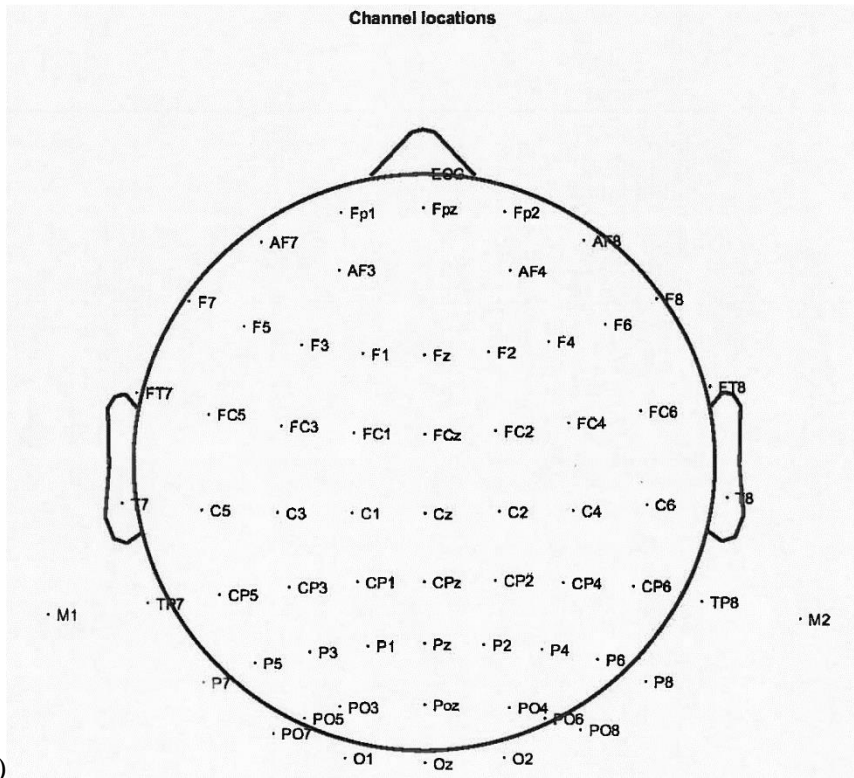


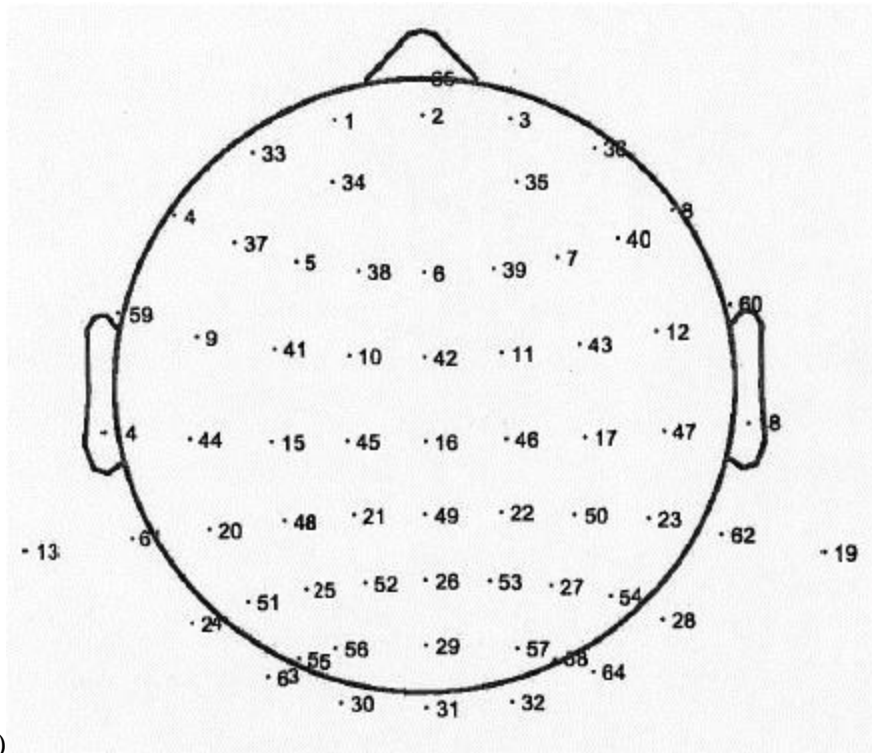
Figure 3-3. Block diagram describes data processing of the study on EEG data recorded from No Interaction 1 (NI 1) and No Interaction 2 (NI 2) phase on each subject

3.2.2 EEG Cluster by Functional Lobes

The standardized placement of scalp electrodes for a classical EEG recording has become common since the adoption of the 10/20 system. The essence of this system is the distance in percentages of the 10/20 range between Nasion-Inion and fixed points. These points are marked as the Frontal pole (Fp), Central (C), Parietal (P), Occipital (O), and Temporal (T). The midline electrodes are marked with a subscript z, which stands for zero. The odd numbers are used as subscript for points over the left hemisphere and even numbers over the right hemisphere.



A)



B)

Figure 3-4. The 10/20 system with 65-electrodes placement scheme

Cleaned and relatively free of artifact EEG data were topographically divided into clusters as listed in Table 20 according to the electrode placement and its corresponding brain region (Figure 3-4). EEG representative for each subsequent brain region was then determined by taking the average across all selected channels.

Table 20. Topographic Distribution of Electrodes according to brain region

EEG Clusters	Brain Region	Electrode (Channel) #
Frontal	Fp1, Fpz, Fp2, F7, F3, Fz, F4, F8, FC5, FC1, FC2, FC6, AF7, AF3, AF4, AF8, F5, F1, F2, F6, FC3, FCz, FC4	23 channels – # 1, 2, 3, 4, 5, 6, 7, 8, 9, 10, 11, 12, 33, 34, 35, 36, 37, 38, 39, 40, 41, 42, 43
Central	C3, Cz, C4, C5, C1, C2, C6	7 channels – # 15, 16, 17, 44, 45, 46, 47
Parietal	CP5, CP1, CP2, CP6, P7, P3, Pz, P4, P8, Poz, CP3, CPz, CP4, P5, P1, P2, P6	17 channels – # 20, 21, 22, 23, 24, 25, 26, 27, 28, 29, 48, 49, 50, 51, 52, 53, 54
Parietal-Occipital	PO5, PO3, PO4, PO6, PO7, PO8	6 channels – # 55, 56, 57, 58, 63, 64
Occipital	O1, Oz, O2	3 channels – # 30, 31, 32
Temporal	T7, T8, FT7, FT8, TP7, TP8	6 channels – # 14, 18, 59, 60, 61, 62

3.2.3 Magnitude Square Coherence (MSC)

In signal processing, a signal, as a function of time, is a representation that provides information in the time domain with perfect temporal resolution. Whereas, the magnitude of the Fourier Transform of the signal shows what frequency components are present with perfect spectral resolution but with no time information since the Fourier Transform fails to convey when in time, different frequency occurs in the signal. Also, the traditional Fourier analysis relies on assumption that signals are periodic, or infinite in time while in fact, many signals in practice are transient and prone to changes over their duration. Most biological signals such as electroencephalography (EEG), electrocardiogram (ECG), or electromyography (EMG) are non-stationary and non-periodic thus, a time-frequency representation is useful to provide both

temporal information and some spectral information simultaneously for signal analysis. Multiple different techniques have been developed including the Short-Term Fourier Transform (STFT)- which is commonly used to formulate a valid time-frequency representation, wavelet methods, Wigner distribution function (WDF), or Gabor-Wigner transform.²⁹

Time-frequency analysis has been studied and developed intensively in the last two decades to provide efficient analysis of signals with a time-varying frequency content, due to its outstanding and informative performance over the traditional frequency-domain approach. A large number of applications where time-frequency analysis is employed are in speech, audio/music, image, and video signal processing to expand and enhance the signal processing capabilities of multimedia signals. For example, Umapathy et al. discusses various applications of time-frequency analysis in audio signal processing to efficiently extract information from audio signals for the purpose of audio coding, music classification, classification of environmental sounds, and water marking.³² Time-frequency analysis has also demonstrated its use in examining physiological data such as EEG, ECG and EMG.^{29,30}

Coherence is the frequency domain measure of the linear association between two time-series. Magnitude-Square Coherence (MSC) - a common coherence analysis technique,³¹ is a function of frequency with values ranging between 0 and 1 that indicate how well two signals correspond to each other at each frequency. A MSC of 0 indicates complete independency of the frequency of two signals, whereas a coherence of 1 indicates the phase coupling or linear dependency of the frequency of two signals. Magnitude-Square Coherence is often used to identify the amount of power shared by two time-series, or signals at a given frequency, which demonstrates whether

one signal is talking to another. If there is a change in X and similar change in Y, then X and Y are talking.

The method to derive the time-frequency coherence was implemented in MATLAB following equations presented in the Lovett and Ropella paper^{22,33}. Magnitude squared coherence (MSC) is defined as the squared absolute value (i.e., magnitude) of the cross-spectrum divided by the product of the power spectra of X and Y in the frequency domain:

$$MSC(f) = \frac{|S_{XY}(f)|^2}{S_{XX}(f) * S_{YY}(f)} \quad (1)$$

Fourier Transform $X_l[k]$ and $Y_l[k]$ of the two signals, $x_l[n]$ and $y_l[n]$ over L overlapping, equal-length segments is the base of the cross-power spectrum. To obtain an unbiased estimation of coherence, ensemble averaging over a window function $w[n]$ can be used. Thereby, the discrete MSC can be described as:

$$MSC = \frac{|\sum_{l=0}^{L-1} X_l[k] Y_l^*[k]|^2}{\sum_{l=0}^{L-1} |X_{l[k]}|^2 \sum_{l=0}^{L-1} |Y_{l[k]}|^2} \quad (2)$$

In which, L is the number of windows used and is given by l and k , the frequency index.

Equation 2 serves as the base for further development of the MSC time-frequency analysis by Lovett and Ropella. The Fourier Transform of each signal is replaced in Equation 2 with the Short-Term Fourier Transform (STFT). The STFT is a time-frequency analog of the Fourier Transform. A l th order Discrete Prolate Spheroidal Sequences (DPSS) window is then used to obtain the short-term minimum bias eigen transform:

$$X_l[n, k] = \sum_{m=0}^{M-1} x[n + m - \frac{M}{2}] v_l[m] e^{-j2\pi mk/M} \quad (3)$$

with n is the time index, k is the frequency index, M is the window length, and m is a variable of summation. The l^{th} window is given as v_l . Equation 3 is then substituted for the Fourier

Transform in Equation 2 to obtain MSC in both the temporal and spectral domain as described in Equation 4.

$$MSC[n, k] = \frac{|\sum_{l=0}^{L-1} X_l[n, k] Y_l^*[n, k]|^2}{\sum_{l=0}^{L-1} |X_l[n, k]|^2 \sum_{l=0}^{L-1} |Y_l[n, k]|^2} \quad (4)$$

Equation 4 was then implemented in MATLAB to analyze the given physiological data. Prior to the analysis of the physiological data, the MSC over time and frequency implementation was tested on two example signals as described in the paper by Lovett and Ropella. Equation 5 to 8 describes the example signals and other related variables. Note that in this example, e_1 and e_2 are mutually uncorrelated Gaussian white noise, $N = 20,000$, $M = 1,200$, $L = 7$, and $f_s = 1$ Hz. The $MSC[n, k]$ is evaluated at $n = 300$ in a time increment of 600 points.

$$x[n] = 2\cos(n\omega_1[n]) + 2\cos(n\omega_2[n]) + e_1[n] \quad (5)$$

$$y[n] = 2\cos(n\omega_1[n]) + e_2[n] \quad (6)$$

$$\omega_1[n] = \frac{n\pi}{10,000} \quad (7)$$

$$\omega_2[n] = \frac{n\pi}{5000} + \frac{\pi}{4} \quad (8)$$

After performance evaluation of the technique using example test signals, the time-frequency coherence was used on the systematically clean (artifact-free) physiological EEG data obtained from seven young healthy adults within the 18-to-24 age range from both NI1 and NI2 sessions.

3.2.4 Statistical Test

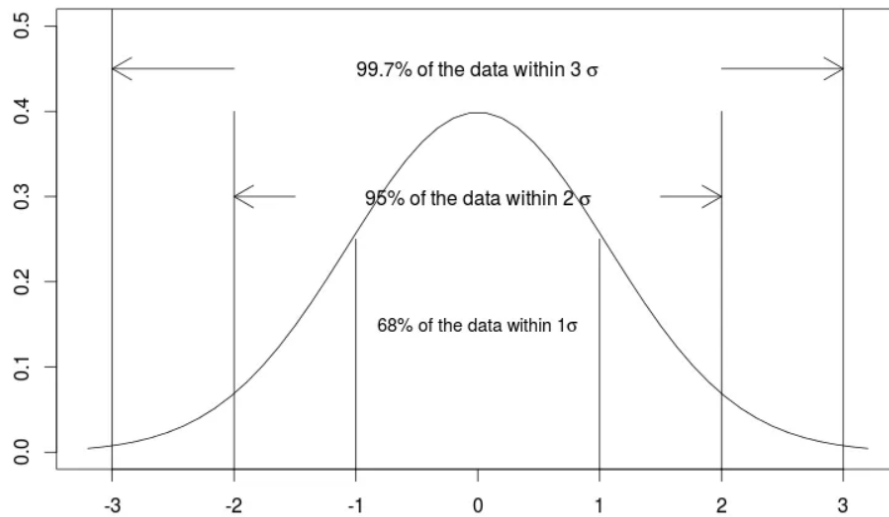


Figure 3-5. The Empirical Rule (68-95-99.7%)

The study utilizes the Empirical rule, which is well known for showing what percentage of values are within a certain range of the mean. About 68% of the values lie within 1 standard deviation of the mean ($\mu \pm 1\sigma$). About 95% of the values lie within 2 standard deviations of the mean ($\mu \pm 2\sigma$). About 99.7% of the values lie within 3 standard deviations of the mean ($\mu \pm 3\sigma$). However, if the data is not normally distributed such interpretation as illustrated in the figure above is not valid thus, it is crucial that the assumption of normality is upheld to set the premise for the test. The study used standard deviation as the metric to show the spread and variability of the data since even for non-normally distributed data, standard deviation can still be used as a standard measure of dispersion.

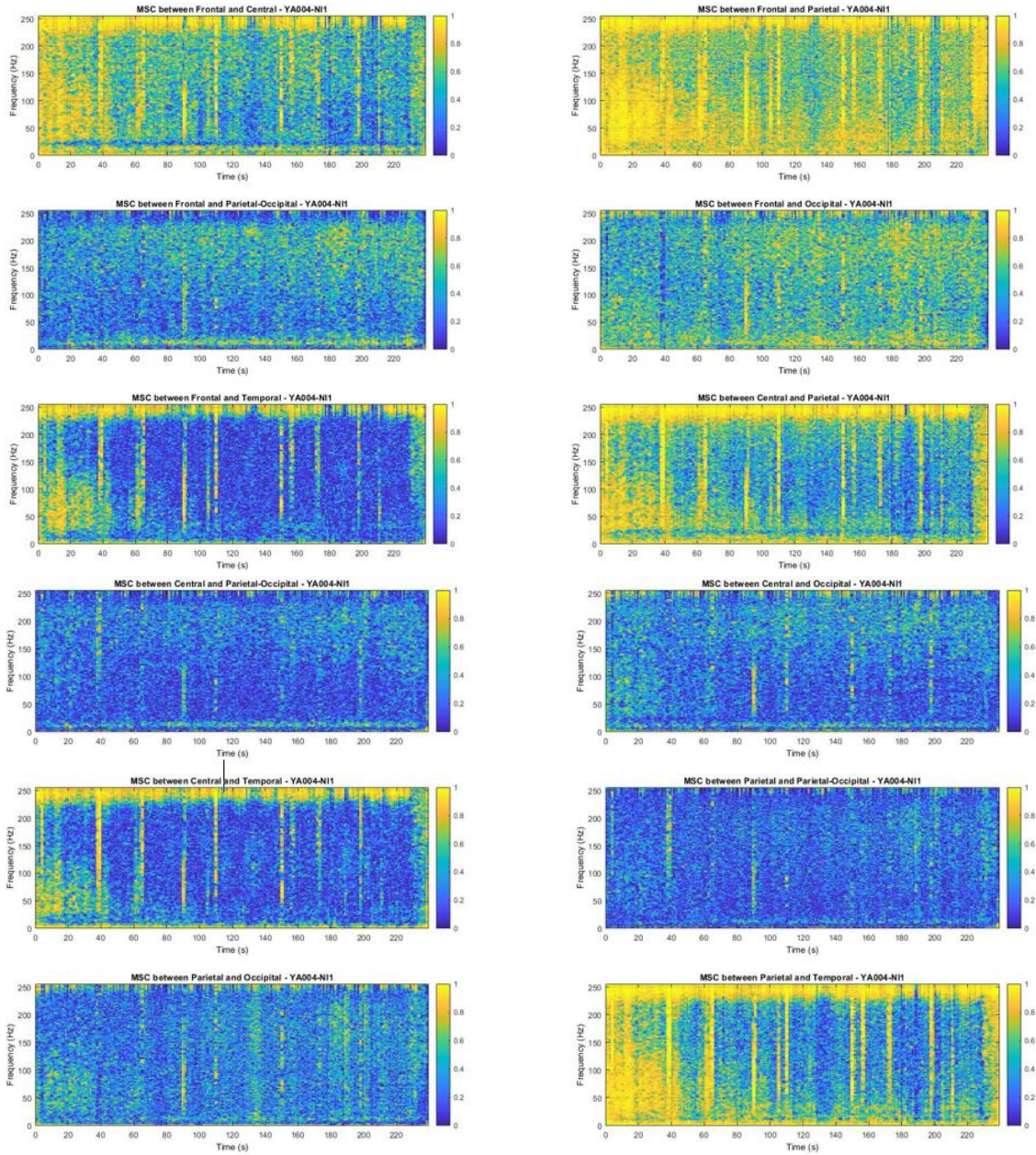
The p-value is defined as the probability of obtaining a result at least as extreme as the current one, assume the null hypothesis is true. Low p-value means the data is incompatible with the null hypothesis thus, the null hypothesis is rejected. When the p-value is high, there is less disagreement between our data and the null hypothesis, thus fail to reject the null hypothesis. To

determine whether a p-value is low or high, we use alpha – the level of significance, it is the cutoff value where we determine whether a p-value is low or high. If the p-value is lower than alpha then we conclude that there is a statistically significant difference between groups. When the p-value is higher than the significance level, we conclude that the observed difference between groups is not statistically significant. A 5% level of significance is most commonly used in medicine based on the consensus of researchers. Using a 5% alpha implies that having a 5% probability of incorrectly rejecting the null hypothesis is acceptable. In this case, if the p-value of the study is less than 5% then there is a statistically significant difference between groups. If the p-value is more than 5% then there is not a statistically significant difference between groups. P-value is calculated using the assumption that the null hypothesis is correct. A paired t-test with 95% confidence interval was used to evaluate if the Trainer had significant impact on the functional neural connectivity and brain cognitive function of healthy young adults in five dominant frequencies by analyzing the changes, or difference between the MSC before and after the Trainer.

Appendix A – Figures

Subject 1

○ *No Interaction 1 – Before the Trainer*



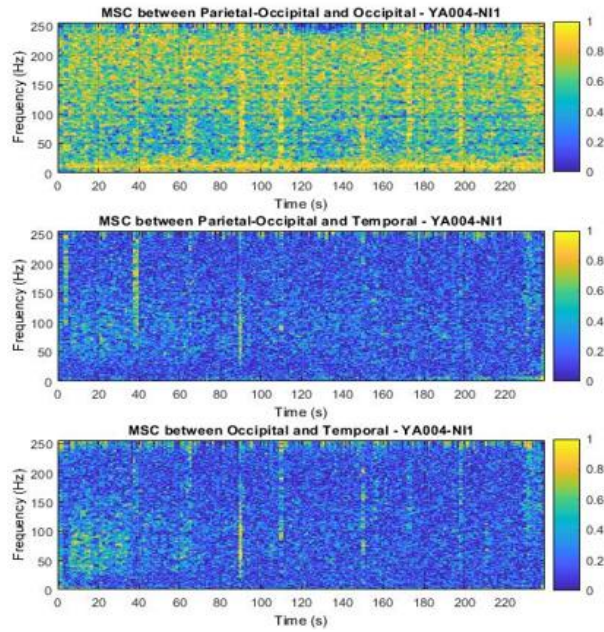
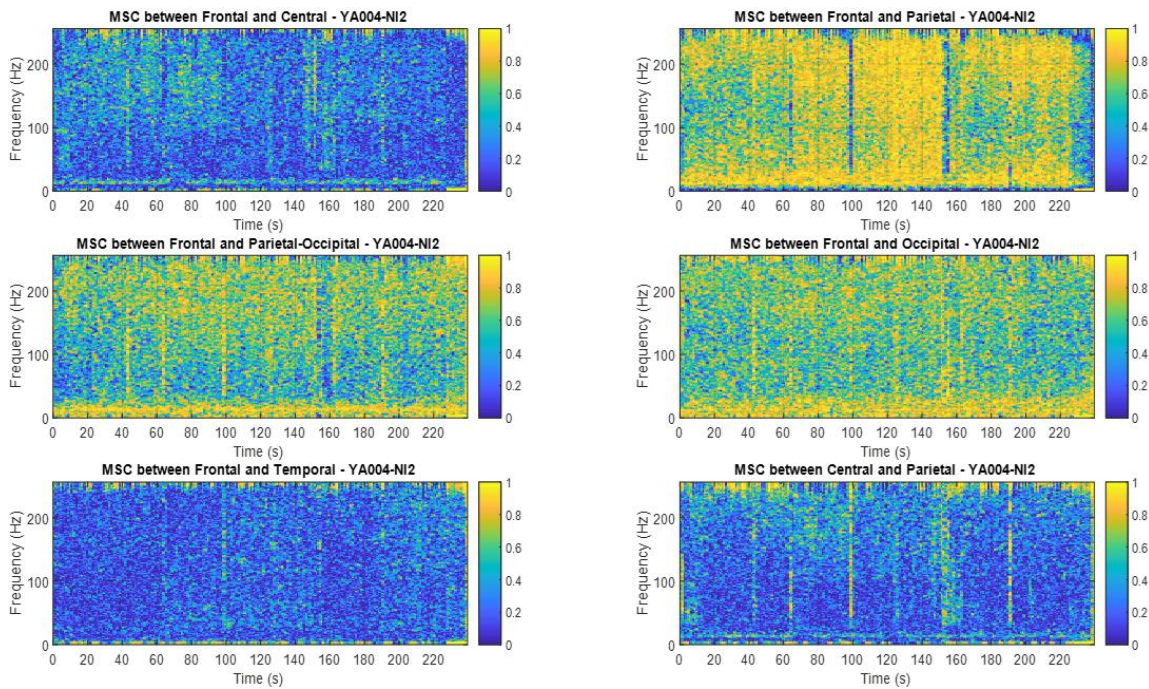


Figure A-1. Magnitude Square Coherence from NI1 – 5-min rest yet awake before the Trainer between various brain region combinations in subject 1 (YA004)

○ *No Interaction 2 – After the Trainer*



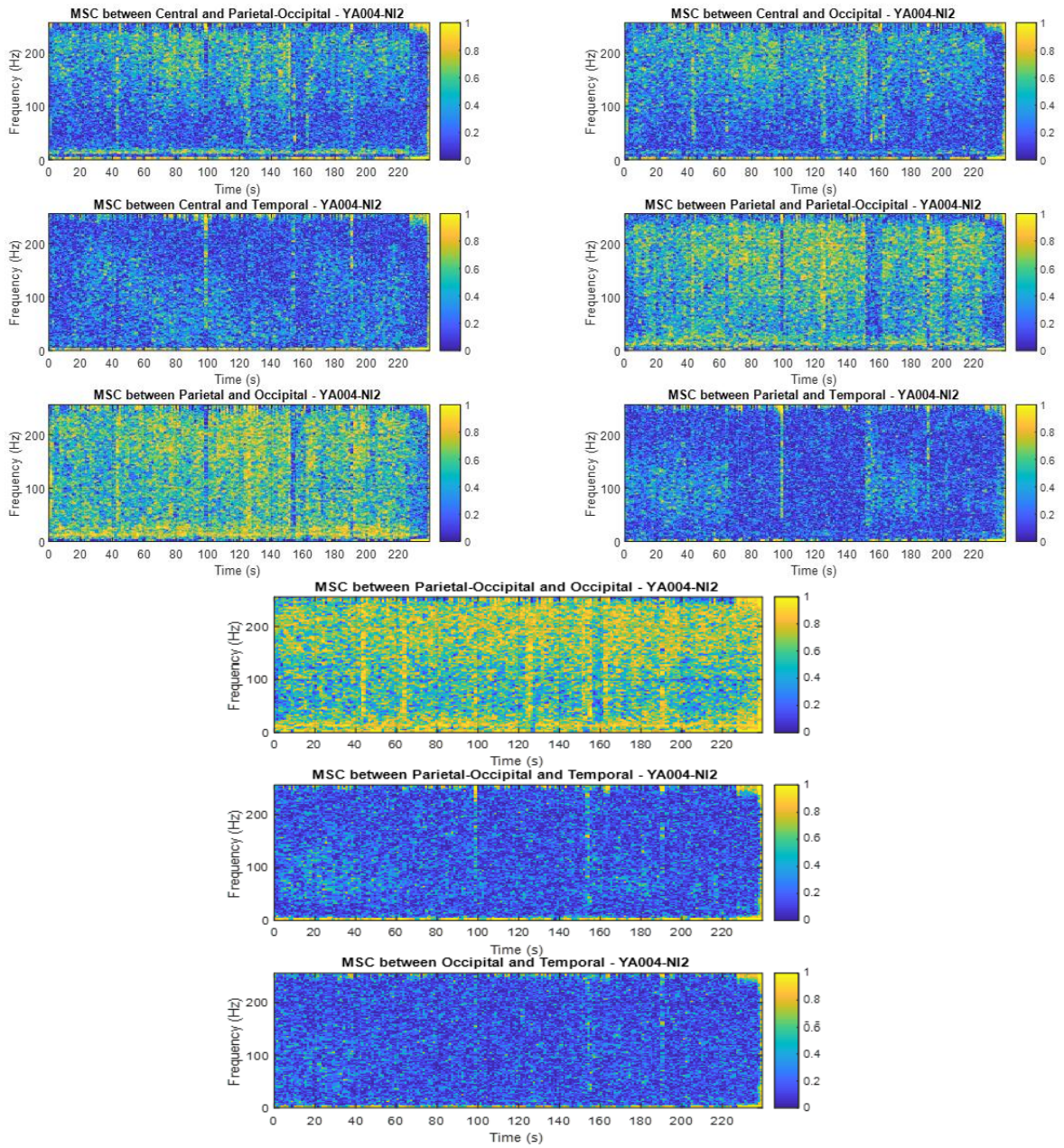
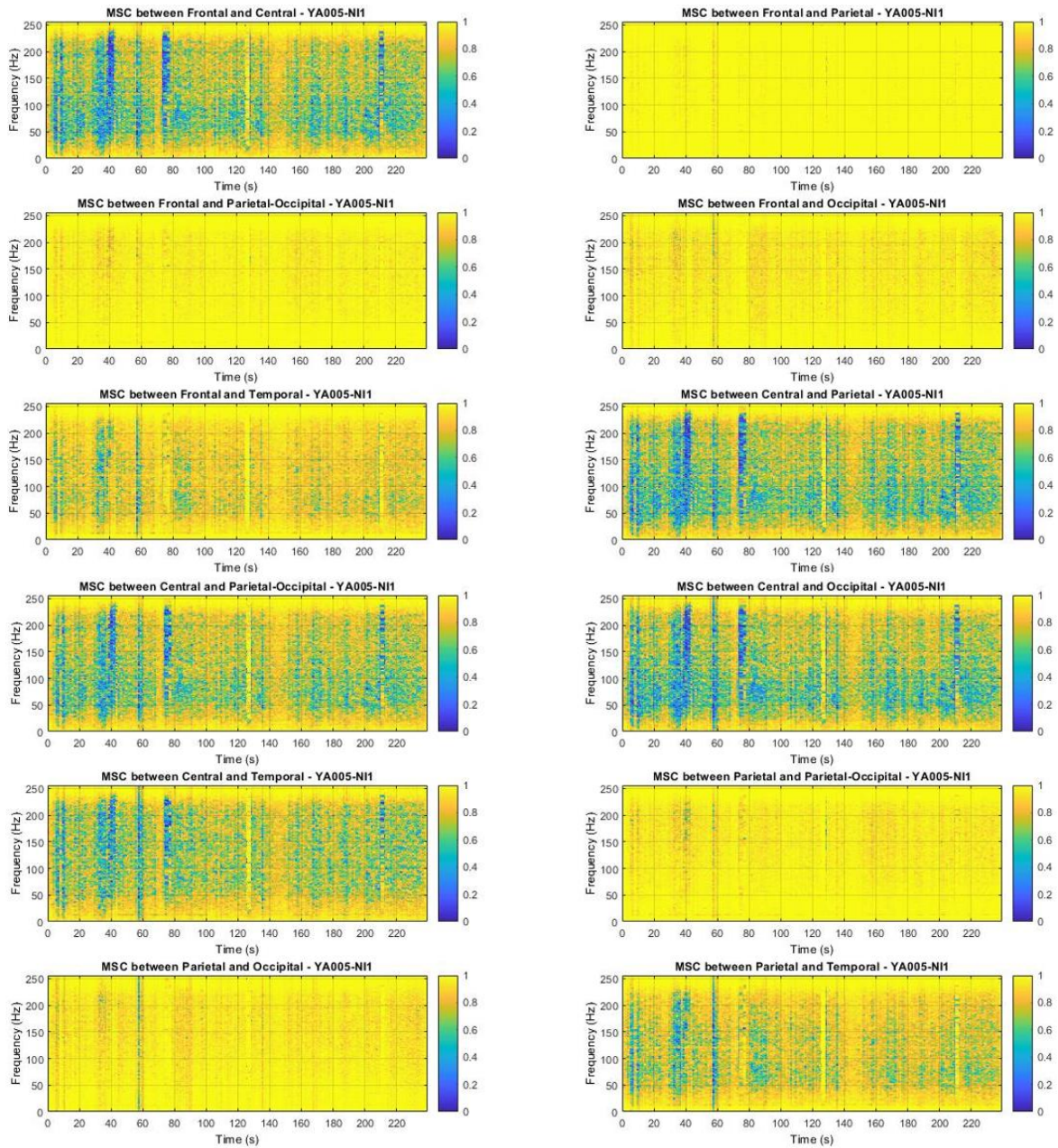


Figure A-2. Magnitude Square Coherence from NI2 – 5-min rest yet awake after the Trainer between various brain region combinations in subject 1 (YA004)

Subject 2

○ *No Interaction 1 – Before the Trainer*



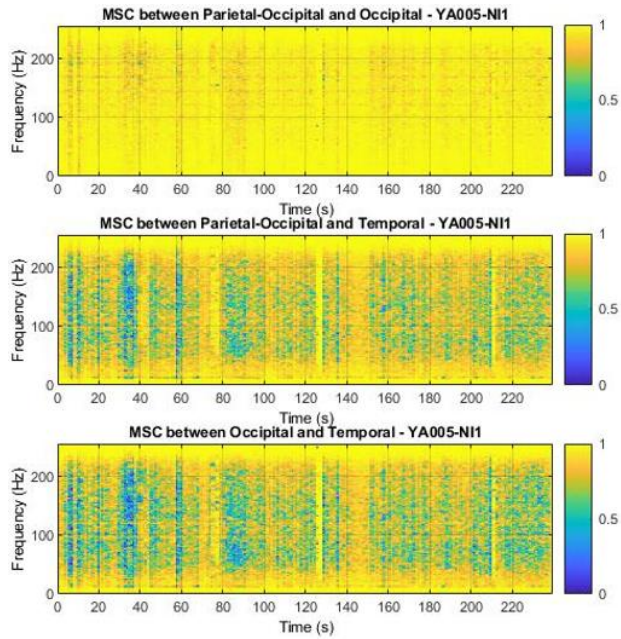
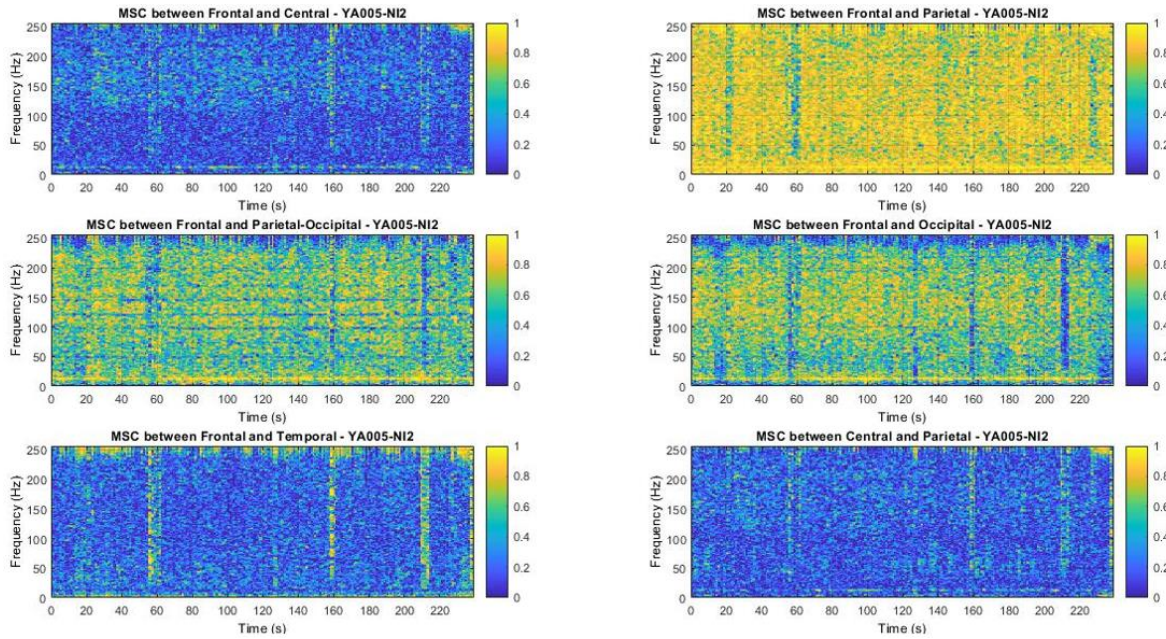


Figure A-3. Magnitude Square Coherence from NI1 – 5-min rest yet awake before the Trainer between various brain region combinations in subject 2 (YA005)

○ *No Interaction 2 – After the Trainer*



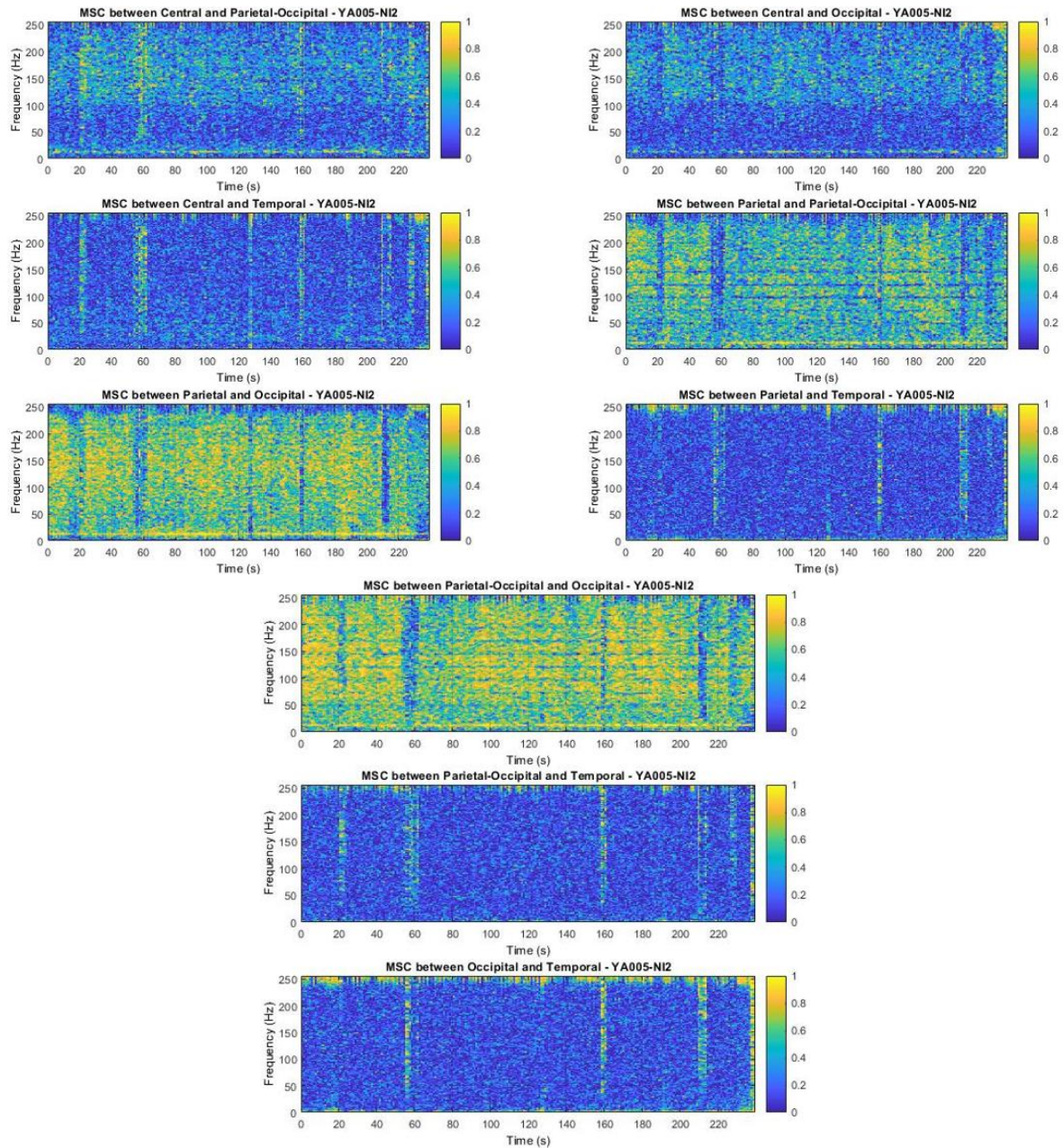
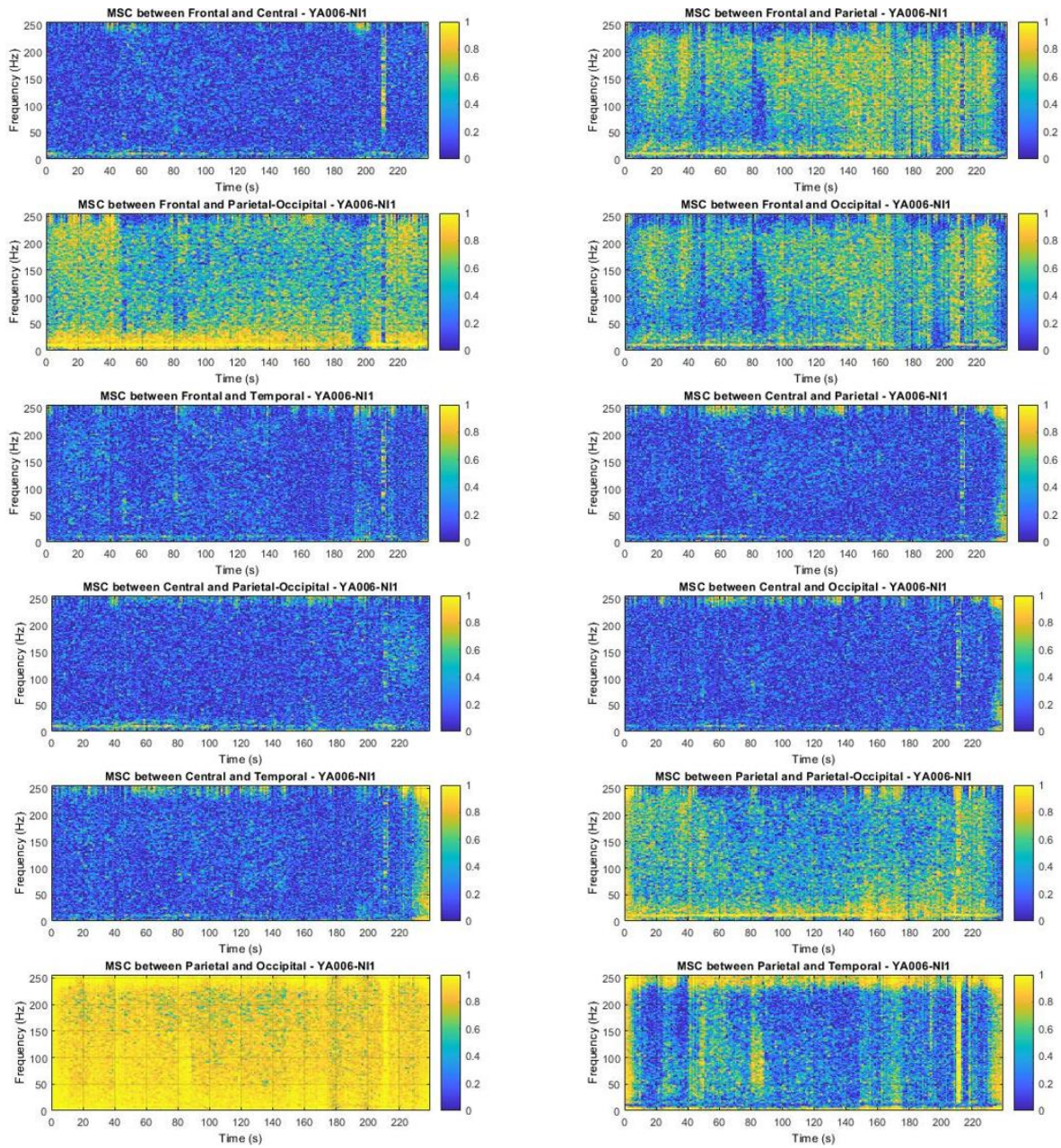


Figure A-4. Magnitude Square Coherence from NI2 – 5-min rest yet awake after the Trainer between various brain region combinations in subject 2 (YA005)

Subject 3

○ *No Interaction 1 – Before the Trainer*



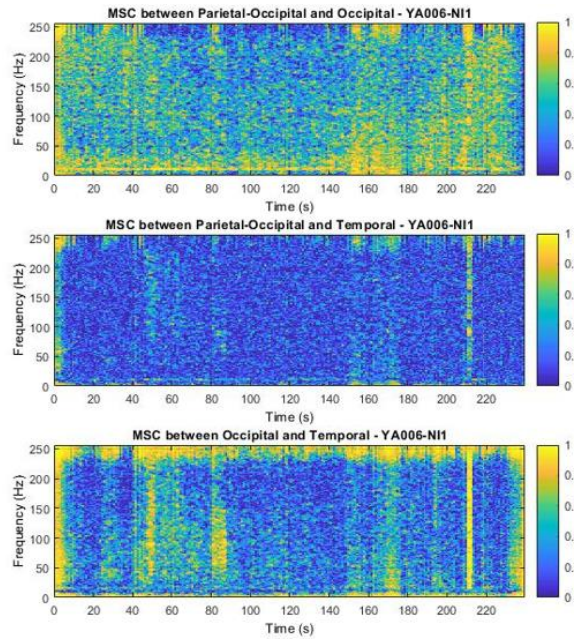
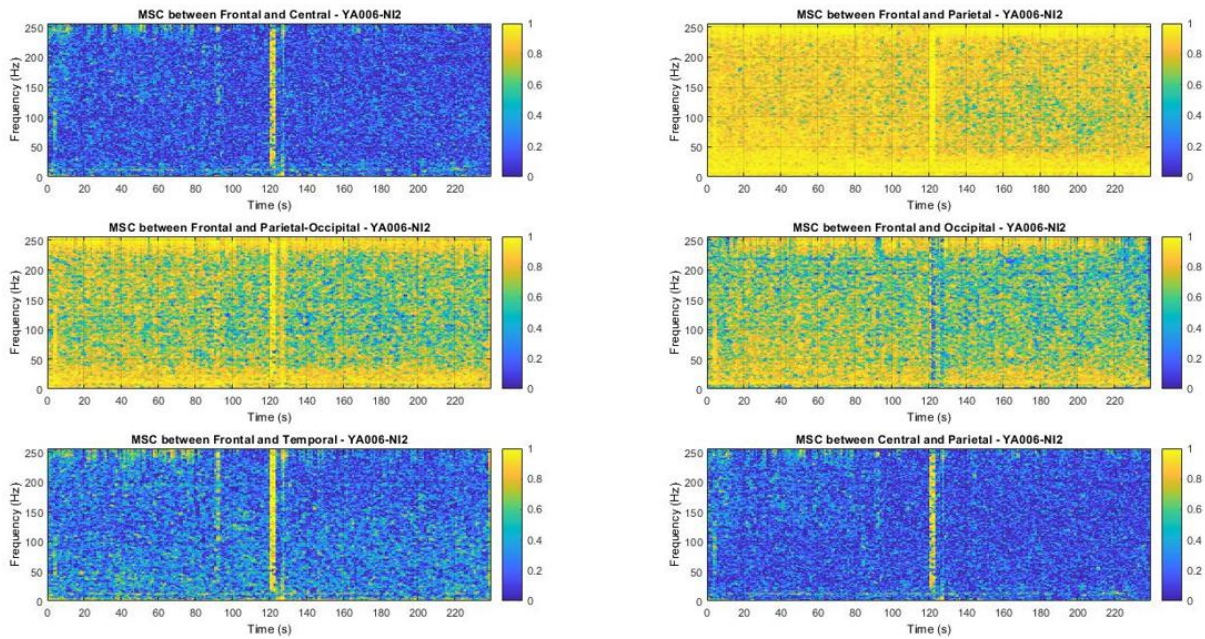


Figure A-5. Magnitude Square Coherence from NI1 – 5-min rest yet awake before the Trainer between various brain region combinations in subject 3 (YA006)

○ *No Interaction 2 – After the Trainer*



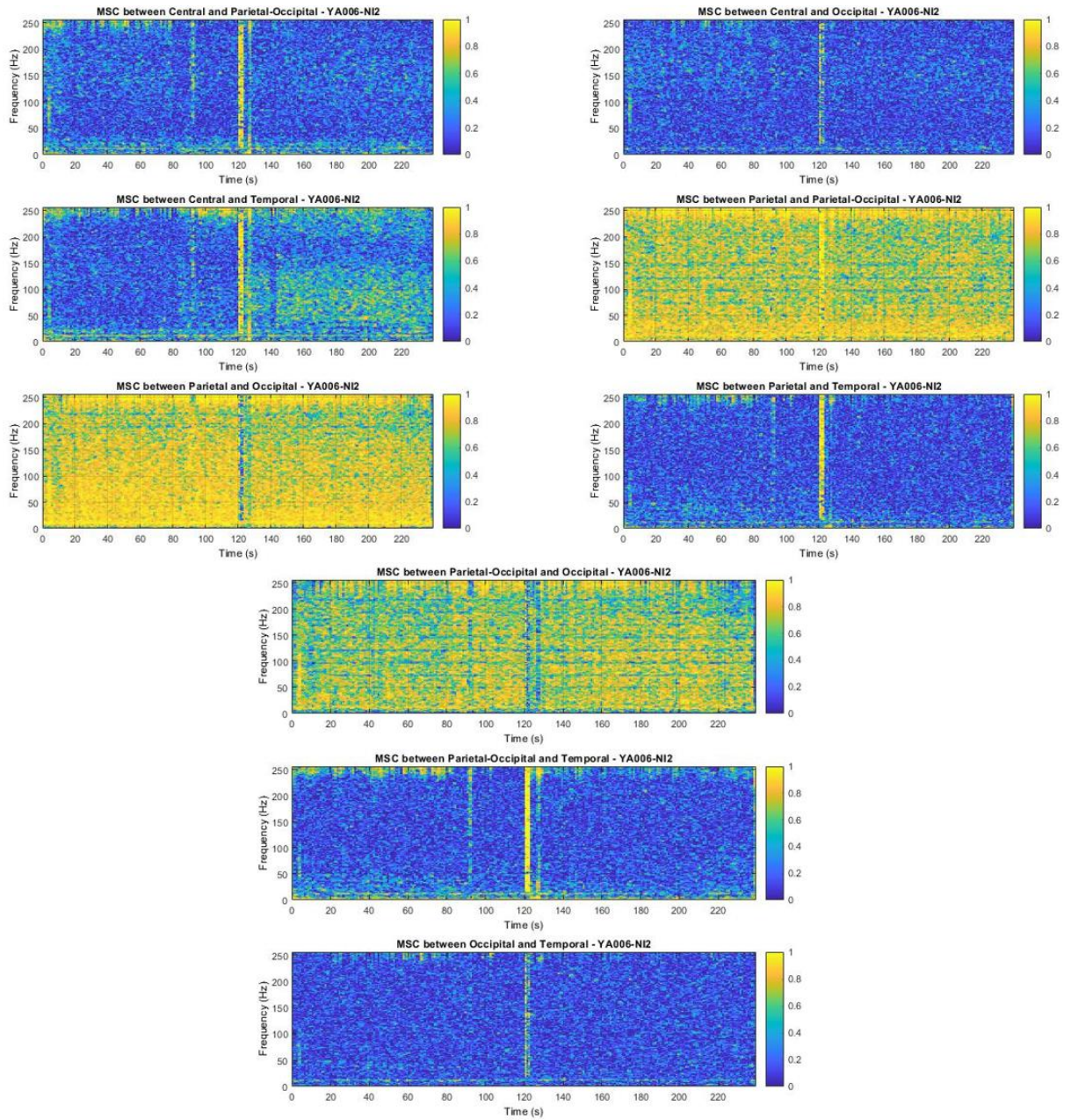
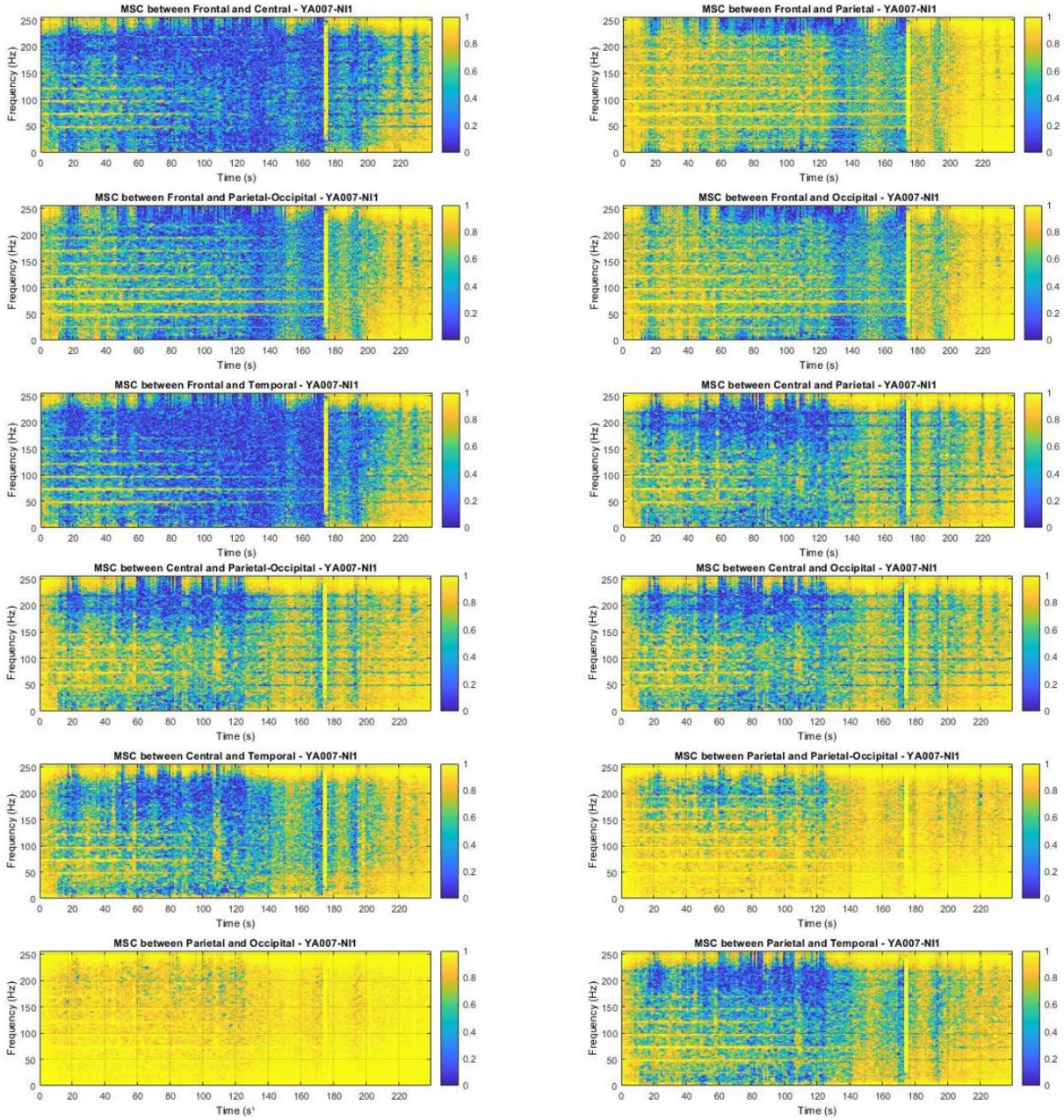


Figure A-6. Magnitude Square Coherence from NI2 – 5-min rest yet awake after the Trainer between various brain region combinations in subject 3 (YA006)

Subject 4

○ *No Interaction 1 – Before the Trainer*



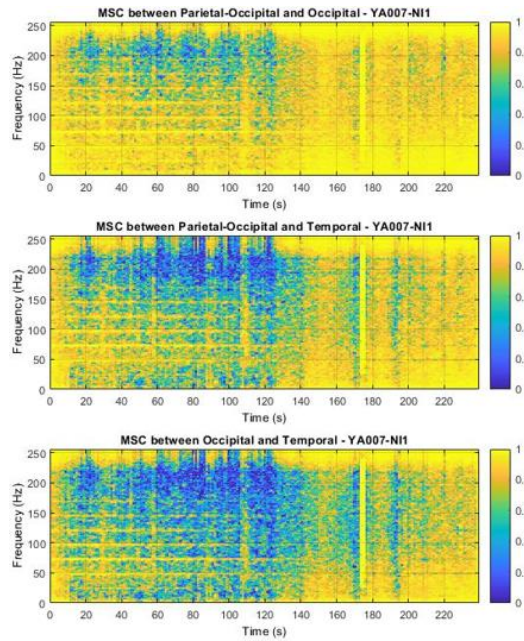
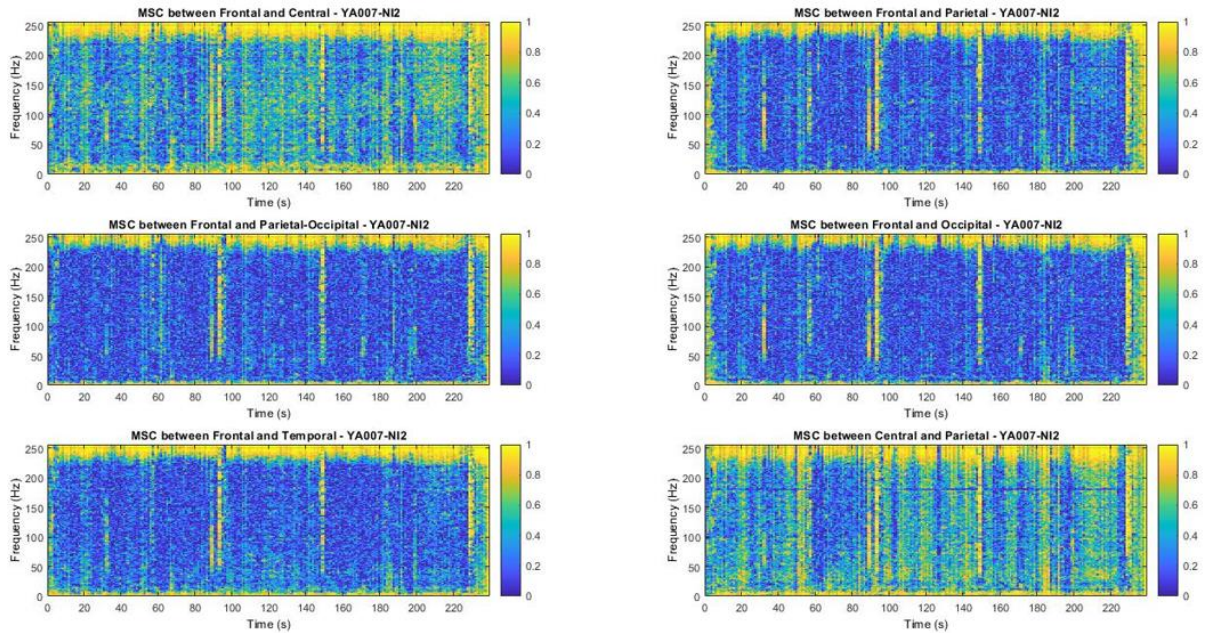


Figure A-7. Magnitude Square Coherence from NI1 – 5-min rest yet awake before the Trainer between various brain region combinations in subject 4 (YA007)

○ *No Interaction 2 – After the Trainer*



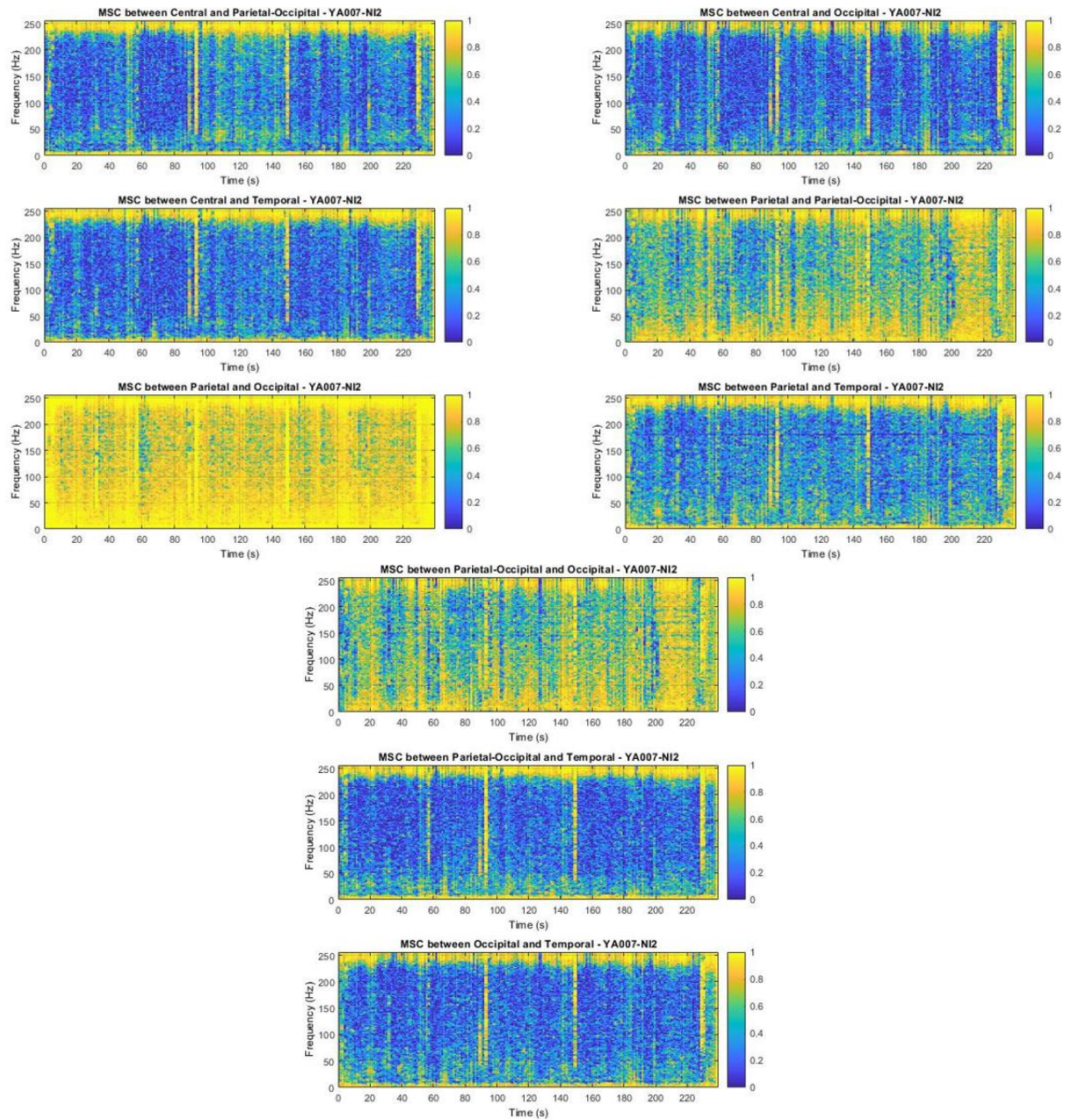
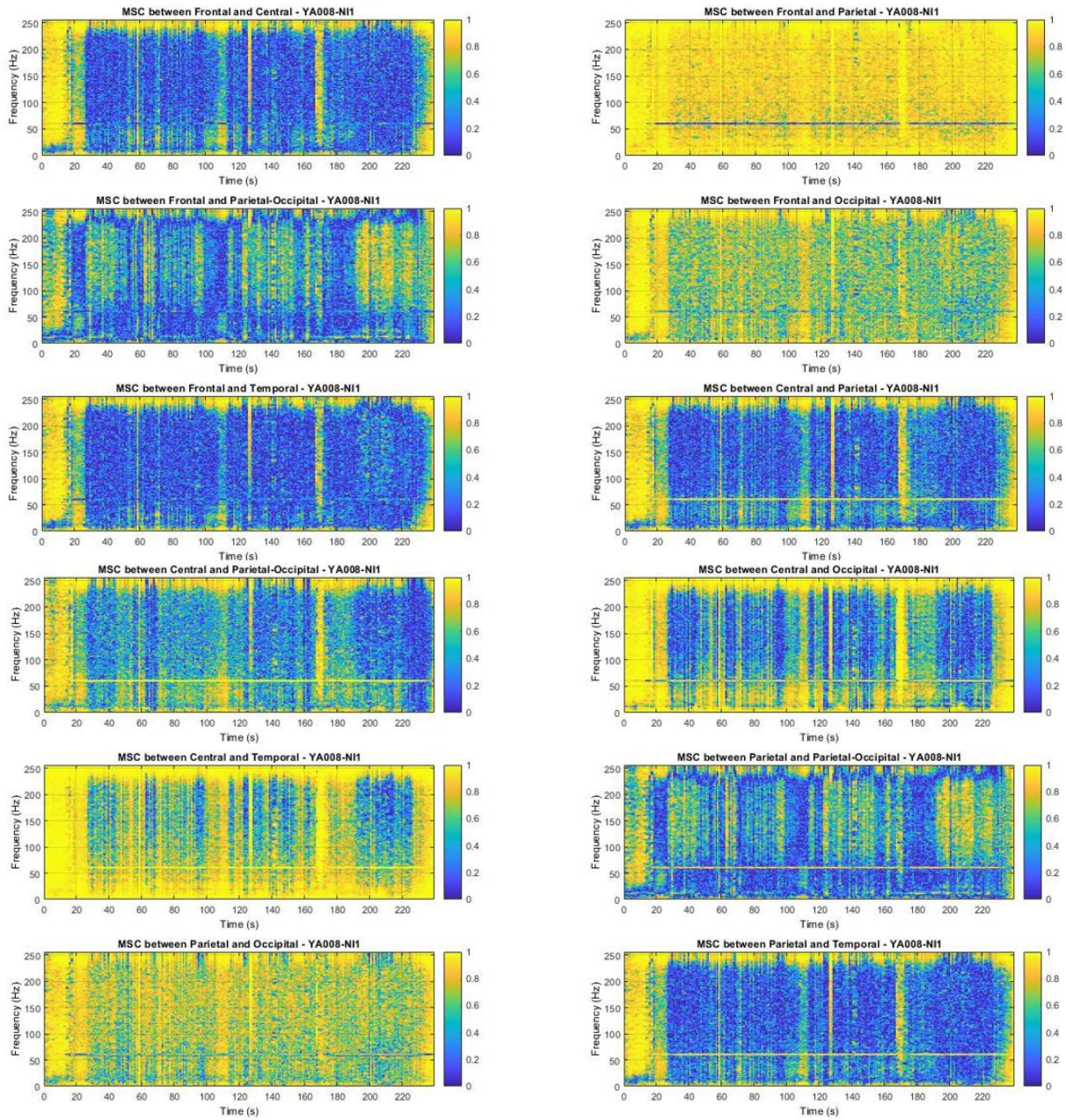


Figure A-8. Magnitude Square Coherence from NI2 – 5-min rest yet awake after the Trainer between various brain region combinations in subject 4 (YA007)

Subject 5

○ *No Interaction 1 – Before the Trainer*



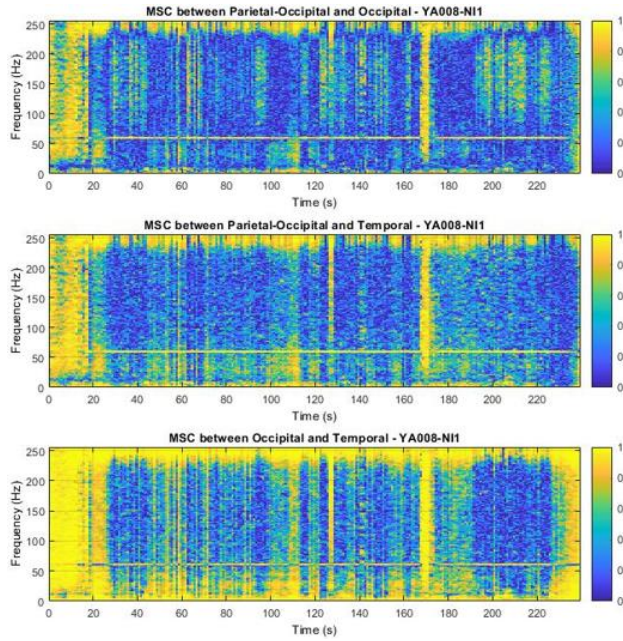
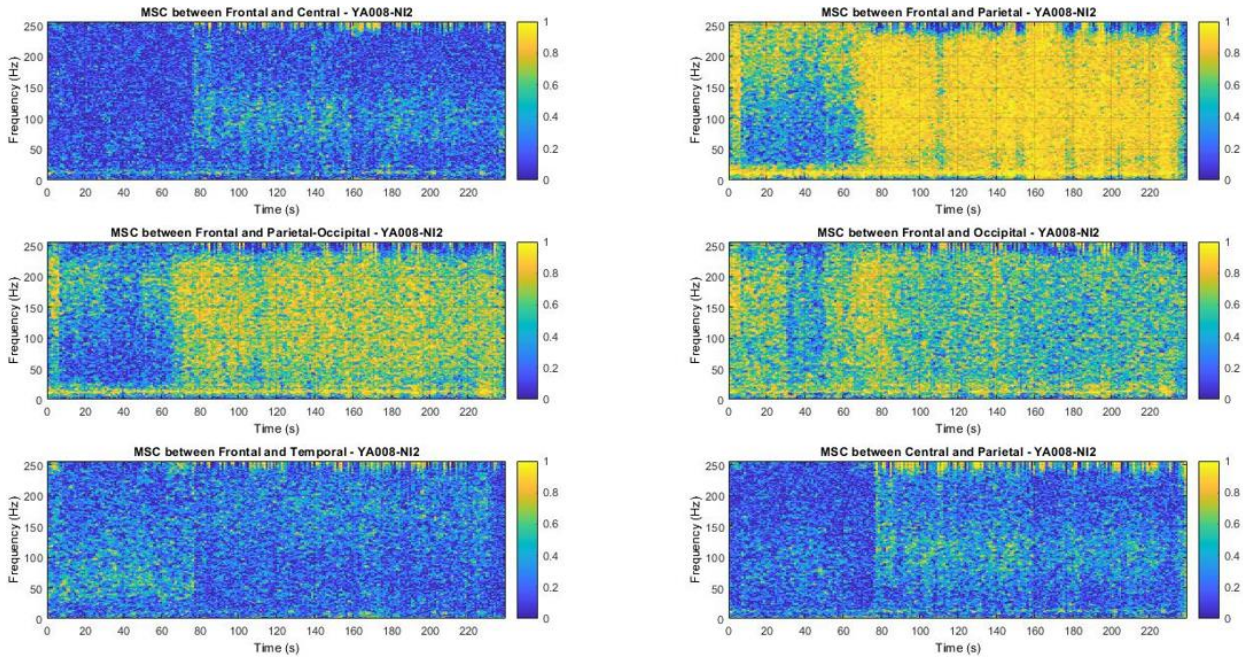


Figure A-9. Magnitude Square Coherence from NI1 – 5-min rest yet awake before the Trainer between various brain region combinations in subject 5 (YA008)

○ *No Interaction 2 – After the Trainer*



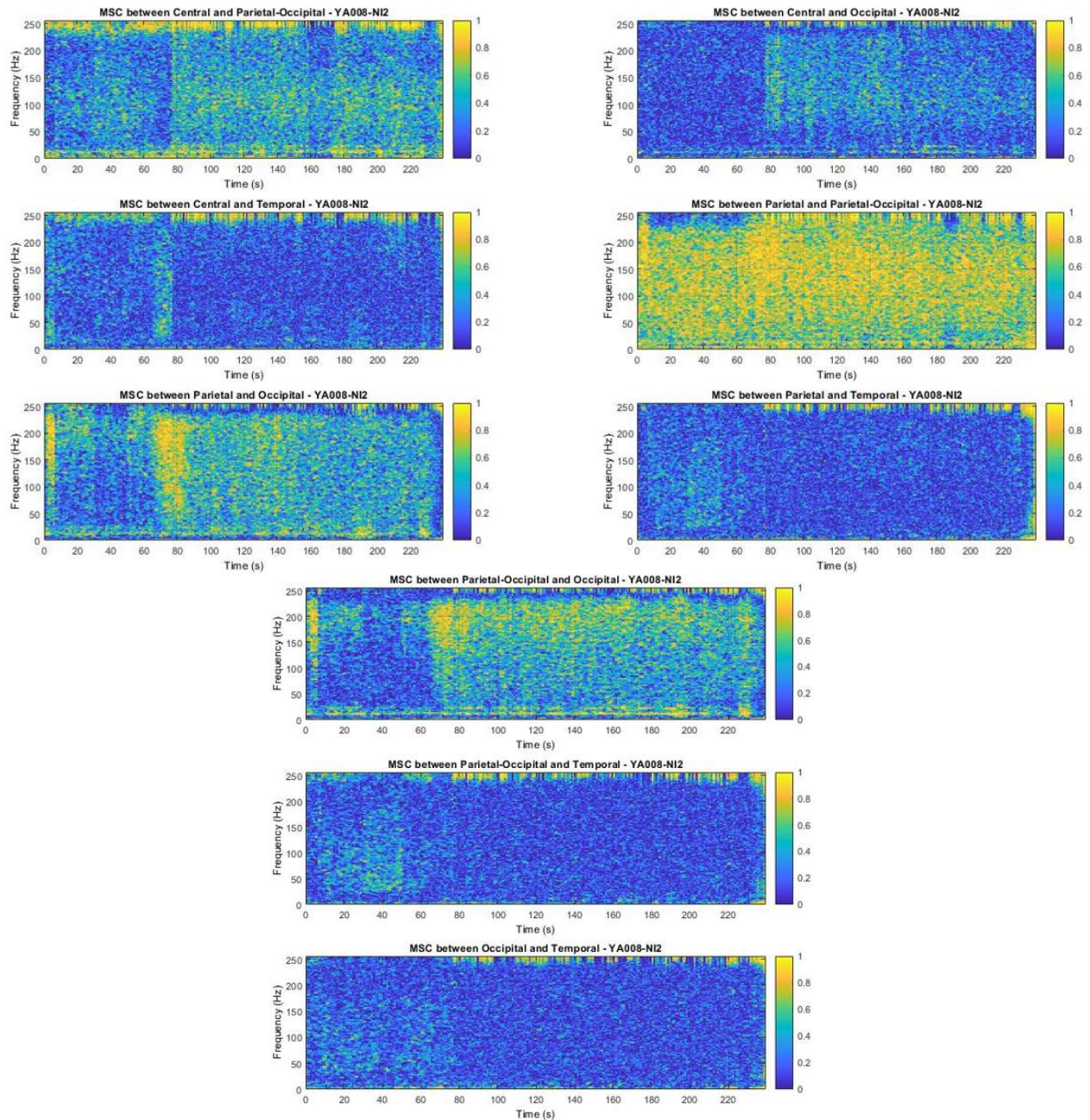
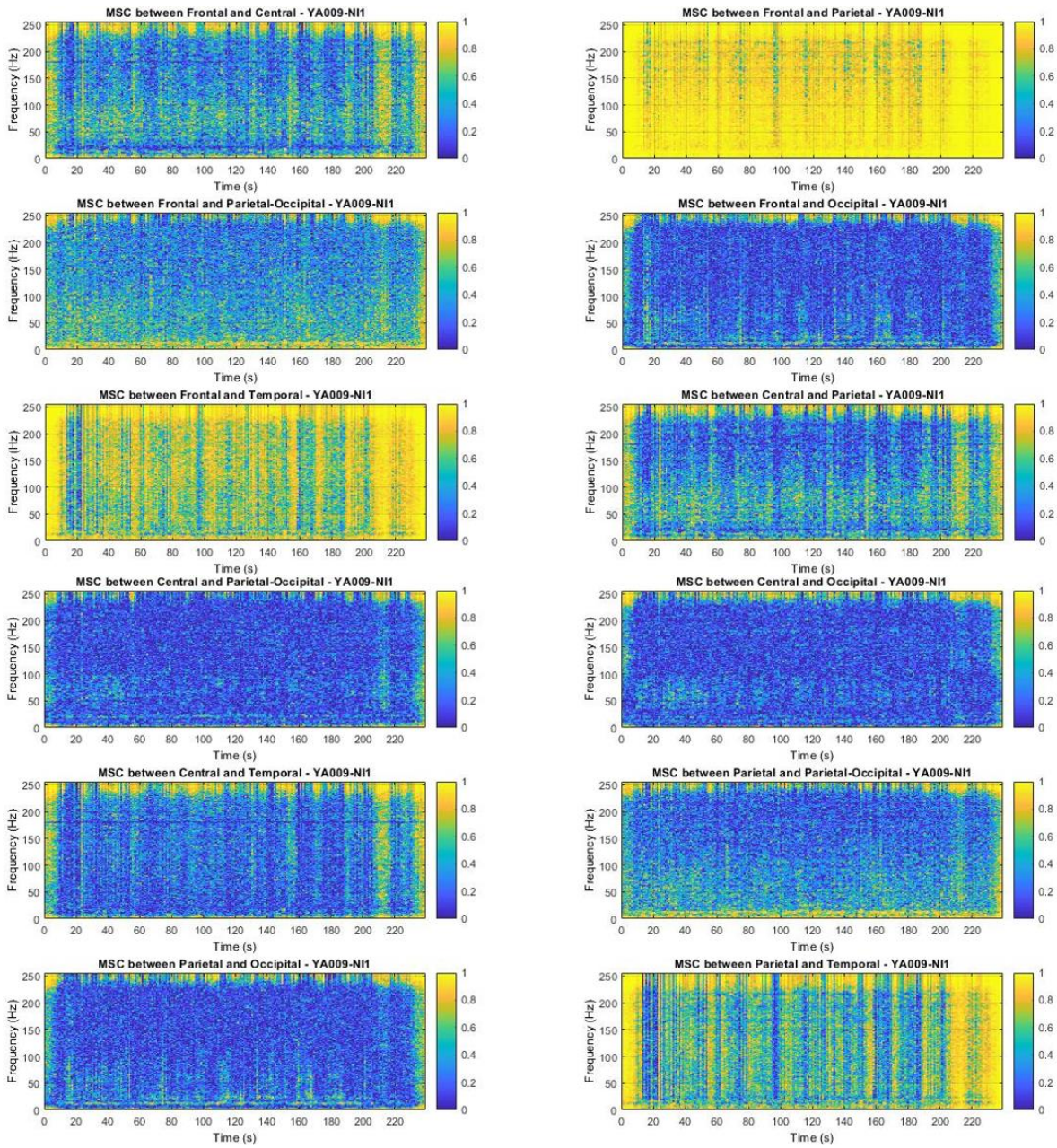


Figure A-10. Magnitude Square Coherence from NI2 – 5-min rest yet awake after the Trainer between various brain region combinations in subject 5 (YA008)

Subject 6

○ *No Interaction 1 – Before the Trainer*



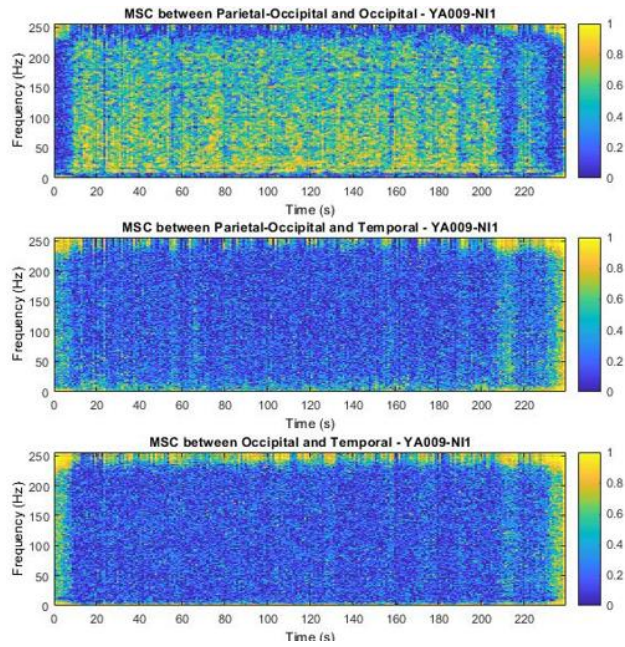
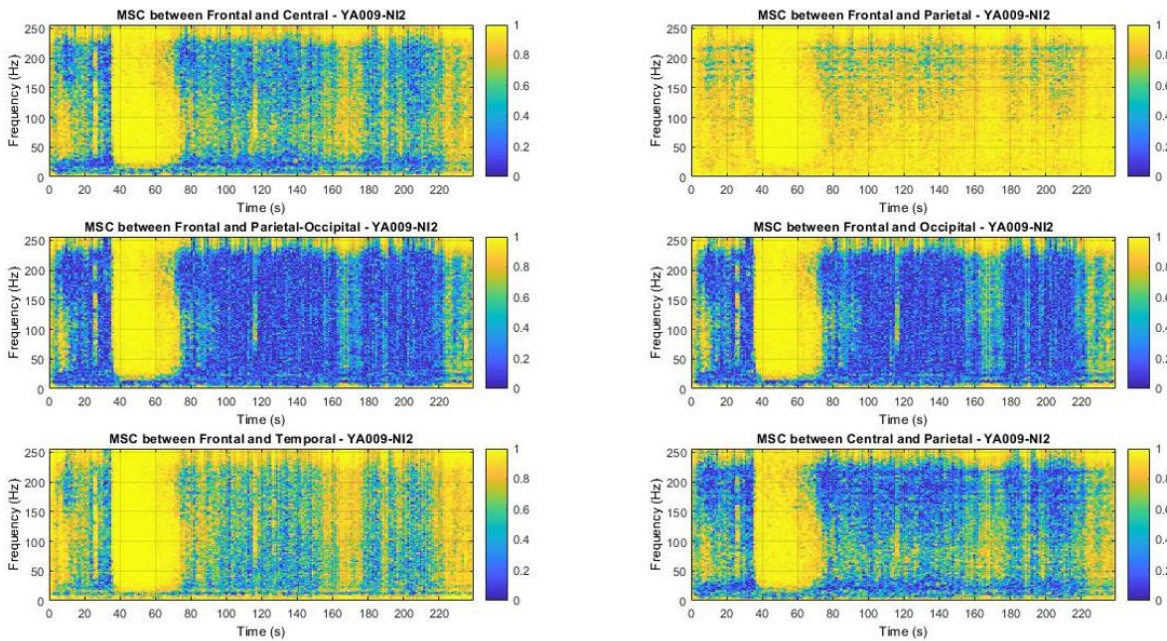


Figure A-11. Magnitude Square Coherence from NI1 – 5-min rest yet awake before the Trainer between various brain region combinations in subject 6 (YA009)

○ *No Interaction 2 – After the Trainer*



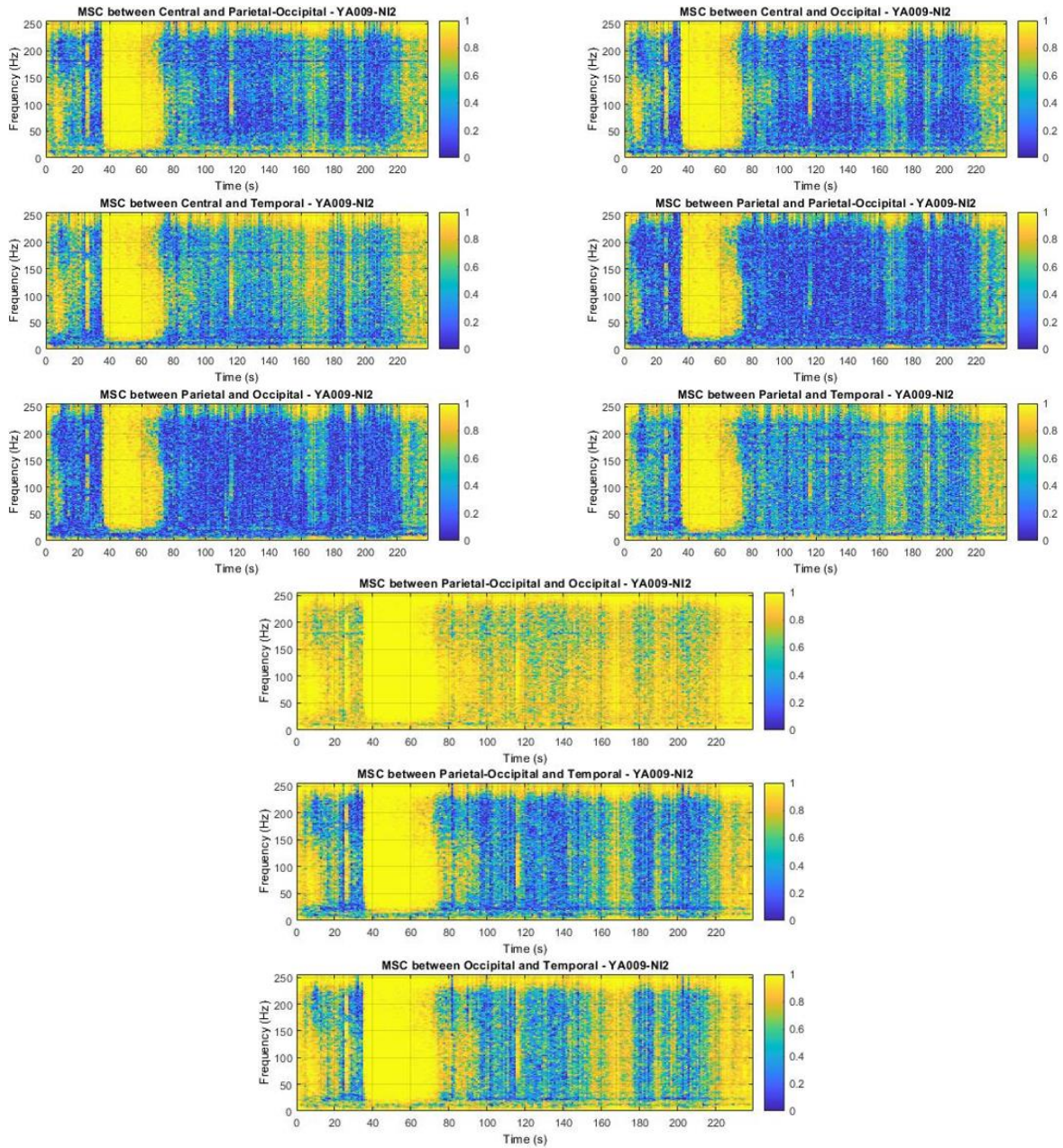
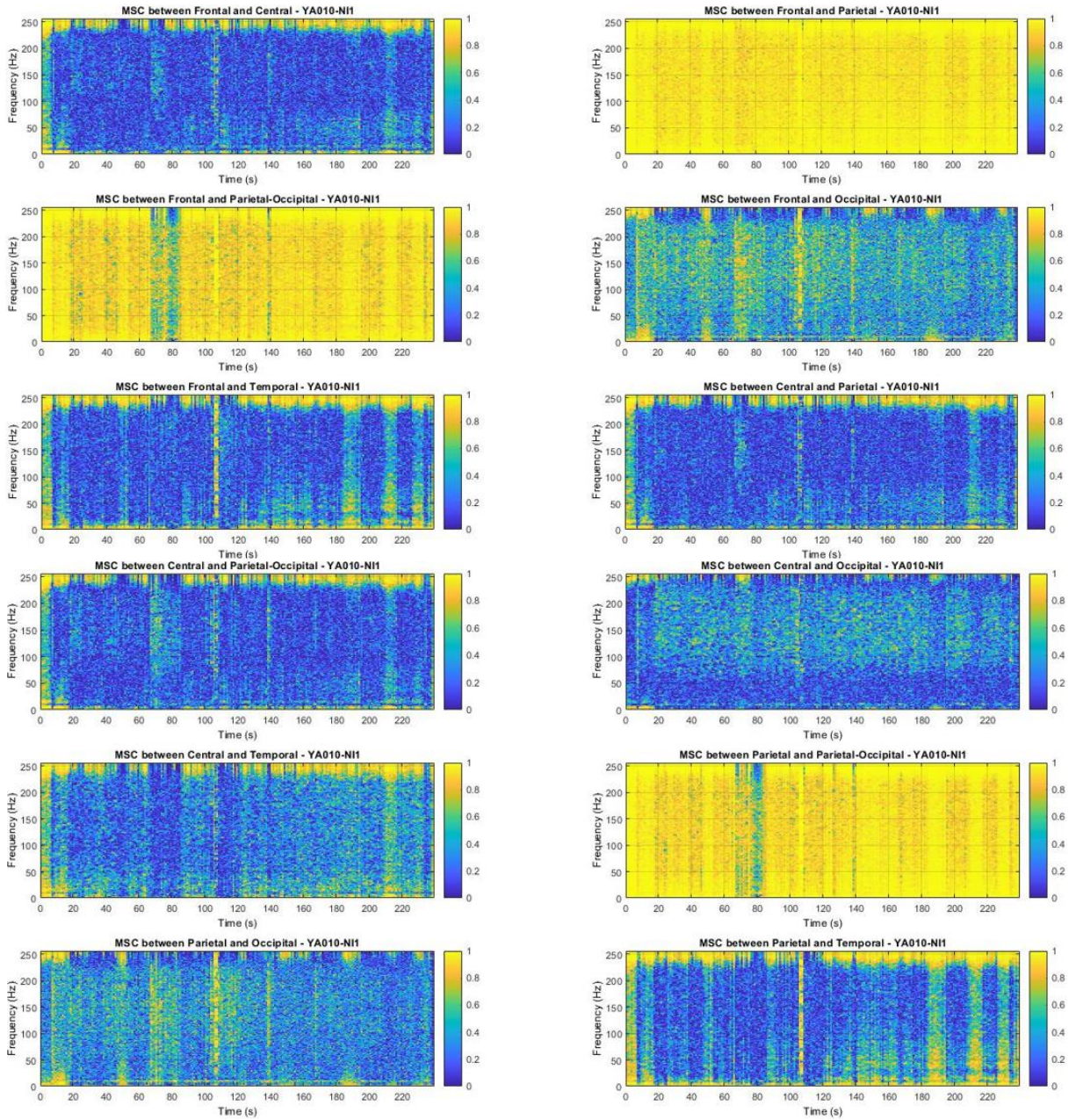


Figure A-12. Magnitude Square Coherence from NI2 – 5-min rest yet awake after the Trainer between various brain region combinations in subject 6 (YA009)

Subject 7

○ *No Interaction 1 – Before the Trainer*



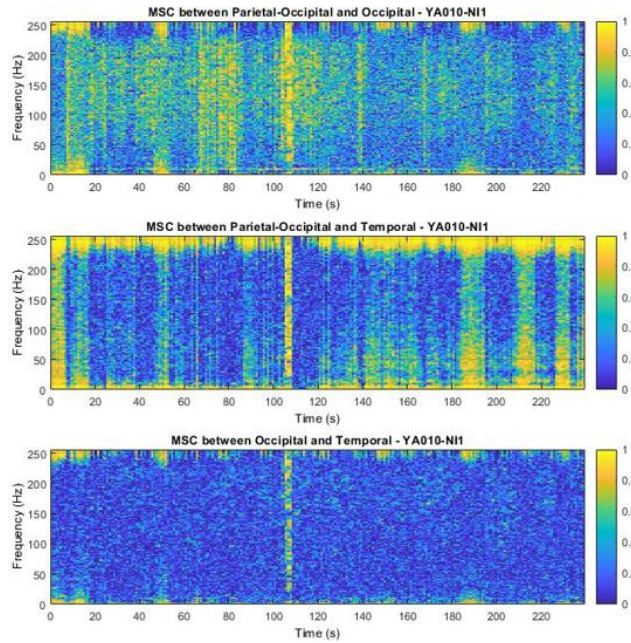
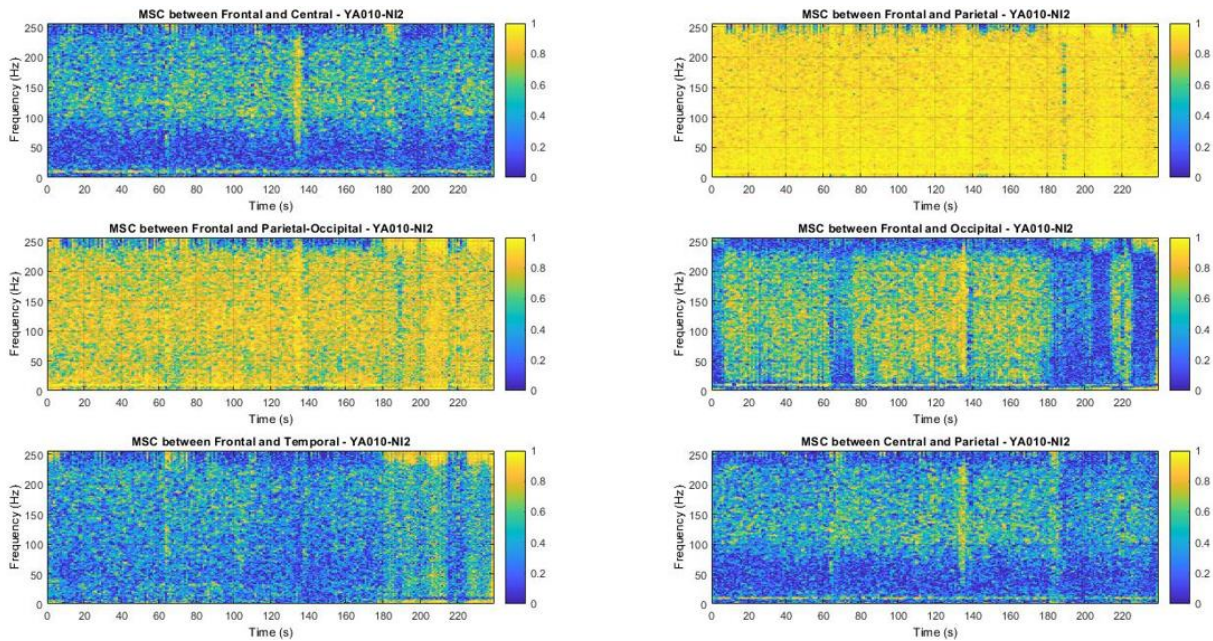


Figure A-13. Magnitude Square Coherence from NI1 – 5-min rest yet awake before the Trainer between various brain region combinations in subject 7 (YA010)

○ *No Interaction 2 – After the Trainer*



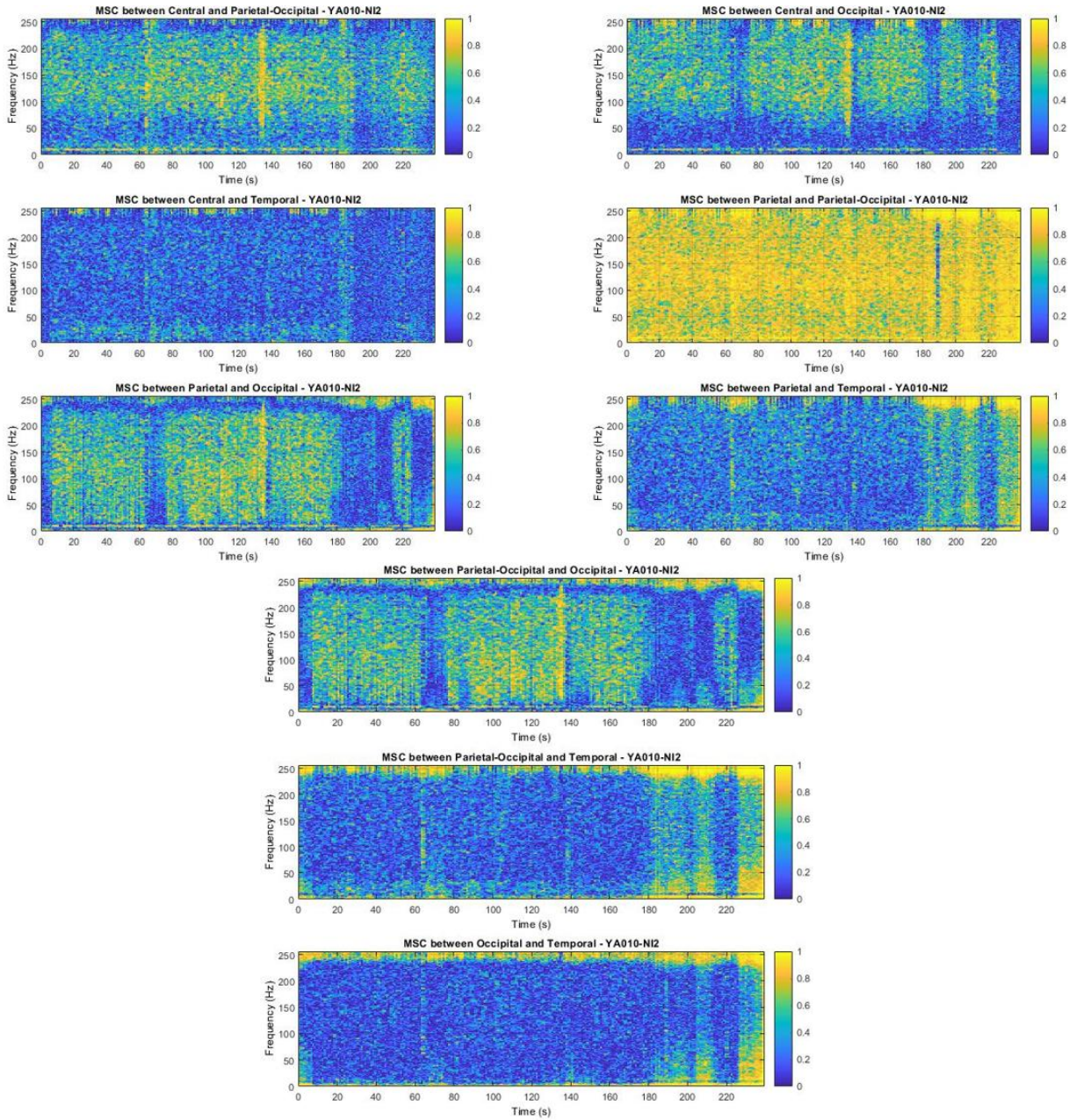


Figure A-14. Magnitude Square Coherence from NI2 – 5-min rest yet awake after the Trainer between various brain region combinations in subject 7 (YA010)

Appendix B – Codes

```
function [icaEEG, opt] = RemoveStrongArtifacts(icaEEG, Comp, Kthr, F)
%
% This function denoise high amplitude artifacts (e.g. ocular) and remove them from the
% Independent Components (ICs).
%
% INPUT:
%
% icaEEG - matrix of ICA components (Nchannel x Nobservations)
%
% Comp   - # of ICs to be denoised and cleaned (can be a vector)
%
% Kthr   - threshold (multiplier) for denoising of artifacts
%         (default Kthr = 1.15)
%
% F      - acquisition frequency
%         (default F = 256 Hz)
%
% OUTPUT:
%
% icaEEG - matrix of cleaned independent components
%
% opt    - vector of threshold values used for filtering of corresponding
%         ICs
%
% NOTE: If a component has no artifacts of a relatively high amplitude
%       the function will skip this component (no action), display a
%       warning and the corresponding output "opt" will be set to zero.
%
% Valeri A. Makarov, vmakarov@opt.ucm.es
% ver 0.1 Sept. 2005
% ver 0.2 May 2006
%

if nargin < 2,
    disp('At least two arguments are required!');
    help RemoveStrongArtifacts
    return;
end
if nargin < 3 || isempty(Kthr), Kthr = 1.15; end
if nargin < 4 || isempty(F), F = 512; end
L = round(F*0.1);
[Nchan, Nobser] = size(icaEEG);
if Nchan > Nobser,
    error('Problem with data orientation, try to transpose the matrix!');
end
N = 2^floor(log2(Nobser));
h = daubcwf(6);
opt = zeros(1,length(Comp));
for c=1:length(Comp),
```



```

Y = icaEEG(Comp(c),1:N);
Sig = median(abs(Y)/0.6745);
Thr = 4*Sig;
idx = find(abs(Y) > Thr);
idx_ext = zeros(1,length(idx)*(2*L+1));
for k=1:length(idx),
    idx_ext((2*L+1)*(k-1)+1:(2*L+1)*k) = [idx(k)-L:idx(k)+L];
end
id_noise=setdiff((1:N), idx_ext);
id_artef=setdiff((1:N), id_noise);
if isempty(id_artef),
    disp(['The component #' num2str(Comp(c)) ' has passed unchanged']);
    continue;
end
thld = 3.6;
KK = 100;
LL = floor(log2(length(Y)));
[xl, xh] = mrdwt(Y, h, LL);
while KK > Kthr,
    thld = thld + 0.5;
    xh = HardTh(xh, thld);
    xd = mirdwt(xl,xh,h,LL);
    xn = Y - xd;
    cn=corrcoef(Y(id_noise),xn(id_noise));
    ca=corrcoef(Y(id_artef),xd(id_artef));
    KK = ca(1,2)/cn(1,2);
end
opt(c) = thld;
Y = icaEEG(Comp(c),end-N+1:end);
icaEEG(Comp(c),1:N) = xn;
LL = floor(log2(length(Y)));
[xl, xh] = mrdwt(Y, h, LL);
xh = HardTh(xh, thld);
xd = mirdwt(xl,xh,h,LL);
xn = Y - xd;
icaEEG(Comp(c),N+1:end) = xn(end-(Nobser-N)+1:end);
disp(['The component #' num2str(Comp(c)) ' has been filtered']);
end

```

```

function [X,f,t] = STFTCoherence(x,M>window,nStart,increment,fs)
% SHORT-TERM FOURIER TRANSFORM function
% author: Ruby Phung
% date: 1/5/2017

% This function requires the following input arguments:
% 1. the input signal, or a time series: x
% 2. the window length: M
% 3. window function: window
% 4. starting time index: nStart
% 5. a time increment of __ points: increment
% 6. sampling frequency: fs

```

```

% and produce X output signal of meaningful points and the corresponding
% frequency and time index, f and t, respectively
k = 1;
N = length(x); % x is the input signal
halfwindow = fix(M/2); % half window size
f = (1:halfwindow)*(fs/M); % frequency vector

% Calculate spectra at each position using Hamming window
for j = nStart:increment:N
    if j+M-1 > length(x)
        x = [x zeros(1,M-(length(x)-j))];
    end
    xwindow = x(j:j+M-1).*window;
    ft = fft(xwindow);
    X(:,k) = ft(1:halfwindow); % meaningful points
    t(k) = j/fs; % calculate time
    k = k + 1; % increment the index

end

end

```

```

function [MSCohere,Freq,Time] = MSC(x,y,fs,M,L)
% MAGNITUDE-SQUARE COHERENCE function
% author: Ruby Phung
% date: 1/5/2017

l = 1:L;
X = cell(1, L); % create a 1xL cell array of empty matrices
Y = cell(1, L); % create a 1xL cell array of empty matrices
Yconj = cell(1,L); % create a 1xL cell array of empty matrices for Y*, aka conjugate

v = dpss(M,L/2); % create a window using dpss function
halfwin = M/2;
increment = M/2;
nStart = 300;

for m = 1:L
    [X{m},f,t] = STFTCoherence(x,M,v(:,m)',nStart,increment,fs);
    [Y{m},f,t] = STFTCoherence(y,M,v(:,m)',nStart,increment,fs);
    Yconj{m} = conj(Y{m});
end

Sxy = zeros(increment, length(t));
for l =1:L
    Sxy = Sxy + X{l}.*Yconj{l};
end
Sxy = abs(Sxy).^2;

Sxx = zeros(increment, length(t));
for l =1:L

```

```

    Sxx = Sxx + abs(X{1}).^2;
end

Syy = zeros(increment, length(t));
for l = 1:L
    Syy = Syy + abs(Y{1}).^2;
end

MSCohere = Sxy./(Sxx.*Syy);
Freq = f;
Time = t;

end

```

```

function [Y] = FrequencyBandExtractMSC(X)
% 5 DOMINANT FREQUENCY BAND EXTRACTION
% author: Ruby Phung
% date: 9/13/2018
%
% Overall MSC returns coherence values across all frequencies (up to 512 Hz)
% and across time (over 4 minutes) thus this function is intended to
% extract the MSC corresponding to 5 dominant frequency bands across time domain then take the
% mean across time domain for that specific frequency

% Extract Delta 1-4 Hz & take the mean across both frequency sub-bands and across time for the
chosen section i.e. NI1 or NI2
delta = mean2(X(1:8,:));
% Theta 5-7 Hz
theta = mean2(X(10:14,:));
% Alpha 8-13 Hz
alpha = mean2(X(16:26,:));
% Beta 14-30 Hz
beta = mean2(X(28:60,:));
% Gamma 31-100 Hz
gamma = mean2(X(62:200,:));

Y = {delta;theta;alpha;beta;gamma};

end

```

```

function [H, pvalue, w] = swtest(x, alpha)
% Shapiro-wilk (Sw) parametric hypothesis test of composite normality.
% [H, pvalue, SWstatistic] = SWTEST(X, ALPHA) performs the
% Shapiro-wilk test to determine if the null hypothesis of
% composite normality is a reasonable assumption regarding the
% population distribution of a random sample X. The desired significance
% level, ALPHA, is an optional scalar input (default = 0.05).
%

```

```

% The Shapiro-wilk and Shapiro-Francia null hypothesis is:
% "X is normal with unspecified mean and variance."
%
% This is an omnibus test, and is generally considered relatively
% powerful against a variety of alternatives.
% Shapiro-wilk test is better than the Shapiro-Francia test for
% Platykurtic sample. Conversely, Shapiro-Francia test is better than the
% Shapiro-wilk test for Leptokurtic samples.
%
% When the series 'X' is Leptokurtic, SWTEST performs the Shapiro-Francia
% test, else (series 'X' is Platykurtic) SWTEST performs the
% Shapiro-wilk test.
%
% [H, pvalue, SWstatistic] = SWTEST(X, ALPHA)
%
% Inputs:
% X - a vector of deviates from an unknown distribution. The observation
% number must exceed 3 and less than 5000.
%
% Optional inputs:
% ALPHA - The significance level for the test (default = 0.05).
%
% Outputs:
% SWstatistic - The test statistic (non normalized).
%
% pvalue - is the p-value, or the probability of observing the given
% result by chance given that the null hypothesis is true. Small values
% of pvalue cast doubt on the validity of the null hypothesis.
%
% H = 0 => Do not reject the null hypothesis at significance level ALPHA.
% H = 1 => Reject the null hypothesis at significance level ALPHA.
%
% Copyright (c) 17 March 2009 by Ahmed Ben Saïda
% Department of Finance, IHEC Sousse - Tunisia
% Email: ahmedbensaïda@yahoo.com
% $ Revision 3.0 $ Date: 18 June 2014 $
%
% References:
%
% - Royston P. "Remark AS R94", Applied Statistics (1995), vol. 44,
% No. 4, pp. 547-551.
% AS R94 -- calculates Shapiro-wilk normality test and P-value
% for sample sizes 3 <= n <= 5000. Handles censored or uncensored data.
% Corrects AS 181, which was found to be inaccurate for n > 50.
% Subroutine can be found at: http://lib.stat.cmu.edu/apstat/R94
%
% - Royston P. "A pocket-calculator algorithm for the Shapiro-Francia test
% for non-normality: An application to medicine", Statistics in Medicine
% (1993a), vol. 12, pp. 181-184.
%
% - Royston P. "A Toolkit for Testing Non-Normality in Complete and
% Censored Samples", Journal of the Royal Statistical Society Series D
% (1993b), vol. 42, No. 1, pp. 37-43.

```



```

%
% - Royston P. "Approximating the Shapiro-wilk W-test for non-normality",
%   Statistics and Computing (1992), Vol. 2, pp. 117-119.
%
% - Royston P. "An Extension of Shapiro and Wilk's W Test for Normality
%   to Large Samples", Journal of the Royal Statistical Society Series C
%   (1982a), Vol. 31, No. 2, pp. 115-124.
%
%
% Ensure the sample data is a VECTOR.
%
if numel(x) == length(x)
    x = x(:);           % Ensure a column vector.
else
    error(' Input sample 'X' must be a vector. ');
end
%
% Remove missing observations indicated by NaN's and check sample size.
%
x = x(~isnan(x));
if length(x) < 3
    error(' Sample vector 'X' must have at least 3 valid observations. ');
end
if length(x) > 5000
    warning('Shapiro-wilk test might be inaccurate due to large sample size (> 5000). ');
end
%
% Ensure the significance level, ALPHA, is a
% scalar, and set default if necessary.
%
if (nargin >= 2) && ~isempty(alpha)
    if ~isscalar(alpha)
        error(' Significance level 'Alpha' must be a scalar. ');
    end
    if (alpha <= 0 || alpha >= 1)
        error(' Significance level 'Alpha' must be between 0 and 1. ');
    end
else
    alpha = 0.05;
end
% First, calculate the a's for weights as a function of the m's
% See Royston (1992, p. 117) and Royston (1993b, p. 38) for details
% in the approximation.
x      = sort(x); % Sort the vector X in ascending order.
n      = length(x);
mtilde = norminv(((1:n)' - 3/8) / (n + 1/4));
weights = zeros(n,1); % Preallocate the weights.
if kurtosis(x) > 3
    % The Shapiro-Francia test is better for leptokurtic samples.
    weights = 1/sqrt(mtilde'*mtilde) * mtilde;
    %
    % The Shapiro-Francia statistic W' is calculated to avoid excessive
    % rounding errors for W' close to 1 (a potential problem in very
    % large samples).

```

```

%
w = (weights' * x)^2 / ((x - mean(x))' * (x - mean(x)));
% Royston (1993a, p. 183):
nu = log(n);
u1 = log(nu) - nu;
u2 = log(nu) + 2/nu;
mu = -1.2725 + (1.0521 * u1);
sigma = 1.0308 - (0.26758 * u2);
newSFstatistic = log(1 - w);
%
% Compute the normalized Shapiro-Francia statistic and its p-value.
%
NormalSFstatistic = (newSFstatistic - mu) / sigma;
% Computes the p-value, Royston (1993a, p. 183).
pValue = 1 - normcdf(NormalSFstatistic, 0, 1);
else

% The Shapiro-wilk test is better for platykurtic samples.
c = 1/sqrt(mtilde'*mtilde) * mtilde;
u = 1/sqrt(n);
% Royston (1992, p. 117) and Royston (1993b, p. 38):
PolyCoef_1 = [-2.706056 , 4.434685 , -2.071190 , -0.147981 , 0.221157 , c(n)];
PolyCoef_2 = [-3.582633 , 5.682633 , -1.752461 , -0.293762 , 0.042981 , c(n-1)];
% Royston (1992, p. 118) and Royston (1993b, p. 40, Table 1)
PolyCoef_3 = [-0.0006714 , 0.0250540 , -0.39978 , 0.54400];
PolyCoef_4 = [-0.0020322 , 0.0627670 , -0.77857 , 1.38220];
PolyCoef_5 = [0.00389150 , -0.083751 , -0.31082 , -1.5861];
PolyCoef_6 = [0.00303020 , -0.082676 , -0.48030];
PolyCoef_7 = [0.459 , -2.273];
weights(n) = polyval(PolyCoef_1 , u);
weights(1) = -weights(n);
if n > 5
    weights(n-1) = polyval(PolyCoef_2 , u);
    weights(2) = -weights(n-1);
    count = 3;
    phi = (mtilde'*mtilde - 2 * mtilde(n)^2 - 2 * mtilde(n-1)^2) / ...
          (1 - 2 * weights(n)^2 - 2 * weights(n-1)^2);
else
    count = 2;
    phi = (mtilde'*mtilde - 2 * mtilde(n)^2) / ...
          (1 - 2 * weights(n)^2);
end
% Special attention when n = 3 (this is a special case).
if n == 3
    % Royston (1992, p. 117)
    weights(1) = 1/sqrt(2);
    weights(n) = -weights(1);
    phi = 1;
end
%
% The vector 'WEIGHTS' obtained next corresponds to the same coefficients
% listed by Shapiro-wilk in their original test for small samples.
%
weights(count : n-count+1) = mtilde(count : n-count+1) / sqrt(phi);

```

```

%
% The Shapiro-wilk statistic w is calculated to avoid excessive rounding
% errors for w close to 1 (a potential problem in very large samples).
%
w = (weights' * x) ^2 / ((x - mean(x))' * (x - mean(x)));
%
% Calculate the normalized w and its significance level (exact for
% n = 3). Royston (1992, p. 118) and Royston (1993b, p. 40, Table 1).
%
newn = log(n);
if (n >= 4) && (n <= 11)
    mu = polyval(PolyCoef_3 , n);
    sigma = exp(polyval(PolyCoef_4 , n));
    gam = polyval(PolyCoef_7 , n);
    newSWstatistic = -log(gam-log(1-w));
elseif n > 11
    mu = polyval(PolyCoef_5 , newn);
    sigma = exp(polyval(PolyCoef_6 , newn));
    newSWstatistic = log(1 - w);
elseif n == 3
    mu = 0;
    sigma = 1;
    newSWstatistic = 0;
end
%
% Compute the normalized Shapiro-wilk statistic and its p-value.
%
NormalSWstatistic = (newSWstatistic - mu) / sigma;
% NormalSWstatistic is referred to the upper tail of N(0,1),
% Royston (1992, p. 119).
pvalue = 1 - normcdf(NormalSWstatistic, 0, 1);
% Special attention when n = 3 (this is a special case).
if n == 3
    pvalue = 6/pi * (asin(sqrt(w)) - asin(sqrt(3/4)));
    % Royston (1982a, p. 121)
end
end
%
% To maintain consistency with existing Statistics Toolbox hypothesis
% tests, returning 'H = 0' implies that we 'Do not reject the null
% hypothesis at the significance level of alpha' and 'H = 1' implies
% that we 'Reject the null hypothesis at significance level of alpha.'
%
H = (alpha >= pvalue);

```

Main script: YA_MSC_Analysis.m

```

eeglab(); % once EEGLAB GUI appears then select File -> Import data -> Using EEGLAB functions and
plugins -> From ANT EEProbe.CNT file

```

```

% 1. Load the selected dataset e.g. YA005_NI1.cnt OR YA005_NI2.cnt

```

```

[EEG] = pop_loadeep_v4(filename); % filename is the raw young adult EEG data from either NI1 or
NI2, e.g. pop_loadeep_v4('YAEEG_004__2017-10-27_09-20-58 NI1.cnt')

% 2. Remove unused/reference channels
EEG = pop_select(EEG, 'channel', [1:64]);

% 3. Resample data from 2048 to 512 Hz
EEG = pop_resample(EEG,512);

% 4. Remove DC value by removing the mean, aka Mean removal from the signal.
% By doing this we can eliminate the dc, i.e., 0Hz noise.
% Here DC component means, the signal positive half cycles average and the negative half cycle is
not zero. if x is the signal then xm=x-mean(x).
datatranspose = detrend(EEG.data','constant'); %Y = detrend(X,'constant') removes just the mean
value from the vector X,
% or the mean value from each column, if X is a matrix.
EEG.data = datatranspose';

% 5. Notch filter for 60 Hz

% Alternating current in the United States and several other countries oscillates at a frequency
of 60 Hz.
% Those oscillations often corrupt measurements and have to be subtracted. Eliminate the 60 Hz
noise with a Butterworth notch filter. Use designfilt to design it.
% The width of the notch is defined by the 59 to 61 Hz frequency interval. The filter removes at
least half the power of the frequency components lying in that range.
% Zero-phase filtering to help preserve features in a filtered time waveform exactly where they
occur in the unfiltered signal.
% zero-phase filters the input data, x, using a digital filter, d. Use designfilt to generate d
based on frequency-response specifications.
d =
designfilt('bandstopiir','FilterOrder',4,'HalfPowerFrequency1',59,'HalfPowerFrequency2',61,...
'DesignMethod','butter','SampleRate',EEG.srate); % 4th-order Butterworth filter
EEG.data = double(EEG.data); % change EEG data to double type as it is a required data type input
for the filtfilt function to work
EEG.data = filtfilt(d,EEG.data);

% 6. Change reference to overall average
EEG = pop_reref( EEG,[]); % for an average reference of 64 channels. The function is actually
averaging the 108 channels, and using
% these as the reference.

% 7. Read in Channel location files
EEG.chanlocs = readlocs('waveguard64final.ced');

% 8. Delete first 30 seconds and last 30 seconds of data
EEG.data = EEG.data(1:64, 30*(EEG.srate)+1:end-30*(EEG.srate));
% remove the first 30 seconds of time and last 30 seconds of times
EEG.times = EEG.times(30*(EEG.srate)+1:end-30*(EEG.srate));

% 9. Find IC's of the data
EEG.data = double(EEG.data);
[weight,sphere] = runica(EEG.data, 'verbose', 'off');
W=weight*sphere; % unmixing matrix

```

```

icaDATA =w*EEG.data; % compute the sources from the data

% 10. Removing Artefacts
% compute the cleaned IC's
[icaDATA2, opt] = RemoveStrongArtifacts(icaDATA,(1:64),1.15,EEG.srate);
% This function denoise high amplitude artifacts (e.g. ocular) and remove them from the
% Independent Components (ICs).

% 11. Reconstruct the EEG signal without the artefactual sources
EEG.data= inv(W)*icaDATA2;

%12. Divided EEG data by functional lobes
Frontal = EEG.data([1:12 33:43],:); % 23 channels
Central = EEG.data([15:17 44:47],:); % 7 channels
Parietal = EEG.data([20:29 48:54],:); % 17 channels
Parietal_Occipital = EEG.data([55:58 63:64],:); % 6 channels
Occipital = EEG.data([30:32],:); % 3 channels
Temporal = EEG.data([14 18 59:62],:); % 6 channels

Frontal_average = single(mean(Frontal));
Central_average = single(mean(Central));
Parietal_average = single(mean(Parietal));
Parietal_Occipital_average = single(mean(Parietal_Occipital));
Occipital_average = single(mean(Occipital));
Temporal_average = single(mean(Temporal));

% 13. Magnitude Square Coherence

fs = 512; % sampling frequency
M = 1024; % window length M
L = 7; % L is the overlapping, equal-length segments of x(n) and y(n),
% which are tapered by a single window function w(n)
[Frontal_Central_coherence,f_FC,t_FC] = MSC(Frontal_average,Central_average,fs,M,L);
[Frontal_Parietal_coherence,f_FP,t_FP] = MSC(Frontal_average,Parietal_average,fs,M,L);
[Frontal_ParietalOccipital_coherence,f_FPO,t_FPO] =
MSC(Frontal_average,Parietal_Occipital_average,fs,M,L);
[Frontal_Occipital_coherence,f_FO,t_FO] = MSC(Frontal_average,Occipital_average,fs,M,L);
[Frontal_Temporal_coherence,f_FT,t_FT] = MSC(Frontal_average,Temporal_average,fs,M,L);

[Central_Parietal_coherence,f_CP,t_CP] = MSC(Central_average,Parietal_average,fs,M,L);
[Central_ParietalOccipital_coherence,f_CPO,t_CPO] =
MSC(Central_average,Parietal_Occipital_average,fs,M,L);
[Central_Occipital_coherence,f_CO,t_CO] = MSC(Central_average,Occipital_average,fs,M,L);
[Central_Temporal_coherence,f_CT,t_CT] = MSC(Central_average,Temporal_average,fs,M,L);

[Parietal_ParietalOccipital_coherence,f_PPO,t_PPO] =
MSC(Parietal_average,Parietal_Occipital_average,fs,M,L);
[Parietal_Occipital_coherence,f_PO,t_PO] = MSC(Parietal_average,Occipital_average,fs,M,L);
[Parietal_Temporal_coherence,f_PT,t_PT] = MSC(Parietal_average,Temporal_average,fs,M,L);

[ParietalOccipital_Occipital_coherence,f_POO,t_POO] =
MSC(Parietal_Occipital_average,Occipital_average,fs,M,L);
[ParietalOccipital_Temporal_coherence,f_POT,t_POT] =
MSC(Parietal_Occipital_average,Temporal_average,fs,M,L);

```

```
[Occipital_Temporal_coherence,f_OT,t_OT] = MSC(Occipital_average,Temporal_average,fs,M,L);
```

```
% 14. Extract coherence from the 5 frequency bands of interest
```

```
MSC_FC_NI1 = FrequencyBandExtractMSC(Frontal_Central_coherence);  
MSC_FP_NI1 = FrequencyBandExtractMSC(Frontal_Parietal_coherence);  
MSC_FPO_NI1 = FrequencyBandExtractMSC(Frontal_ParietalOccipital_coherence);  
MSC_FO_NI1 = FrequencyBandExtractMSC(Frontal_Occipital_coherence);  
MSC_FT_NI1 = FrequencyBandExtractMSC(Frontal_Temporal_coherence);  
  
MSC_CP_NI1 = FrequencyBandExtractMSC(Central_Parietal_coherence);  
MSC_CPO_NI1 = FrequencyBandExtractMSC(Central_ParietalOccipital_coherence);  
MSC_CO_NI1 = FrequencyBandExtractMSC(Central_Occipital_coherence);  
MSC_CT_NI1 = FrequencyBandExtractMSC(Central_Temporal_coherence);  
  
MSC_PPO_NI1 = FrequencyBandExtractMSC(Parietal_ParietalOccipital_coherence);  
MSC_PO_NI1 = FrequencyBandExtractMSC(Parietal_Occipital_coherence);  
MSC_PT_NI1 = FrequencyBandExtractMSC(Parietal_Temporal_coherence);  
  
MSC_POO_NI1 = FrequencyBandExtractMSC(ParietalOccipital_Occipitalcoherence);  
MSC_POT_NI1 = FrequencyBandExtractMSC(ParietalOccipital_Temporal_coherence);  
MSC_OT_NI1 = FrequencyBandExtractMSC(Occipital_Temporal_coherence);
```

```
figure(1);hold on  
subplot(3,2,1);  
imagesc(t_FC,f_FC,Frontal_Central_coherence); grid on; title('MSC between Frontal and Central -  
YA005-NI1');  
colorbar('EastOutside'); set(gca,'YDir','normal');caxis([0 1])  
xlabel('Time (s)'); xlim([0 max(t_FC)]);set(gca,'XTick',(0:20:240))  
ylabel('Frequency (Hz)');ylim([0 max(f_FC)]);  
  
subplot(3,2,2);  
imagesc(t_FP,f_FP,Frontal_Parietal_coherence); grid on; title('MSC between Frontal and Parietal -  
YA005-NI1');  
colorbar('EastOutside'); set(gca,'YDir','normal');caxis([0 1])  
xlabel('Time (s)'); xlim([0 max(t_FP)]);set(gca,'XTick',(0:20:240))  
ylabel('Frequency (Hz)');ylim([0 max(f_FP)]);  
  
subplot(3,2,3);  
imagesc(t_FPO,f_FPO,Frontal_ParietalOccipital_coherence); grid on; title('MSC between Frontal and  
Parietal-Occipital - YA005-NI1');  
colorbar('EastOutside'); set(gca,'YDir','normal');caxis([0 1])  
xlabel('Time (s)'); xlim([0 max(t_FPO)]);set(gca,'XTick',(0:20:240))  
ylabel('Frequency (Hz)');ylim([0 max(f_FPO)]);  
  
subplot(3,2,4);  
imagesc(t_FO,f_FO,Frontal_Occipital_coherence); grid on; title('MSC between Frontal and Occipital  
- YA005-NI1');  
colorbar('EastOutside'); set(gca,'YDir','normal');caxis([0 1])  
xlabel('Time (s)'); xlim([0 max(t_FO)]);set(gca,'XTick',(0:20:240))  
ylabel('Frequency (Hz)');ylim([0 max(f_FO)]);  
  
subplot(3,2,5);
```

```

imagesc(t_FT,f_FT,Frontal_Temporal_coherence); grid on; title('MSC between Frontal and Temporal -
YA005-NI1');
colorbar('EastOutside'); set(gca,'YDir','normal');caxis([0 1])
xlabel('Time (s)'); xlim([0 max(t_FT)]);set(gca,'XTick',(0:20:240))
ylabel('Frequency (Hz)');ylim([0 max(f_FT)]);

subplot(3,2,6);
imagesc(t_CP,f_CP,Central_Parietal_coherence); grid on; title('MSC between Central and Parietal -
YA005-NI1');
colorbar('EastOutside'); set(gca,'YDir','normal');caxis([0 1])
xlabel('Time (s)'); xlim([0 max(t_CP)]);set(gca,'XTick',(0:20:240))
ylabel('Frequency (Hz)');ylim([0 max(f_CP)]);hold off

figure(2); hold on
subplot(3,2,1);
imagesc(t_CPO,f_CPO,Central_ParietalOccipital_coherence); grid on; title('MSC between Central and
Parietal-Occipital - YA005-NI1');
colorbar('EastOutside'); set(gca,'YDir','normal');caxis([0 1])
xlabel('Time (s)'); xlim([0 max(t_CPO)]);set(gca,'XTick',(0:20:240))
ylabel('Frequency (Hz)');ylim([0 max(f_CPO)]);

subplot(3,2,2);
imagesc(t_CO,f_CO,Central_Occipital_coherence); grid on; title('MSC between Central and Occipital
- YA005-NI1');
colorbar('EastOutside'); set(gca,'YDir','normal');caxis([0 1])
xlabel('Time (s)'); xlim([0 max(t_CO)]);set(gca,'XTick',(0:20:240))
ylabel('Frequency (Hz)');ylim([0 max(f_CO)]);

subplot(3,2,3);
imagesc(t_CT,f_CT,Central_Temporal_coherence); grid on; title('MSC between Central and Temporal -
YA005-NI1');
colorbar('EastOutside'); set(gca,'YDir','normal');caxis([0 1])
xlabel('Time (s)'); xlim([0 max(t_CT)]);set(gca,'XTick',(0:20:240))
ylabel('Frequency (Hz)');ylim([0 max(f_CT)]);

subplot(3,2,4);
imagesc(t_PPO,f_PPO,Parietal_ParietalOccipital_coherence); grid on; title('MSC between Parietal
and Parietal-Occipital - YA005-NI1');
colorbar('EastOutside'); set(gca,'YDir','normal');caxis([0 1])
xlabel('Time (s)'); xlim([0 max(t_PPO)]);set(gca,'XTick',(0:20:240))
ylabel('Frequency (Hz)');ylim([0 max(f_PPO)]);

subplot(3,2,5);
imagesc(t_PO,f_PO,Parietal_Occipital_coherence); grid on; title('MSC between Parietal and
Occipital - YA005-NI1');
colorbar('EastOutside'); set(gca,'YDir','normal');caxis([0 1])
xlabel('Time (s)'); xlim([0 max(t_PO)]);set(gca,'XTick',(0:20:240))
ylabel('Frequency (Hz)');ylim([0 max(f_PO)]);

subplot(3,2,6);
imagesc(t_PT,f_PT,Parietal_Temporal_coherence); grid on; title('MSC between Parietal and Temporal
- YA005-NI1');
colorbar('EastOutside'); set(gca,'YDir','normal');caxis([0 1])

```

```

xlabel('Time (s)'); xlim([0 max(t_PT)]);set(gca,'XTick',(0:20:240))
ylabel('Frequency (Hz)');ylim([0 max(f_PT)]);hold off

figure(3); hold on
subplot(3,1,1);
imagesc(t_POO,f_POO,ParietalOccipital_Occipitalcoherence); grid on; title('MSC between Parietal-
Occipital and Occipital - YA005-NI1');
colorbar('EastOutside'); set(gca,'YDir','normal');caxis([0 1])
xlabel('Time (s)'); xlim([0 max(t_POO)]);set(gca,'XTick',(0:20:240))
ylabel('Frequency (Hz)');ylim([0 max(f_POO)]);

subplot(3,1,2);
imagesc(t_POT,f_POT,ParietalOccipital_Temporal_coherence); grid on; title('MSC between Parietal-
Occipital and Temporal - YA005-NI1');
colorbar('EastOutside'); set(gca,'YDir','normal');caxis([0 1])
xlabel('Time (s)'); xlim([0 max(t_POT)]);set(gca,'XTick',(0:20:240))
ylabel('Frequency (Hz)');ylim([0 max(f_POT)]);

subplot(3,1,3);
imagesc(t_OT,f_OT,Occipital_Temporal_coherence); grid on; title('MSC between Occipital and
Temporal - YA005-NI1');
colorbar('EastOutside'); set(gca,'YDir','normal');caxis([0 1])
xlabel('Time (s)'); xlim([0 max(t_OT)]);set(gca,'XTick',(0:20:240))
ylabel('Frequency (Hz)');ylim([0 max(f_OT)]);
hold off

```

```

% load('YA005-NI2 MSC_ 2nd run.mat')

MSC_FC_NI2 = FrequencyBandExtractMSC(Frontal_Central_coherence);
MSC_FP_NI2 = FrequencyBandExtractMSC(Frontal_Parietal_coherence);
MSC_FPO_NI2 = FrequencyBandExtractMSC(Frontal_ParietalOccipital_coherence);
MSC_FO_NI2 = FrequencyBandExtractMSC(Frontal_Occipital_coherence);
MSC_FT_NI2 = FrequencyBandExtractMSC(Frontal_Temporal_coherence);

MSC_CP_NI2 = FrequencyBandExtractMSC(Central_Parietal_coherence);
MSC_CPO_NI2 = FrequencyBandExtractMSC(Central_ParietalOccipital_coherence);
MSC_CO_NI2 = FrequencyBandExtractMSC(Central_Occipital_coherence);
MSC_CT_NI2 = FrequencyBandExtractMSC(Central_Temporal_coherence);

MSC_PPO_NI2 = FrequencyBandExtractMSC(Parietal_ParietalOccipital_coherence);
MSC_PO_NI2 = FrequencyBandExtractMSC(Parietal_Occipital_coherence);
MSC_PT_NI2 = FrequencyBandExtractMSC(Parietal_Temporal_coherence);

MSC_POO_NI2 = FrequencyBandExtractMSC(ParietalOccipital_Occipitalcoherence);
MSC_POT_NI2 = FrequencyBandExtractMSC(ParietalOccipital_Temporal_coherence);
MSC_OT_NI2 = FrequencyBandExtractMSC(Occipital_Temporal_coherence);

```

```

figure(1); hold on
subplot(3,2,1);
imagesc(t_FC,f_FC,Frontal_Central_coherence); grid on; title('MSC between Frontal and Central -
YA005-NI2');
colorbar('EastOutside'); set(gca,'YDir','normal');caxis([0 1])

```



```

xlabel('Time (s)'); xlim([0 max(t_FC)]);set(gca,'XTick',(0:20:240))
ylabel('Frequency (Hz)');ylim([0 max(f_FC)]);

subplot(3,2,2);
imagesc(t_FP,f_FP,Frontal_Parietal_coherence); grid on; title('MSC between Frontal and Parietal -
YA005-NI2');
colorbar('EastOutside'); set(gca,'YDir','normal');caxis([0 1])
xlabel('Time (s)'); xlim([0 max(t_FP)]);set(gca,'XTick',(0:20:240))
ylabel('Frequency (Hz)');ylim([0 max(f_FP)]);

subplot(3,2,3);
imagesc(t_FPO,f_FPO,Frontal_ParietalOccipital_coherence); grid on; title('MSC between Frontal and
Parietal-Occipital - YA005-NI2');
colorbar('EastOutside'); set(gca,'YDir','normal');caxis([0 1])
xlabel('Time (s)'); xlim([0 max(t_FPO)]);set(gca,'XTick',(0:20:240))
ylabel('Frequency (Hz)');ylim([0 max(f_FPO)]);

subplot(3,2,4);
imagesc(t_FO,f_FO,Frontal_Occipital_coherence); grid on; title('MSC between Frontal and Occipital
- YA005-NI2');
colorbar('EastOutside'); set(gca,'YDir','normal');caxis([0 1])
xlabel('Time (s)'); xlim([0 max(t_FO)]);set(gca,'XTick',(0:20:240))
ylabel('Frequency (Hz)');ylim([0 max(f_FO)]);

subplot(3,2,5);
imagesc(t_FT,f_FT,Frontal_Temporal_coherence); grid on; title('MSC between Frontal and Temporal -
YA005-NI2');
colorbar('EastOutside'); set(gca,'YDir','normal');caxis([0 1])
xlabel('Time (s)'); xlim([0 max(t_FT)]);set(gca,'XTick',(0:20:240))
ylabel('Frequency (Hz)');ylim([0 max(f_FT)]);

subplot(3,2,6);
imagesc(t_CP,f_CP,Central_Parietal_coherence); grid on; title('MSC between Central and Parietal -
YA005-NI2');
colorbar('EastOutside'); set(gca,'YDir','normal');caxis([0 1])
xlabel('Time (s)'); xlim([0 max(t_CP)]);set(gca,'XTick',(0:20:240))
ylabel('Frequency (Hz)');ylim([0 max(f_CP)]);hold off

```

```

figure(2); hold on
subplot(3,2,1);
imagesc(t_CPO,f_CPO,Central_ParietalOccipital_coherence); grid on; title('MSC between Central and
Parietal-Occipital - YA005-NI2');
colorbar('EastOutside'); set(gca,'YDir','normal');caxis([0 1])
xlabel('Time (s)'); xlim([0 max(t_CPO)]);set(gca,'XTick',(0:20:240))
ylabel('Frequency (Hz)');ylim([0 max(f_CPO)]);

subplot(3,2,2);
imagesc(t_CO,f_CO,Central_Occipital_coherence); grid on; title('MSC between Central and Occipital
- YA005-NI2');
colorbar('EastOutside'); set(gca,'YDir','normal');caxis([0 1])
xlabel('Time (s)'); xlim([0 max(t_CO)]);set(gca,'XTick',(0:20:240))
ylabel('Frequency (Hz)');ylim([0 max(f_CO)]);

```

```

subplot(3,2,3);
imagesc(t_CT,f_CT,Central_Temporal_coherence); grid on; title('MSC between Central and Temporal -
YA005-NI2');
colorbar('EastOutside'); set(gca,'YDir','normal');caxis([0 1])
xlabel('Time (s)'); xlim([0 max(t_CT)]);set(gca,'XTick',(0:20:240))
ylabel('Frequency (Hz)');ylim([0 max(f_CT)]);

subplot(3,2,4);
imagesc(t_PPO,f_PPO,Parietal_ParietalOccipital_coherence); grid on; title('MSC between Parietal
and Parietal-Occipital - YA005-NI2');
colorbar('EastOutside'); set(gca,'YDir','normal');caxis([0 1])
xlabel('Time (s)'); xlim([0 max(t_PPO)]);set(gca,'XTick',(0:20:240))
ylabel('Frequency (Hz)');ylim([0 max(f_PPO)]);

subplot(3,2,5);
imagesc(t_PO,f_PO,Parietal_Occipital_coherence); grid on; title('MSC between Parietal and
Occipital - YA005-NI2');
colorbar('EastOutside'); set(gca,'YDir','normal');caxis([0 1])
xlabel('Time (s)'); xlim([0 max(t_PO)]);set(gca,'XTick',(0:20:240))
ylabel('Frequency (Hz)');ylim([0 max(f_PO)]);

subplot(3,2,6);
imagesc(t_PT,f_PT,Parietal_Temporal_coherence); grid on; title('MSC between Parietal and Temporal
- YA005-NI2');
colorbar('EastOutside'); set(gca,'YDir','normal');caxis([0 1])
xlabel('Time (s)'); xlim([0 max(t_PT)]);set(gca,'XTick',(0:20:240))
ylabel('Frequency (Hz)');ylim([0 max(f_PT)]);hold off

```

```

figure(3); hold on
subplot(3,1,1);
imagesc(t_POO,f_POO,ParietalOccipital_Occipitalcoherence); grid on; title('MSC between Parietal-
Occipital and Occipital - YA005-NI2');
colorbar('EastOutside'); set(gca,'YDir','normal');caxis([0 1])
xlabel('Time (s)'); xlim([0 max(t_POO)]);set(gca,'XTick',(0:20:240))
ylabel('Frequency (Hz)');ylim([0 max(f_POO)]);

subplot(3,1,2);
imagesc(t_POT,f_POT,ParietalOccipital_Temporal_coherence); grid on; title('MSC between Parietal-
Occipital and Temporal - YA005-NI2');
colorbar('EastOutside'); set(gca,'YDir','normal');caxis([0 1])
xlabel('Time (s)'); xlim([0 max(t_POT)]);set(gca,'XTick',(0:20:240))
ylabel('Frequency (Hz)');ylim([0 max(f_POT)]);

subplot(3,1,3);
imagesc(t_OT,f_OT,Occipital_Temporal_coherence); grid on; title('MSC between Occipital and
Temporal - YA005-NI2');
colorbar('EastOutside'); set(gca,'YDir','normal');caxis([0 1])
xlabel('Time (s)'); xlim([0 max(t_OT)]);set(gca,'XTick',(0:20:240))
ylabel('Frequency (Hz)');ylim([0 max(f_OT)]);
hold off

```

```

% load('Combined MSC in 5 freq band 15 lobes combination_YA005.mat');

% Extract Delta 1-4 Hz
Delta_005 = [MSC_FC_NI1{1},MSC_FP_NI1{1},MSC_FPO_NI1{1},MSC_FO_NI1{1},MSC_FT_NI1{1},...
    MSC_CP_NI1{1},MSC_CPO_NI1{1},MSC_CO_NI1{1},MSC_CT_NI1{1},MSC_PPO_NI1{1},...
    MSC_PO_NI1{1},MSC_PT_NI1{1},MSC_POO_NI1{1},MSC_POT_NI1{1},MSC_OT_NI1{1};...
    MSC_FC_NI2{1},MSC_FP_NI2{1},MSC_FPO_NI2{1},MSC_FO_NI2{1},MSC_FT_NI2{1},...
    MSC_CP_NI2{1},MSC_CPO_NI2{1},MSC_CO_NI2{1},MSC_CT_NI2{1},MSC_PPO_NI2{1},...
    MSC_PO_NI2{1},MSC_PT_NI2{1},MSC_POO_NI2{1},MSC_POT_NI2{1},MSC_OT_NI2{1}];

% Theta 5-7 Hz
Theta_005 = [MSC_FC_NI1{2},MSC_FP_NI1{2},MSC_FPO_NI1{2},MSC_FO_NI1{2},MSC_FT_NI1{2},...
    MSC_CP_NI1{2},MSC_CPO_NI1{2},MSC_CO_NI1{2},MSC_CT_NI1{2},MSC_PPO_NI1{2},...
    MSC_PO_NI1{2},MSC_PT_NI1{2},MSC_POO_NI1{2},MSC_POT_NI1{2},MSC_OT_NI1{2};...
    MSC_FC_NI2{2},MSC_FP_NI2{2},MSC_FPO_NI2{2},MSC_FO_NI2{2},MSC_FT_NI2{2},...
    MSC_CP_NI2{2},MSC_CPO_NI2{2},MSC_CO_NI2{2},MSC_CT_NI2{2},MSC_PPO_NI2{2},...
    MSC_PO_NI2{2},MSC_PT_NI2{2},MSC_POO_NI2{2},MSC_POT_NI2{2},MSC_OT_NI2{2}];

% Alpha 8-13 Hz
Alpha_005 = [MSC_FC_NI1{3},MSC_FP_NI1{3},MSC_FPO_NI1{3},MSC_FO_NI1{3},MSC_FT_NI1{3},...
    MSC_CP_NI1{3},MSC_CPO_NI1{3},MSC_CO_NI1{3},MSC_CT_NI1{3},MSC_PPO_NI1{3},...
    MSC_PO_NI1{3},MSC_PT_NI1{3},MSC_POO_NI1{3},MSC_POT_NI1{3},MSC_OT_NI1{3};...
    MSC_FC_NI2{3},MSC_FP_NI2{3},MSC_FPO_NI2{3},MSC_FO_NI2{3},MSC_FT_NI2{3},...
    MSC_CP_NI2{3},MSC_CPO_NI2{3},MSC_CO_NI2{3},MSC_CT_NI2{3},MSC_PPO_NI2{3},...
    MSC_PO_NI2{3},MSC_PT_NI2{3},MSC_POO_NI2{3},MSC_POT_NI2{3},MSC_OT_NI2{3}];

% Beta 14-30 Hz
Beta_005 = [MSC_FC_NI1{4},MSC_FP_NI1{4},MSC_FPO_NI1{4},MSC_FO_NI1{4},MSC_FT_NI1{4},...
    MSC_CP_NI1{4},MSC_CPO_NI1{4},MSC_CO_NI1{4},MSC_CT_NI1{4},MSC_PPO_NI1{4},...
    MSC_PO_NI1{4},MSC_PT_NI1{4},MSC_POO_NI1{4},MSC_POT_NI1{4},MSC_OT_NI1{4};...
    MSC_FC_NI2{4},MSC_FP_NI2{4},MSC_FPO_NI2{4},MSC_FO_NI2{4},MSC_FT_NI2{4},...
    MSC_CP_NI2{4},MSC_CPO_NI2{4},MSC_CO_NI2{4},MSC_CT_NI2{4},MSC_PPO_NI2{4},...
    MSC_PO_NI2{4},MSC_PT_NI2{4},MSC_POO_NI2{4},MSC_POT_NI2{4},MSC_OT_NI2{4}];

% Gamma 31-100 Hz
Gamma_005 = [MSC_FC_NI1{5},MSC_FP_NI1{5},MSC_FPO_NI1{5},MSC_FO_NI1{5},MSC_FT_NI1{5},...
    MSC_CP_NI1{5},MSC_CPO_NI1{5},MSC_CO_NI1{5},MSC_CT_NI1{5},MSC_PPO_NI1{5},...
    MSC_PO_NI1{5},MSC_PT_NI1{5},MSC_POO_NI1{5},MSC_POT_NI1{5},MSC_OT_NI1{5};...
    MSC_FC_NI2{5},MSC_FP_NI2{5},MSC_FPO_NI2{5},MSC_FO_NI2{5},MSC_FT_NI2{5},...
    MSC_CP_NI2{5},MSC_CPO_NI2{5},MSC_CO_NI2{5},MSC_CT_NI2{5},MSC_PPO_NI2{5},...
    MSC_PO_NI2{5},MSC_PT_NI2{5},MSC_POO_NI2{5},MSC_POT_NI2{5},MSC_OT_NI2{5}];

```

Main script: YA_StatisticalAnalysis.m

```

clear all; close all;clc;

load('Grand Poplulation MSC in 5 frequency bands NI1 & NI2.mat');

```

1. Calculate the change in coherence, aka Δ MSC in 5 frequency bands

```
deltaMSC_Delta = Grand_Delta_NI2 - Grand_Delta_NI1; % change in coherence (MSC) in DELTA
frequency 1-4 Hz
deltaMSC_Theta = Grand_Theta_NI2 - Grand_Theta_NI1; % change in coherence (MSC) in THETA
frequency 5-7 Hz
deltaMSC_Alpha = Grand_Alpha_NI2 - Grand_Alpha_NI1; % change in coherence (MSC) in ALPHA
frequency 8-13 Hz
deltaMSC_Beta = Grand_Beta_NI2 - Grand_Beta_NI1; % change in coherence (MSC) in BETA frequency
14-30 Hz
deltaMSC_Gamma = Grand_Gamma_NI2 - Grand_Gamma_NI1; % change in coherence (MSC) in GAMMA
frequency 31-100 Hz
```

2. Run the Shapiro-Wilk test for normality in the data - Verification of normal distribution assumption for the paired t-test

```
%%%%%%%%%%%%%%%%%%%%%%%%%%%%%%%%%%%%%%%%%%%%%%%%%%%%%%%%%%%%%%%%%%%%%%%%
%   H = 0 => Do not reject the null hypothesis at significance level ALPHA.
%   H = 1 => Reject the null hypothesis at significance level ALPHA.
%%%%%%%%%%%%%%%%%%%%%%%%%%%%%%%%%%%%%%%%%%%%%%%%%%%%%%%%%%%%%%%%%%%%%%%%
[r,c] = size(deltaMSC_Delta);
for i = 1:c
    [H_Delta(i),pval_Delta(i),w_Delta(i)] = swtest(deltaMSC_Delta(:,i),0.05);
end

[r,c] = size(deltaMSC_Theta);
for i = 1:c
    [H_Theta(i),pval_Theta(i),w_Theta(i)] = swtest(deltaMSC_Theta(:,i),0.05);
end

[r,c] = size(deltaMSC_Alpha);
for i = 1:c
    [H_Alpha(i),pval_Alpha(i),w_Alpha(i)] = swtest(deltaMSC_Alpha(:,i),0.05);
end

[r,c] = size(deltaMSC_Beta);
for i = 1:c
    [H_Beta(i),pval_Beta(i),w_Beta(i)] = swtest(deltaMSC_Beta(:,i),0.05);
end

[r,c] = size(deltaMSC_Gamma);
for i = 1:c
    [H_Gamma(i),pval_Gamma(i),w_Gamma(i)] = swtest(deltaMSC_Gamma(:,i),0.05);
end

H = [H_Delta;H_Theta;H_Alpha;H_Beta;H_Gamma];
% put those in a Table form
% H = array2table(H);
% rename the correct header for each row
% H.Properties.RowNames = {'Delta','Theta','Alpha','Beta','Gamma'};
% H.Properties.VariableNames =
{'FC','FP','FPO','FO','FT','CP','CPO','CO','CT','PPO','PO','PT','POO','POT','OT'};
```

```

disp('          WILK-SHAPIRO NORMALITY TEST');
disp(H);

pval_wilkShapiro = [pval_Delta;pval_Theta;pval_Alpha;pval_Beta;pval_Gamma];
% put those in a Table form
pval_wilkShapiro = array2table(pval_wilkShapiro);
% rename the correct header for each row
pval_wilkShapiro.Properties.RowNames = {'Delta','Theta','Alpha','Beta','Gamma'};
pval_wilkShapiro.Properties.VariableNames =
{'FC','FP','FPO','FO','FT','CP','CPO','CO','CT','PPO','PO','PT','POO','POT','OT'};
disp('          WILK-SHAPIRO NORMALITY TEST');
disp(pval_wilkShapiro);

```

3. Paired T-test - a parametric test

```

%%%%%%%%%%%%%%%%%%%%%%%%%%%%%%%%%%%%%%%%%%%%%%%%%%%%%%%%%%%%%%%%%%%%%%%%
% H = 0 indicates the null hypothesis (mean or the change is zero) can NOT be rejected
% H = 1 indicates that the null hypothesis can be rejected at the 5% level
% => there is in deed a change in coherence
%%%%%%%%%%%%%%%%%%%%%%%%%%%%%%%%%%%%%%%%%%%%%%%%%%%%%%%%%%%%%%%%%%%%%%%%
[r,c] = size(deltaMSC_Delta);
for i = 1:c
    [h_ttest_Delta(i),p_ttest_Delta(i)] = ttest(deltaMSC_Delta(:,i),0,'tail','left');
end

[r,c] = size(deltaMSC_Theta);
for i = 1:c
    [h_ttest_Theta(i),p_ttest_Theta(i)] = ttest(deltaMSC_Theta(:,i),0,'tail','left');
end

[r,c] = size(deltaMSC_Alpha);
for i = 1:c
    [h_ttest_Alpha(i),p_ttest_Alpha(i)] = ttest(deltaMSC_Alpha(:,i),0,'tail','left');
end

[r,c] = size(deltaMSC_Beta);
for i = 1:c
    [h_ttest_Beta(i),p_ttest_Beta(i)] = ttest(deltaMSC_Beta(:,i),0,'tail','left');
end

[r,c] = size(deltaMSC_Gamma);
for i = 1:c
    [h_ttest_Gamma(i),p_ttest_Gamma(i)] = ttest(deltaMSC_Gamma(:,i),0,'tail','left');
end
H_ttest = [h_ttest_Delta;h_ttest_Theta;h_ttest_Alpha;h_ttest_Beta;h_ttest_Gamma];
% % put those in a Table form
% H_ttest = array2table(H_ttest);
% % rename the correct header for each row
% H_ttest.Properties.RowNames = {'Delta','Theta','Alpha','Beta','Gamma'};
% H_ttest.Properties.VariableNames =
{'FC','FP','FPO','FO','FT','CP','CPO','CO','CT','PPO','PO','PT','POO','POT','OT'};

```

```
disp('          PAIRED T-TEST');
disp(H_ttest);
```

4. Wilcoxon sign-rank test - a nonparametric test equivalent of the paired t-test

```
%%%%%%%%%%%%%%%%%%%%%%%%%%%%%%%%%%%%%%%%%%%%%%%%%%%%%%%%%%%%%%%%%%%%%%%%
% H = 0 indicates the null hypothesis cannot be rejected at the 5% level
% H = 1 indicates the null hypothesis can be rejected at the 5% level
%%%%%%%%%%%%%%%%%%%%%%%%%%%%%%%%%%%%%%%%%%%%%%%%%%%%%%%%%%%%%%%%%%%%%%%%

[row,col] = size(deltaMSC_Delta);
for ii = 1:col
    [P_signrank_Delta(ii),H_signrank_Delta(ii)] = signrank(deltaMSC_Delta(:,ii),0,'tail','left');
end

[row,col] = size(deltaMSC_Theta);
for ii = 1:col
    [P_signrank_Theta(ii),H_signrank_Theta(ii)] = signrank(deltaMSC_Theta(:,ii),0,'tail','left');
end

[row,col] = size(deltaMSC_Alpha);
for ii = 1:col
    [P_signrank_Alpha(ii),H_signrank_Alpha(ii)] = signrank(deltaMSC_Alpha(:,ii),0,'tail','left');
end

[row,col] = size(deltaMSC_Beta);
for ii = 1:col
    [P_signrank_Beta(ii),H_signrank_Beta(ii)] = signrank(deltaMSC_Beta(:,ii),0,'tail','left');
end

[row,col] = size(deltaMSC_Gamma);
for ii = 1:col
    [P_signrank_Gamma(ii),H_signrank_Gamma(ii)] = signrank(deltaMSC_Gamma(:,ii),0,'tail','left');
end

H_signrank =
[H_signrank_Delta;H_signrank_Theta;H_signrank_Alpha;H_signrank_Beta;H_signrank_Gamma];
% put those in a Table form
% H_signrank = array2table(H_signrank);
% rename the correct header for each row
% H_signrank.Properties.RowNames = {'Delta','Theta','Alpha','Beta','Gamma'};
% H_signrank.Properties.VariableNames =
{'FC','FP','FPO','FO','FT','CP','CPO','CO','CT','PPO','PO','PT','POO','POT','OT'};
disp('          WILCOXON SIGN-RANK TEST');
disp(H_signrank);

% P_signrank =
[P_signrank_Delta;P_signrank_Theta;P_signrank_Alpha;P_signrank_Beta;P_signrank_Gamma];
% put those in a Table form
% P_signrank = array2table(P_signrank);
% rename the correct header for each row
% P_signrank.Properties.RowNames = {'Delta','Theta','Alpha','Beta','Gamma'};
```



```
% P_signrank.Properties.VariableNames =  
{'FC','FP','FPO','FO','FT','CP','CPO','CO','CT','PPO','PO','PT','POO','POT','OT'};  
% disp(P_signrank);
```

Bibliography

1. Butler, C., “Effects of Powered Mobility on Self-Initiated Behavior of Young Children with Locomotor Disability”, 1986, *Developmental Medicine and Child Neurology*, Vol 28, 325-332.
2. Deitz, J. et al, “Powered Mobility and Preschoolers with Complex Developmental Delays”, 2002, *American Journal of Occupational Therapy*, Vol 56, 86-96.
doi:10.5014/ajot.56.1.86
3. Zweifel, Nadina, "Changes in the EEG Spectrum of a Child with Severe Disabilities in Response to Power Mobility Training" (2016). Masters Theses. 799.
4. Usoro, Joshua O., "Information Theoretic EEG Analysis of Children with Severe Disabilities in Response to Power Mobility Training: A Pilot Study" (2017). Masters Theses. 837.
5. Kenyon, L. et al, “Power Mobility Training for Young Children with Multiple, Severe Impairments: A Case Series.”, 2016, *Phys Occup Ther Pediatr.*, 2638 (January): 1-16.
doi:10.3109/01942638.2015.1108380.
6. Kenyon L. et al, “Promoting Self-exploration and Function Through an Individualized Power Mobility Training Program.”, 2015, *Pediatr Phys Ther.*, Vol 27(2), 200-206.
doi:10.1097/PEP.0000000000000129.
7. Sauseng, P. et al, “What does phase information of oscillatory brain activity tell us about cognitive processes?”, 2008, *Neuroscience and Biobehavioral Reviews*, Vol 32, 1001-1013

8. Deitz, J. et al, "Powered Mobility and Preschoolers with Complex Developmental Delays", 2002, American Journal of Occupational Therapy, Vol 56, 86-96.
doi:10.5014/ajot.56.1.86.
9. Wong, K.F. et al, "Robust Time-Varying Multivariate Coherence Estimation: Application to Electroencephalogram Recordings During General Anesthesia", 2011, Conf Proc IEEE Eng Med Biol Soc., 4725-4728
10. Fein G, Raz J, Brown F, Merrin E. "Common reference coherence data are confounded by power and phase effects". EEG Clin Neurophysiol 1988; 69: 581–4.
11. Herculano-Houzel S. "The human brain in numbers: a linearly scaled-up primate brain". Front Hum Neurosci. 2009; 3:31. doi:10.3389/neuro.09.031.2009
12. Maurer, K., Dierks, T., 1991. "Atlas of Brain Mapping". Springer
13. Mitchell, D.J., McNaughton, N., Flanagan, D., Kirk, I.J., 2008. Frontal–midline theta from the perspective of hippocampal "theta.". Prog. Neurobiol. 86, 156–185.
14. Nunez, P.L., Wingeier, B.M., Silberstein, R.B., 2001. "Spatial-temporal structures of human alpha rhythms: theory, microcurrent sources, multiscale measurements, and global binding of local networks". Hum. Brain Mapp. 13, 125–164.
15. Srinivasan, R., Winter, W.R., Nunez, P.L., 2006. "Source analysis of EEG oscillations using high-resolution EEG and MEG." Prog. Brain Res. 159, 29–42. doi:10.1016/S0079-6123(06)59003-X.3d.
16. Baumeister J, Barthel T, Geiss KR, Weiss M (2008). "Influence of phosphatidylserine on cognitive performance and cortical activity after induced stress". Nutritional Neuroscience. 11 (3): 103–110. doi:10.1179/147683008X301478.

17. Lalo, E; Gilbertson, T; Doyle, L; Di Lazzaro, V; Cioni, B; Brown, P (2007). "Phasic increases in cortical beta activity are associated with alterations in sensory processing in the human". *Experimental Brain Research. Experimentelle Hirnforschung. Experimentation Cerebrale*. 177 (1): 137–45. doi:10.1007/s00221-006-0655-8.
18. Lubar J, White N, Swartwood M, Swartwood J. "Methylphenidate effects on global and complex measures of EEG". *Paediat Neurol* 1999; 21: 633–7.
19. Shaw J. "An introduction to the coherence function and its use in the EEG signal analysis". *J Med Eng Technol* 1981; 5: 279–88.
20. Delorme A, Makeig S. "EEGLAB: An open source toolbox for analysis of single-trial EEG dynamics including independent component analysis". *J Neurosci Methods* 2004; 134:9-21
21. Ungureanu M, Bigan C, Strungaru R, Lazarescu V. "Independent component analysis applied in biomedical signal processing". *Meas Sci Rev* 2004; 4:18.
22. Lovett, E.G. & Ropella, K.M. *Ann Biomed Eng* (1997) 25: 975.
doi:10.1007/BF02684133
23. Brazier MA. "Spread of seizure discharges in epilepsy: anatomical and electrophysiological considerations". *Exp Neurol*. 1972;36(2):263–72.
24. Hines, T. (2018, April). "Anatomy of the Brain", Mayfield Clinic. Retrieved August 6, 2019, from <https://mayfieldclinic.com/pe-anatbrain.htm>
25. Timmons, D. (n.d.). "Anatomy of the Brain and Spinal Cord". Retrieved August 7, 2019, from <https://www.seattlecca.org/diseases/brain-spinal-cord-cancers/brain-spinal-cord-cancers-facts/anatomy-brain-and-spinal-cord>
26. Orekhova E V., Stroganova T a., Posikera IN, Elam M. "EEG theta rhythm in infants and preschool children". *Clin Neurophysiol*. 2006;117(5):1047-1062.

doi: 10.1016/j.clinph.2005.12.027

27. Egri, Csilla, and Peter Ruben. "Action Potentials: Generation and Propagation." ELS, John Wiley & Sons, Inc., 16 Apr. 2012, doi: 10.1002/9780470015902.a0000278.pub2

28. V. Sakkalis, "Review of advanced techniques for the estimation of brain connectivity measured with eeg/meg," *Computers in Biology and Medicine*, vol. 41, no. 12, pp. 1110-1117, 2011.

29. Roach, B. J., & Mathalon, D. H. (2008). "Event-Related EEG Time-Frequency Analysis: An Overview of Measures and An Analysis of Early Gamma Band Phase Locking in Schizophrenia". *Schizophrenia Bulletin*, 34(5), 907-926. doi:10.1093/schbul/sbn093

30. Infantosi, A.F.C., Melges, D.B., & Tierra-Criollo, C.J. (2006). "Use of magnitude-squared coherence to identify the maximum driving response band of the somatosensory evoked potential". *Brazilian Journal of Medical and Biological Research*, 39(12), 1593-1603.

doi:10.1590/S0100-879X2006001200011

31. Esmaili S, Krishnan S, Raahemifar K: "Audio watermarking using time-frequency characteristics". *Canadian Journal of Electrical and Computer Engineering* 2003, 28(2):57-61.

doi:10.1109/CJECE.2003.1532509

32. Umopathy, K., Ghoraani, B. & Krishnan, S. *EURASIP J. Adv. Signal Process.* (2010)

2010: 451695. doi:10.1155/2010/451695

33. Lovett, E.G. & Ropella, K.M. *Ann Biomed Eng* (1997) 25: 975.

doi:10.1007/BF02684133

34. Duffy, F. H., Mcanulty, G. B., & Albert, M. (1996). "Effects of age upon interhemispheric EEG coherence in normal adults". *Neurobiology of Aging*, 17(4), 587-599.

doi:10.1016/S0197-4580(96)00007-3

35. Delorme A, Makeig S. "EEGLAB: An open source toolbox for analysis of single-trial EEG dynamics including independent component analysis". *J Neurosci Methods* 2004; 134:9-21.
36. Ungureanu M, Bigan C, Strungaru R, Lazarescu V. "Independent component analysis applied in biomedical signal processing". *Meas Sci Rev* 2004; 4:18.
37. Vigário RN. "Extraction of ocular artefacts from EEG using independent component analysis". *Electroencephalogr Clin Neurophysiol* 1997; 103:395-404.
38. Leuchter AF, Cook IA, Hunter AM, Cai C, Horvath S (2012) "Resting-State Quantitative Electroencephalography Reveals Increased Neurophysiologic Connectivity in Depression". *PLoS ONE* 7(2): e32508. doi: 10.1371/journal.pone.0032508.
39. Li Y, Kang C, Qu X, Zhou Y, Wang W, Hu Y. "Depression-Related Brain Connectivity Analyzed by EEG Event-Related Phase Synchrony Measure". *Frontiers in Human Neuroscience*. 2016; 10:477. doi:10.3389/fnhum.2016.00477.
40. Suhhova A., Bachmann M., Aadamsoo K., Vöhma Ü., Lass J., Hinrikus H. (2009) "EEG Coherence as Measure of Depressive Disorder" In: Vander Sloten J., Verdonck P., Nyssen M., Haeisen J. (eds) 4th European Conference of the International Federation for Medical and Biological Engineering. IFMBE Proceedings, vol 22. Springer, Berlin, Heidelberg
41. Markovska-Simoska, S., Pop-Jordanova, N., & Pop-Jordanov, J. (2018). "Inter- and Intra-Hemispheric EEG Coherence Study in Adults with Neuropsychiatric Disorders". *Prilozi*, 39(2-3), 5–19. doi: 10.2478/prilozi-2018-0037
42. Coben R., Clarke AR, Hudspeth W., (2008) Barry RJ. "EEG power and coherence in autistic spectrum disorder", *Clinical neurophysiology*, Vol: 119, Issue: 5, Page: 1002-9
43. Niedermeyer, E., da Silva, F.H.L., (1993). "Electroencephalography, Basic Principles, Clinical Applications, and Related Fields", 3rd ed.

44. Maurer, K., Dierks, T., (1991). “Atlas of Brain Mapping”. Springer
45. Nunez, P.L., Wingeier, B.M., Silberstein, R.B., (2001). “Spatial-temporal structures of human alpha rhythms: theory, microcurrent sources, multiscale measurements, and global binding of local networks”. *Hum. Brain Mapp.* 13, 125–164
46. Song J, Tucker DM, Gilbert T, Hou J, Mattson C, Luu P, et al. “Methods for examining electrophysiological coherence in epileptic networks”. *Front Neurol.* 2013; 4:55
47. Elisevich K, Shukla N, Moran JE, Smith BJ, Schultz L, Mason KM, et al. “An Assessment of MEG Coherence Imaging in the Study of Temporal Lobe Epilepsy”. *Epilepsia.* 2011a; 52 (6):1110–9
48. Bowyer S, Gjini K, Zhu X, Kim L, Moran J, Rizvi S, et al. “Potential Biomarkers of Schizophrenia from MEG Resting-State Functional Connectivity Networks: Preliminary Data”. *J Behav Brain Sci.* 2015; 5:1–11. doi:10.4236/jbbs.2015.51001.
49. Boutros NN, Galloway MP, Ghosh S, Gjini K, Bowyer SM. “Abnormal coherence imaging in panic disorder: a magnetoencephalography investigation”. *Neuroreport.* 2013;24(9):487–91.
50. Lajiness-O'Neill R, Richard AE, Moran JE, Olszewski A, Pawluk L, Jacobson D, et al. “Neural synchrony examined with magnetoencephalography (MEG) during eye gaze processing in autism spectrum disorders: preliminary findings”. *J Neurodev Disord.* 2014;6(1):15.
51. Knott, V., Mahoney, C., Kennedy, S., Evans, K., 2001. “EEG power, frequency, asymmetry and coherence in male depression”. *Psychiatry Research: Neuroimaging Section* 106 pages 123–140.

52. Debener, S., Beauducel, A., Nessler, D., Brocke, B., Heilemann, H., Keyser, J. “Is resting anterior EEG alpha asymmetry a trait marker for depression? Findings for healthy adults and clinically depressed patients”. *Neuropsychobiology* 41 (2000), 31–37.
53. Leuchter AF, Cook IA, Hunter AM, Cai C, Horvath S (2012) “Resting-State Quantitative Electroencephalography Reveals Increased Neurophysiologic Connectivity in Depression”. *PLoS ONE* 7(2): e32508. doi: 10.1371/journal.pone.0032508.
54. Li Y, Kang C, Qu X, Zhou Y, Wang W, Hu Y. “Depression-Related Brain Connectivity Analyzed by EEG Event-Related Phase Synchrony Measure”. *Frontiers in Human Neuroscience*. 2016; 10:477. doi:10.3389/fnhum.2016.00477.
55. Leon Petchkovsky, Kirstin Robertson-Gillam, Juri Kropotov & Michael Petchkovsky. “Using QEEG parameters (asymmetry, coherence, and P3a Novelty response) to track improvement in depression after choir therapy *Advances in Mental Health Promotion*”, *Prevention and Early Intervention*; 11:3, 257-267, doi: 10.5172/jamh. 2013.11.3.257.
56. Xing M, Tadayonnejad R, MacNamara A, et al. “Resting-state theta band connectivity and graph analysis in generalized social anxiety disorder”. *NeuroImage: Clinical*. 2017; 13: 24-32. doi: 10.1016/j.nicl.2016.11.009
57. Hanslmayr S, Klimesch W, Sauseng P, et al. “Visual discrimination performance is related to decreased alpha amplitude but increased phase locking”. *Neurosci Lett*. 2005;375(1):64-68. doi: 10.1016/j.neulet.2004.10.092
58. Uchida, S., Maehara, T., Hirai, N., Okubo, Y., Shimizu, H., 2001. “Cortical oscillations in human medial temporal lobe during wakefulness and all-night sleep”. *Brain Res*. 891, 7–19.

59. Gross J, Schmitz F, Schnitzler I, Kessler K, Shapiro K, Hommel B, et al. “Modulation of long-range neural synchrony reflects temporal limitations of visual attention in humans”. *Proc Natl Acad Sci U S A*. 2004;101(35):13050–5.
60. Fogassi, L. et al, “Motor functions of the parietal lobe”, 2005, *Neurobiology*, Vol 15, 626-631
61. Wagner, A.D. et al, “Parietal lobe contributions to episodic memory retrieval”, 2005, *TRENDS in Cognitive Sciences*, Vol 9, No. 9
62. Husain, M. et al, “Space and the parietal cortex”, 2006, *TRENDS in Cognitive Sciences*, Vol 11, No. 1
63. Aftanas LI, Golocheikine SA. “Non-linear dynamic complexity of the human EEG during meditation”. *Neurosci Lett* 2002; 330:143-6.